THE
PHYSICAL REVIEW
A Journal of Experimental and Theoretical Physics
VOL. 45, NO. 2 JANUARY 15, 1934 SECOND SERIES

The Radium-Uranium Ratio and the Number of Actinouranium Isotopes

ARTHUR E. RUARK AND FORREST WESTERN, *Departments of Physics, University of Pittsburgh and Missouri Valley College*
(Received December 7, 1933)

The radium-uranium ratio V is given by $E(1-\frac{1}{2}nB)/Z$ where $2E$ and Z are respectively the numbers of alpha-particles emitted per sec. per g of U or of Ra; B is essentially equal to the actinium "branching" ratio; and n is the number of actinouranium isotopes. Data on V, E, Z and B are considered in order to determine whether $n=1$ or 2. The results speak strongly in favor of the existence of only one actinouranium isotope.

SEVERAL lines of evidence support the view that the parent of the actinium series is a uranium isotope of weight 235.[1] Further evidence can be obtained from data on the rates of disintegration of radium and uranium, together with the radium-uranium ratio, which is numerically equal to the weight of radium in equilibrium with one gram of uranium. Let E be one-half the number of alpha-particles emitted per second by all the isotopes in one gram of uranium; Z, the number of alpha-particles emitted per gram of radium per second; V, the radium-uranium ratio; and let

$$B=\lambda_{Ac}N_{Ac}/\lambda_{U\ I}N_{U\ I}, \qquad (1)$$

where the λ's are decay constants and N_{Ac} is the number of actinium atoms in equilibrium with $N_{U\ I}$ atoms of U I. For practical purposes, B is equal to the so-called actinium branching ratio. Then if n is the number of actinouranium isotopes, we find that

$$V=(E/Z)(1-nB/2). \qquad (2)$$

Eight recent papers yield the mean value

$$Z=(3.695\pm0.017)10^{10}\ \text{particles/g}\cdot\text{sec.},$$

where the uncertainty is the average deviation from the mean. Kovarik and Adams[2] obtained

$$E=12{,}385\ \text{particles/g}\cdot\text{sec.}$$

with 1 percent uncertainty. Thus $E/Z=(3.35\pm0.05)10^{-7}$, while B lies between 0.03 and 0.04.[3] To obtain information about n, we may use Eq. (2) and the above values of E and Z to compute values of V for the extreme values of B and for $n=1$ and 2; and shall compare the results with experimental values of V. The computed values in Table I are uncertain by 0.05, if we accept the above estimates of the uncertainties of E and Z.

TABLE I.

n	B	10^7V
1	0.03	3.30
	0.04	3.28_5
2	0.03	3.25
	0.04	3.22

Experimental determinations of V depend for their accuracy on the selection of unaltered minerals so it is not surprising that the recorded

[1] Hahn, Zeits. f. anorg. Chemie **147**, 16 (1925); Western and Ruark, Phys. Rev. **44**, 675 (1933).

[2] Kovarik and Adams, Phys. Rev. **40**, 718 (1932).

[3] Western and Ruark, reference 1.

values cover a considerable range. The work of Gleditsch and Qviller[4] on uranothorites yielded values from 1.98 to 3.20. They found that low values of V are associated with low values of the lead ratio, indicating leaching of radium and of thorium lead. However, Heimann and Marckwald[5] proved the essential constancy of V for pitchblende specimens from many of the principal uranium deposits of the world. These observations justify us in confining attention to those determinations which have been made with pitchblende. We present here (Table II) such determinations of 10^7V, referring to the treatise of Meyer and Schweidler for bibliography:

TABLE II.

Soddy and Pirrett	1910–11	3.15
Heimann and Marckwald	1913	3.32_8
Becker and Jannasch	1915	3.383 to 3.415
Lind and Roberts	1920	3.40 ± 0.03

The value of Soddy and Pirrett departs so far from the others and from any value which is possible on the basis of Eq. (2) that we are safe in disregarding it. The mean of the others is 3.37_5, while the International Radium Standards Commission[6] adopts the value 3.40 found by Lind and Roberts and by Becker and Jannasch. This value is strongly supported by the fact that the amount of radium available to Lind and Roberts for the preparation of their standard solutions was over 200 mg. This eliminates many uncertainties from their results. It makes little difference whether we take the mean or the value of the Commission. The conclusion is the same; namely, that *the experimental values speak strongly in favor of the hypothesis that there is a single actinouranium isotope.*

It is probable that the discrepancy between the experimental value of V and those given in Table I for the cases $n=1$, $B=0.03$ or 0.04, will be resolved by slight changes in the values assigned to all the quantities V, E and Z. As they stand, the data indicate a low value of B, but the change produced in the computed value of 10^7V by passing from $B=0.03$ to $B=0.04$ is so small that no real light is thrown on the question.

[4] Gleditsch and Qviller, Phil. Mag. **14**, 233 (1932).

[5] Heimann and Marckwald, Phys. Zeits. **14**, 303 (1913).

[6] Report of the International Radium-Standards Commission, 1930, Rev. Mod. Phys. **3**, 427 (1931).

The Natural Widths of the *L*-Series Lines in the X-Ray Spectra of Elements 74 to 83

JOHN H. WILLIAMS,* *Ryerson Laboratory, University of Chicago*

(Received November 20, 1933)

The full widths at half-maximum of the $L\alpha_1$, $L\beta_1$, $L\beta_2$ and $L\gamma_1$ lines of Bi, Pb, Tl, Au, Pt, Ir and W have been measured with Allison's double spectrometer in the (1, +1) position equipped with previously calibrated calcite crystals of high perfection. The results in X.U. are given in the table. The widths are uncorrected for the finite resolving power of the crystals or for the geometrical divergence of the x-ray beam. Approximate small corrections have been made for interfering lines. Relative wave-lengths of neighboring lines are given. Empirical relations between the energy widths of the lines investigated and the atomic number and the electron transitions involved are suggested. The effects of alloys of the elements on the widths observed are discussed.

Line	74 W	77 Ir	78 Pt	79 Au	81 Tl	82 Pb	83 Bi
$L\alpha_1$	1.26	1.19	1.17	1.13	1.11	1.05	1.03
$L\beta_1$	0.943	0.822	0.804	0.785	0.743		0.700
$L\beta_2$	1.38	1.17	1.14	1.06	1.00		.895
$L\gamma_1$	1.01	0.923	0.837	0.791	0.741	0.698	.669

INTRODUCTION

AN empirical knowledge of the natural widths of x-ray lines has been attained in the past few years by the use of the double crystal x-ray spectrometer devised by Ehrenberg and Mark[1] and Davis and Purks.[2] Many investigators have measured the widths of the *K*-series lines of various elements[3] but little is known about the widths of the lines in the *L*-series. Preliminary experiments on the widths of a few lines in the *L*-series of lead and thallium performed by Allison[4] and in tungsten by Ehrenberg and von Susich[5] showed that *L*-series lines were much wider than *K*-series lines of the same wave-length. The widths of twelve lines in the *L*-series spectrum of uranium were investigated by the author[6] in a study of possible correlations between the widths and the transitions involved. Spencer[7] studied the width of Ag $L\alpha_1$ with a "universal" double spectrometer and obtained the large value of 4.5 X.U. for the width at half-maximum.

The present experiments investigated the widths of the $L\alpha_1$, $L\beta_1$, $L\beta_2$ and $L\gamma_1$ lines of W(74), Ir(77), Pt(78), Au(79), Tl(81), Pb(82) and Bi(83).

The measurements were all obtained with the crystals in the (1, +1) position (in the notation of Allison and Williams[8]). In this position, where the crystal faces are not parallel, the dispersion of the instrument is finite. Widths are obtained for the lines that are much greater than those expected from the diffraction pattern of the crystals and hence must be attributed principally to the natural widths of the lines themselves.

APPARATUS AND OPERATING CONDITIONS

The double crystal x-ray spectrometer used in this research has been described previously.[9, 10] The slits limiting the vertical and horizontal divergence of the x-ray beam were 49.6 and 14.5 cm apart, respectively. Table I gives the experimental conditions. α_m is the maximum horizontal divergence of the x-ray beam passing through two slits of equal width a that are L_H cm apart and is equal to a/L_H. ϕ_m is the maximum vertical divergence and is similarily equal to b/L_V.

The crystals used in this investigation were

* National Research Fellow.

[1] Ehrenberg and Mark, Zeits. f. Physik **42**, 807 (1927).

[2] Davis and Purks, Proc. Nat. Acad. Sci. **13**, 419 (1927).

[3] See reference 1 in Allison, Phys. Rev. **44**, 63 (1933).

[4] S. K. Allison, Phys. Rev. **34**, 176 (1929).

[5] Ehrenberg and von Susich, Zeits. f. Physik **42**, 823 (1927).

[6] J. H. Williams, Phys. Rev. **37**, 1431 (1931).

[7] R. C. Spencer, Phys. Rev. **38**, 630 (1931).

[8] Allison and Williams, Phys. Rev. **35**, 149 (1930).

[9] S. K. Allison, Phys. Rev. **44**, 63 (1933).

[10] S. K. Allison, Phys. Rev. **41**, 1 (1932).

TABLE I. *Experimental conditions.*

Element	Line	Voltage (kv)	Current (m.a.)	α_m $\times 10^{-3}$	ϕ_m $\times 10^{-2}$
83 Bi	$L\alpha_1$	36.5	3.1	6.9	1.2
	β_1	"	3.0	"	1.1
	β_2	"	"	"	1.2
	γ_1	41.0	4.1	"	1.4
82 Pb	$L\alpha_1$	36.5	4.0	5.5	1.4
	γ_1	42.5	8.0	6.9	1.2
81 Tl	$L\alpha_1$	36.5	2.5	6.9	1.2
	β_1	"	2.6	"	1.4
	β_2	"	2.5	"	"
	γ_1	39.5	2.0	"	"
79 Au	$L\alpha_1$	36.5	3.0	7.4	1.4
	β_1	"	3.3	8.3	1.2
	β_2	"	3.4	"	1.4
	γ_1	39.5	3.3	"	"
78 Pt	$L\alpha_1$	36.5	3.3	8.3	1.1
	β_1	"	"	"	1.2
	β_2	38.2	3.5	"	1.4
	γ_1	39.5	3.1	"	"
77 Ir	$L\alpha_1$	36.5	3.3	8.3	1.4
	β_1	"	3.6	"	"
	β_2	38.6	3.8	"	"
	γ_1	39.5	"	"	"
74 W	$L\alpha_1$	36.5	3.0	8.3	1.4
	β_1	"	3.3	"	"
	β_2	39.5	3.4	"	"
	γ_1	"	"	"	"

Allison's[10] calcites III*A* and III*B* which had been shown to approximate closely the theory of reflection by perfect calcite crystals. Measurements with Pt $L\alpha_1$ and Pb $L\alpha_1$ reflected from the crystals in the (1, −1) position showed that the crystals had not deteriorated during the course of this investigation.

The x-ray tube and targets were of a design previously described by Allison.[9] Bi, Pb and Tl were melted into circular cavities in the faces of standard copper base targets. In the case of Tl the surface was filed and then covered with naphthalene to prevent oxidization. The naphthalene evaporated quickly when the tube was evacuated. Au and Pt sheets were soft-soldered to a flat copper face. Ir was silver-soldered into the cavity and W was first spot-welded with nickel and then silver-soldered to a standard base target.

EXPERIMENTAL PROCEDURE

The curves were taken by rotating crystal *B* about a vertical axis lying in the plane of its reflecting face while crystal *A* remained stationary. DuMond and Hoyt[11] have pointed out that this method may introduce errors because, as crystal *B* is rotated through small steps, the x-ray beam is reflected from different parts of the crystals and also, the central beam comes from different parts of the focal spot of the tube. By rotating both crystals simultaneously in a manner that satisfies the geometrical conditions, Allison[9] has shown that for the Co $K\alpha$ lines, which have an angular width of 0.82 and 0.94 X.U., widths are obtained which agree with those obtained by the former method of operation. Since the widths of the lines observed in the present experiment were of the same order of magnitude as those examined by Allison, the method of rotating crystal *B* alone is justified. A further test of the method was made with Tl $L\beta_1$, $L\beta_2$ lines of wave-lengths 1012.99 and 1008.22 X.U., respectively. The width of either $L\beta_1$ or $L\beta_2$ was found to be independent of the setting of crystal *A* at values between the limiting reflection angles imposed by the above wave-lengths. Thus it is felt that the method of single rotation will yield curves that are not influenced by the movements of the observed beam over the focal spot or the reflecting crystal faces.

CORRECTIONS TO THE OBSERVED WIDTHS

The three factors that may be considered to affect the observed widths are: the horizontal and vertical divergence of the x-ray beam and the finite resolving power of the calcite crystals. Allison[9] has discussed the question of these corrections for *small* values of α_m and ϕ_m and has shown that the geometrical divergence of the incident beam contributes a negligible amount to the width calculated for monochromatic radiation. In the case of real line radiation possessing a finite wave-length spread, with the limits on α_m and ϕ_m of the order of magnitude of those given in Table I, geometrical contributions may be neglected. The contributions of the finite resolving power of the crystals to the observed widths are not so well known. The widths observed when the crystals are in the (1, −1) position[10] show that this width is from 8 to 12 percent of the widths of the lines examined here in the

[11] DuMond and Hoyt, Phys. Rev. **36**, 1702 (1930).

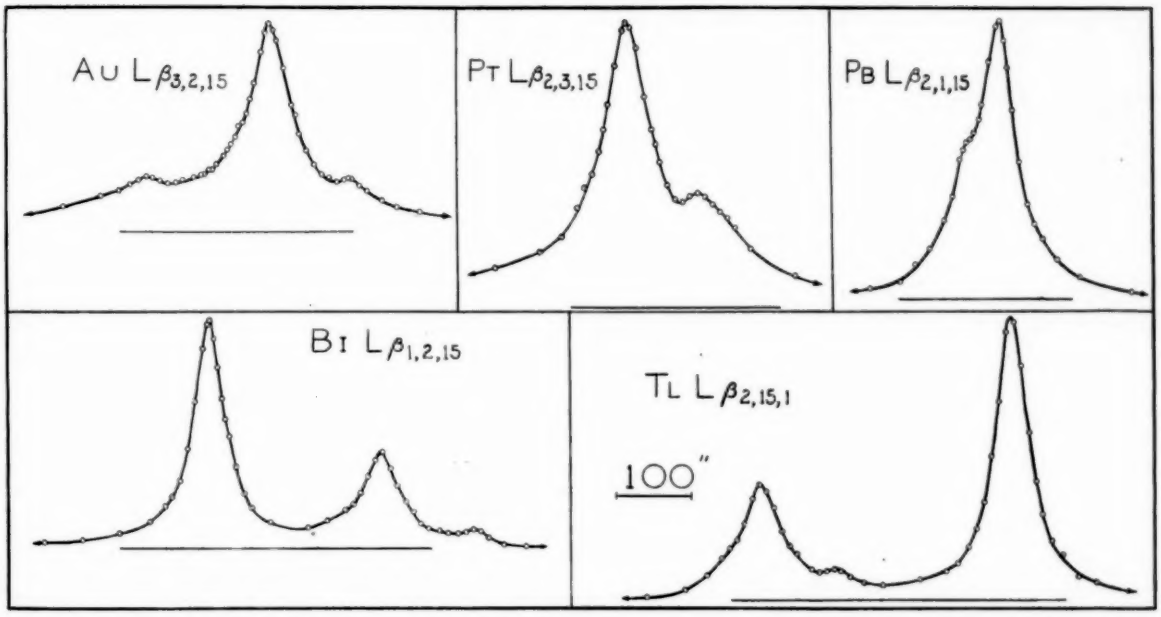

FIG. 1. Curves of L-series lines obtained in the (1, +1) position by rotating crystal B alone. The vertical scale of intensity is not the same for all the curves. The horizontal scale of angular rotation of crystal B from an arbitrary zero is the same for all the curves. The horizontal lines beneath the curves are the base line intensities measured at least 500″ on either side of the peaks.

(1, +1) position. Laue[12] has shown that the actual shape of a single crystal diffraction pattern cannot be obtained from the (1, −1) curve and so any treatment is necessarily handicapped by the assumption of an arbitrary function for this shape, even if empirical functions are known[13] for the (1, −1) rocking curve shape. The results of this experiment are therefore uncorrected for the three possible effects.

The widths of most of the lines examined are not influenced by neighboring lines except in the case of the doublet $L\beta_2$, $L\beta_{15}$ in all the elements, the neighboring lines $L\beta_2$, $L\beta_3$ in Au, $L\beta_2$, $L\beta_3$ in Pt, and the coincident lines $L\beta_1$, $L\beta_2$ in Pb. The doublet $L\beta_2$, $L\beta_{15}$ has a relative intensity of 9 to 1 predicted by an extension of the Burger and Dorgelo[14] sum rules and experimentally proven by measurements on uranium and thorium by Allison.[4] The relative intensity $L\beta_2/L\beta_{15}$ for Au, Tl and Bi was here estimated to be 10, 9 and 8.5, respectively. Considerations of the curves showed that the influence of $L\beta_{15}$ on the width of $L\beta_2$ was negligible. Estimates were made from large scale plots of the small contribution of $L\beta_3$ to Au $L\beta_2$ and Pt $L\beta_2$. Curves of the interfering lines and of the group $L\beta_1$, $L\beta_2$, $L\beta_{15}$ in Tl, Pb and Bi are shown in Fig. 1.

All the principal lines examined were symmetrical to within the accuracy of the measurements so that the ratio of the part of the width lying to the long wave-length side of the maximum ordinate to that part on the short wave-length side was 1.00 ± 0.05. In striking contrast to these results are the measurements of Allison[9] and others on Cu $K\alpha_1$ where the ratio is 1.4 although the wave-length is approximately the same as W $L\alpha_1$.

By assuming that the principal lines are perfectly symmetrical one can split the composite curve into its separate parts and obtain values for the relative wave-lengths of neighboring lines from the measured angular separation and the known dispersion of the instrument. By taking the most intense line as the reference line and assigning to it a wave-length given by Siegbahn,[15]

[12] Laue, Zeits. f. Physik **72**, 472 (1932).
[13] A. Hoyt, Phys. Rev. **40**, 477 (1932).
[14] Burger and Dorgelo, Zeits. f. Physik **23**, 258 (1924).
[15] M. Siegbahn, *Spektroskopie der Röntgenstrahlen*, second edition.

TABLE II. *Relative wave-lengths of overlapping lines in X.U.*

Element	$L\beta_1$	$L\beta_2$	$L\beta_{15}$	$L\beta_3$
Bi (83)	(950.02)	953.33 953.24*	955.14 955.08*	
Pb (82)	(980.83)	980.15 980.83*		
Tl (81)	(1012.99)	1008.14 1008.22*	1009.69 1010.0 *	
Au (79)		(1068.01)	1069.54 1069.9 *	1065.61 1065.50*
Pt (78)		(1099.74)	1101.34 1101.65*	

the relative wave-lengths shown in Table II have been obtained. Values of the wave-lengths of Ir $L\beta_{15}$ and W $L\beta_{15}$ are not given because $L\beta_2$ has become so wide that the derived values are unreliable. The values in parentheses are the reference wave-lengths and the starred values are Siegbahn's values for the wave-lengths.

RESULTS

Table III shows the values of the widths, $\Delta\theta$, in seconds of arc obtained for the full width at half maximum of the various lines in the (1, +1) position. From these the values of $\Delta\lambda$ in X.U., ΔV in volts and $(\Delta\nu/R)^{\frac{1}{2}}$ are calculated by the following equations:

$$\Delta\lambda = (\tfrac{1}{2})\lambda \cot\theta\Delta\theta \qquad (1)$$

$$(\Delta\nu/R)^{\frac{1}{2}} = 9.5460\times10^{2}\lambda^{-1}(\Delta\lambda)^{\frac{1}{2}} \qquad (2)$$

$$\Delta V = 1.2336\times10^{7}\Delta\lambda/\lambda^{2} \qquad (3)$$

where $\Delta\lambda$ and λ are in X.U.

TABLE III. *Experimental results on the natural widths.*

Line	λ (X.U.)[15]	$\Delta\theta$	$\Delta\lambda$ (X.U.)	$(\Delta\nu/R)^{\frac{1}{2}}$	$\Delta\nu$ (volts)
83 Bi $L\alpha_1$	1141.50	71.5″	1.03	0.849	9.76
$L\beta_1$	950.02	48.3	0.700	.841	9.57
$L\beta_2$	953.24	61.7	0.895	.947	12.1
$L\gamma_1$	811.43	46.0	0.669	.963	12.5
82 Pb $L\alpha_1$	1172.58	73.3	1.05	.837	9.47
$L\gamma_1$	838.01	48.0	0.698	.952	12.3
81 Tl $L\alpha_1$	1204.93	77.2	1.11	.834	9.41
$L\beta_1$	1012.99	51.3	0.743	.812	8.93
$L\beta_2$	1008.22	69.2	1.00	.948	12.2
$L\gamma_1$	865.71	51.0	0.741	.949	12.2
79 Au $L\alpha_1$	1273.77	78.4	1.13	.795	8.57
$L\beta_1$	1081.28	54.3	0.785	.782	8.28
$L\beta_2$	1068.01	73.2	1.06	.919	11.4
$L\gamma_1$	924.61	54.5	0.791	.918	11.4
78 Pt $L\alpha_1$	1310.33	81.5	1.17	.788	8.40
$L\beta_1$	1117.58	55.7	0.804	.766	7.94
$L\beta_2$	1099.74	79.0	1.14	.927	11.6
$L\gamma_1$	955.99	57.7	0.837	.913	11.3
77 Ir $L\alpha_1$	1348.47	83.2	1.19	.773	8.08
$L\beta_1$	1155.40	57.0	0.822	.749	7.59
$L\beta_2$	1132.97	81.3	1.17	.913	11.3
$L\gamma_1$	988.76	63.7	0.923	.927	11.6
74 W $L\alpha_1$	1473.36	88.5	1.26	.727	7.16
$L\beta_1$	1279.17	65.7	0.943	.725	7.11
$L\beta_2$	1242.03	95.8	1.38	.902	10.1
$L\gamma_1$	1096.30	70.0	1.01	.875	10.4
92 U[16] $L\alpha_1$	908.33	61.3	0.890	0.991	13.3
$L\beta_1$	718.07	42.0	.612	1.04	14.6
$L\beta_2$	752.68	53.1	.774	1.12	16.8
$L\gamma_1$	612.83	35.3	.516	1.12	16.9

The angular widths are estimated to be correct to within ±2 percent for $L\alpha_1$, ±3 percent for $L\beta_1$ and ±5 percent for $L\beta_2$ and $L\gamma_1$. In general three or more curves were taken of each line.

Fig. 2 and Fig. 3 show the variation of $\Delta\lambda$ and $(\Delta\nu/R)^{\frac{1}{2}}$ as a function of atomic number. The points in Fig. 3 lie on straight lines to within the

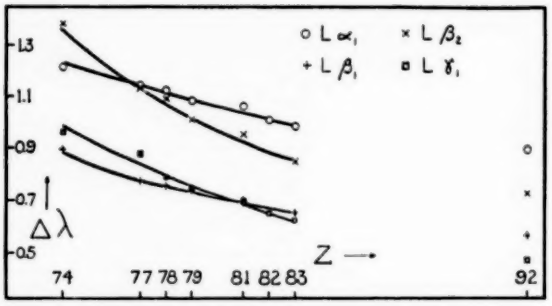

FIG. 2. The full width in X.U. at half-maximum of *L*-series lines as a function of atomic number.

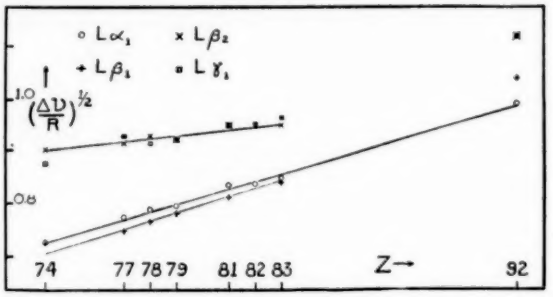

FIG. 3. The square root of the frequency width of *L*-series lines as a function of atomic number.

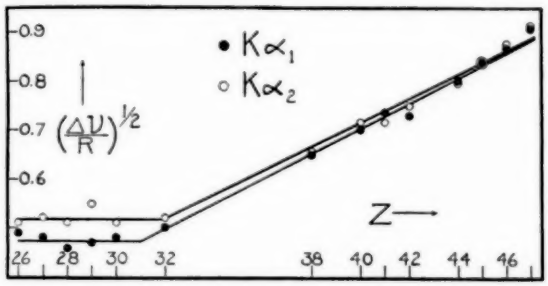

FIG. 4. The square root of the frequency width of the $K\alpha$ lines as a function of atomic number plotted from Allison's[9] data.

experimental error. In order to see if this empirical linear relationship existed in the K-series, Allison's[9] results were plotted with the same variables and are shown in Fig. 4. It is seen that straight lines may be drawn through the experimental points with a change in slope at Z equal to 31 or 32. Allison has pointed out that in this region the M_{IV}, M_V shells have just become filled and that in the solid state the distortion of the shells may extend above 29 Cu where the spectroscopic data give evidence of a complete $3d$ level. On this basis it is evident that the L transitions examined in this research are not affected by the filling of outer shells in the region 74 W to 83 Bi. The values[16] of $(\Delta\nu/R)^{\frac{1}{2}}$ for U $L\beta_1$, $L\beta_2$ and $L\gamma_1$ do not fall on the extrapolated lines. This might indicate changing conditions in the unexamined region which is unfortunately meager in elements easily available for solid x-ray targets.

The generalizations drawn by the author[6] from the voltage widths of the L-series lines of uranium are somewhat confirmed by the present results. The $L\beta_2$ and $L\gamma_1$ voltage widths agree and it may be more than fortuitous that these lines involve transitions from similar initial and final orbits and the eccentricities of these orbits on the Sommerfeld theory are the same as well as the changes in the quantum numbers. The neighboring values of the voltage widths of $L\alpha_1$ and $L\beta_1$ might be correlated with the fact that the lines involve transitions between energy levels differing only in the magnitude of j but agreeing in changes in quantum numbers and have the same ellipticity of the orbits. It should be pointed out that the conclusion of experimenters[17] working with the photographic method that $L\alpha_1$ is the narrowest L-series line on a wave-length scale is definitely in error.

Parratt[18] has reported changes in the width of Mn $K\alpha_1$ in alloys of Mn–Ni, Mn–Cu and Mn–Cr but no changes in a 50–50 Mn–Fe alloy. In order to see if this effect was evident in the L-series the width of Pb $L\alpha_1$ was examined from various alloys of Pb and Sb. No changes in the width were observed but this might well be due to the fact that the levels here involved are more deeply buried in the atom than the Mn levels investigated by Parratt. Also the alloy chosen might correspond to the Mn–Fe alloy which showed no effect on the width of Mn $K\alpha_1$. All the elements used in the determination of the natural widths shown in Table III were of sufficient purity not to be influenced by this effect except that a layer of oxide might have been on the Tl despite the precautions.

The agreement between the present results and the previous meager results[4, 5] on the natural widths of the L-series lines is not at all good. However, the previous measurements were obtained when the technique of the instrument was just being acquired and it is felt that the disagreement is not to be taken seriously. The better crystals and the more accurate adjustments of the instrument in the present experiments are certain to yield more accurate values for the widths.

In conclusion I wish to express my sincere thanks to Professor S. K. Allison for placing his laboratory at my disposal and for the many favors extended by him in the past few years. I am also indebted to the members of Ryerson Laboratory for the use of their many laboratory facilities and for their helpful interest.

[16] The values for uranium have been recalculated from reference 6 by the same method as the above.

[17] Coster, Zeits. f. Physik **45**, 797 (1927).

[18] L. G. Parratt, Phys. Rev. **44**, 328 (1933).

Note on the Ionization Potential of Fe II

J. C. DOBBIE, *Solar Physics Laboratory, Cambridge, England*

(Received November 25, 1933)

Two new high terms, e^6D and e^4D, have been found in the spark spectrum of iron which are in series with known low terms. The principal ionization potential for Fe II is thus found to be 16.16 volts.

IN the course of analysis of the unclassified lines of Fe II which is now being undertaken at the Solar Physics Observatory, Cambridge, England, with a view to the extension of the multiplet scheme started by H. N. Russell,[1] two new high-lying terms, $e^6D(77{,}861.4)$ and $e^4D(79{,}439.3)$ have been identified.

The arrangements of the multiplets which these terms, belonging to the configuration $d^{n-2}\cdot s$, form by their combinations with the odd triad $d^{n-2}p\ z^4P°$, $D°$, $F°$ are set out in Tables I and II. The intensities, placed after the wave-length, have been estimated on an arbitrary scale. The theoretical wave number is shown in brackets below the observed.

The measurements of these new multiplet lines have been made from plates, taken by Mr. Moss, of the polar lines of iron. They appear on these plates most strongly at the positive pole and faintly in the core in the case of the stronger lines and not at all in the case of the weaker lines. In Exner and Haschek's spark spectrum of iron the lines in question either do not appear or are broad and diffuse.

Many hundreds of unclassified lines of Fe II appear on our plates as polar lines of all degrees of enhancement ranging from those which are nearly as strong in the core as at the poles (i.e., high level lines of Fe I) to those which are very strong at the pole compared with the core (i.e., lines corresponding to transitions from high terms in Fe II such as those recorded in this note).

Since the new terms $d^{n-2}\cdot s\ e^6D$ and $d^{n-2}\cdot s\ e^4D$ are the second members of their respective series, the first members being the low-lying $d^{n-2}s\ a^6D$ and $d^{n-2}s\ a^4D$ terms, the ionization potential of Fe II may be calculated with a fair degree of accuracy.

Taking the levels of highest inner quantum number $a^4D_{3\frac{1}{2}}(7955.3)$ and $e^4D_{3\frac{1}{2}}(79{,}439.3)$ as representing the first two terms of the quartet series and expressing the difference 71,484.0 as the difference between two Rydberg terms, we find

$$71{,}484.0 = 4\times 109{,}737.1\{1/(1.877783)^2 - 1/(2.877783)^2\}$$
$$= 124{,}486.6 - 53{,}002.6,$$

where the value 109,737.1 has been taken for the Rydberg constant.[2]

The series limit becomes $7955.3+124{,}486.6 = 132{,}441.9$. From a comparison of the limits obtained from a Ritz formula for series in which more than two terms are known, with those obtained from a Rydberg formula from the first two terms, Russell[3] finds that in the case of the neutral elements of the iron group the limit obtained from a Rydberg formula is higher than that obtained from a Ritz formula and that a fair correction may be made to the former by assuming a percentage error of $4.5\times 10^{-5}\times$ length of series.

In the case of the ionized elements he shows that the computed percentage error

$$0.25\times 4.5\times 10^{-5}\times \text{length of series}$$

is in good agreement with the actual error for Ca II and Zn II to which elements the Ritz formula is applicable.

[1] H. N. Russell, Astrophys. J. **64**, 194 (1926).

[2] Bacher and Goudsmit, *Atomic Energy States*, page 544.

[3] H. N. Russell, Astrophys. J. **66**, 233 (1927).

TABLE I.

		$e^6D_{4\frac{1}{2}}$ 77861.4	376.2	$e^6D_{3\frac{1}{2}}$ 78237.6	287.7	$e^6D_{2\frac{1}{2}}$ 78525.3	200.3	$e^6D_{1\frac{1}{2}}$ 78725.6	118.3	$e^6D_{\frac{1}{2}}$ 78843.9
$z^6F^\circ_{5\frac{1}{2}}$	41968.08	2785.21(15) 35893.3 (3.4)								
$z^6F^\circ_{4\frac{1}{2}}$	42114.86	2796.65(7) 35746.6 (6.6)		2767.52(20)[a] 36123.0 (2.7)						
$z^6F^\circ_{3\frac{1}{2}}$	42237.06	—		2776.92(8) 36000.4 (0.5)		2754.90(10) 36288.0 (8.2)				
$z^6F^\circ_{2\frac{1}{2}}$	42334.86			2784.48(2) 35902.8 (2.7)		2762.35(7) 36190.6 (0.5)		2747.14(6) 36390.8 (0.7)		
$z^6F^\circ_{1\frac{1}{2}}$	42401.33					—		2752.17(7) 36324.1 (4.3)		—[b]
$z^6F^\circ_{\frac{1}{2}}$	42439.87							2755.09(0) 36285.5 (5.7)		2746.14(4) 36403.8 (4.1)
$z^6D^\circ_{4\frac{1}{2}}$	38459.02	2537.15(8)[c] 39402.6 (2.4)		2513.16(3) 39778.6 (8.6)						
$z^6D^\circ_{3\frac{1}{2}}$	38660.06	2550.16(5) 39201.5 (1.4)		2525.93(6) 39577.5 (7.5)		2507.69(3) 39865.3 (5.2)				
$z^6D^\circ_{2\frac{1}{2}}$	38858.99			2538.69(4) 39378.7 (8.6)		2520.27(3) 39666.3 (6.3)		2507.61(5) 39866.8 (6.6)		
$z^6D^\circ_{1\frac{1}{2}}$	39013.23					2530.11(10) 39512.3 (2.1)		—		2509.87(4) 39830.7 (0.7)
$z^6D^\circ_{\frac{1}{2}}$	39109.33							2523.46(3) 39616.4 (6.3)		2515.94(1) 39734.8 (4.6)
$z^6P^\circ_{3\frac{1}{2}}$	42658.26	2839.82(10) 35203.1 (3.2)		2809.79(8) 35579.2 (9.3)		2787.25(5) 35866.9 (7.0)				
$z^6P^\circ_{2\frac{1}{2}}$	43238.61			2856.40(8) 34999.0 (9.0)		2833.10(8) 35286.7 (6.7)		2817.11(6) 35487.0 (7.0)		
$z^6P^\circ_{1\frac{1}{2}}$	43620.98					2864.13(5) 34904.3 (4.3)		2847.79(6) 35104.6 (4.6)		2838.22(8) 35222.8 (3.0)

[a] A blend. [b] Covered by the Fe II line 2743.196. [c] Very diffuse core line slightly enhanced.

Applying this correction, therefore, to the value 132,441.9 found above for the series limit in the case of the quartets, we obtain for the corrected limit the value 130,698.

The length of the series now becomes

$$130{,}698 - 7955 = 122{,}743,$$

which value represents the energy (15.14 volts) required to remove an s electron from the $d^{n-2}s\ a^4D_{3\frac{1}{2}}$ state or 16.12 from the ground state $a^6D_{4\frac{1}{2}}$.

TABLE II.

		$e^4D_{3\frac{1}{2}}$ 79439.3	446.1	$e^4D_{2\frac{1}{2}}$ 79885.4	292.5	$e^4D_{1\frac{1}{2}}$ 80177.9	168.1	$e^4D_{\frac{1}{2}}$ 80346.0
$z^4F^\circ_{4\frac{1}{2}}$	44232.55	2839.53(12) 35206.6 (6.7)						
$z^4F^\circ_{3\frac{1}{2}}$	44753.83	—		2845.61(15)[a] 35131.6 (1.6)				
$z^4F^\circ_{2\frac{1}{2}}$	45079.87	—		—		2848.33(8) 35098.0 (8.0)		
$z^4F^\circ_{1\frac{1}{2}}$	45289.86			—		2865.47(3) 34888.1 (8.0)		2851.73(10)[b] 35056.1 (6.1)
$z^4D^\circ_{3\frac{1}{2}}$	44446.91	2856.93(9) 34992.3 (2.4)		—				
$z^4D^\circ_{2\frac{1}{2}}$	44784.80	2884.78(7) 34654.5 (4.5)		2848.12(8) 35100.5 (0.6)		2824.58(2) 35393.0 (3.1)		
$z^4D^\circ_{1\frac{1}{2}}$	45044.23			—		2845.44(7) 35133.6 (3.7)		2831.89(3) 35301.8 (1.8)
$z^4D^\circ_{\frac{1}{2}}$	45206.55					2858.65(5) 34971.5 (1.4)		2844.97(6) 35139.4 (9.4)
$z^4P^\circ_{2\frac{1}{2}}$	46967.52	3078.71(9) 32471.9 (1.8)		3036.98(7) 32917.8 (7.9)		3010.23(3) 33210.5 (0.4)		
$z^4P^\circ_{1\frac{1}{2}}$	47389.88			3076.46(8) 32495.5 (5.5)		3049.01(7) 32787.9 (8.0)		3033.46(3) 32956.2 (6.1)
$z^4P^\circ_{\frac{1}{2}}$	47626.18					3071.14(5) 32551.7 (1.7)		3055.37(8) 32719.7 (9.8)

[a] Blended with the Fe I line 2845.595.

[b] Blended with the Fe I line 2851.797.

In the case of the sextet series, the empirically corrected length of series becomes 131,259 representing an ionization potential of 16.19 volts.

The mean of these, 16.16 volts, may be adopted as the "principal ionization potential" which represents the difference in energy between the normal states of the Fe II and of the Fe III atom.

The values 16.19 volts for the sextet series and 15.14 volts for the quartet series are in excellent agreement with the values 16.15 volts and 15.12 volts found by Russell[3] from the empirical formulae

$$C=0.601Z+0.13M$$

and

$$D=0.601Z-0.13M,$$

where C and D represent the second ionization potentials of the atoms of the iron group obtained by the removal of an s electron from the $d^{n-2}s$ state for higher and lower multiplicities, respectively. In these formulae Z is the atomic number of the neutral element and M the magnetic moment of the incomplete shell of d electrons, which increases from a single magneton in Sc II to five in Mn II and then diminishes to one in Cu II.

Large Electronic Isotope Effects in Molecular Spectra

HERRICK L. JOHNSTON,* *Department of Chemistry, Ohio State University*

(Received November 21, 1933)

The large electronic isotope effect in the spin coupling of $^2\Pi$-terms, reported by Johnston and Dawson for boron monoxide and for the heads of the OH[2] bands is confirmed by measurements of the fine line structure in the isotopic OH bands. Both for BO and for OH the observed increase in the doublet spacings, in the molecule with the heavier isotope, agrees closely with the results to be expected from Hill and Van Vleck's theoretical treatment of spin coupling energy, although their equations do not so well reproduce the separate doublets. This isotope effect is zero at the band origins, increases to a maximum (which amounts to 20 cm^{-1} in the 0″ vibrational level of OH) and approaches zero asymptotically at high rotational quantum numbers. A large electronic isotope effect in Λ-doubling is also observed for OH. This effect, which is zero at the band origin and increases with increasing rotation, amounts to 17 cm^{-1} at $K=25$. It is not correctly accounted for by Van Vleck's equations for Λ-doubling although *ratios* of the Λ-doublets in OH[1] and OH[2] are correctly given, for a case *b* molecule. No noticeable effect was observed on the spacings of the $^2\Sigma$-doublets in the excited state of OH.

IN the conventional treatment of the isotope effect in molecular spectra only vibrational and rotational effects are regarded as significant. Electronic effects have been sought in shifts in the origins of band systems but in the few instances in which some evidence of such a shift has been found the effect has usually amounted to only a few hundredths of a wave number and has been scarcely beyond the limits of experimental error.

Some time ago Johnston and Dawson[1] reported the presence of a large electronic shift (amounting to approximately 10 cm^{-1} in the lines at the head of the (1,0) band) in the spectrum of $O^{16}H^2$ and mentioned that the effect may also be observed, although to a lesser degree, in the spectrum of boron monoxide. This effect results from the influence of atomic mass on the energy of coupling in the $^2\Pi$-terms of these molecules. The spacings of these spin doublets are *wider* for the *heavier* molecules in contrast to the usual isotopic influence on the vibrational and rotational spacings.

We now wish to present this more fully with the additional evidence gained from the analysis of the fine structure[2] of the individual bands of $O^{16}H^2$. We also find a large electronic isotope effect (amounting to 17 cm^{-1} at $K=25$) associated with the separation of the components of the Λ-doublets in the normal state of OH.

The isotopic effects on the spacings of the spin components associated with the $^2\Pi$-electronic terms for BO and for OH, respectively, are plotted in Figs. 1 and 2. The experimental values

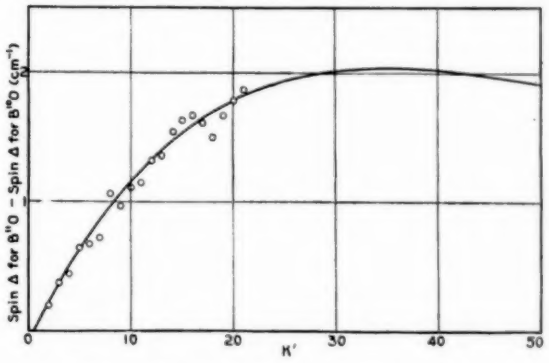

FIG. 1. Isotope effect in the width of the $^2\Pi$-components of BO. Full line, theoretical curve; circles, observed values (computed from the data of Jenkins and McKellar).

* Fellow of the John Simon Guggenheim Memorial Foundation and in residence in the II Physical Institute, Göttingen, Germany, while this material was prepared.

[1] Johnston and Dawson, Naturwiss. **21**, 495 (1933).

[2] Unpublished work of Johnston and Dawson, based on photographs obtained by Dawson with water containing 35 percent heavy hydrogen furnished by Professor G. N. Lewis.

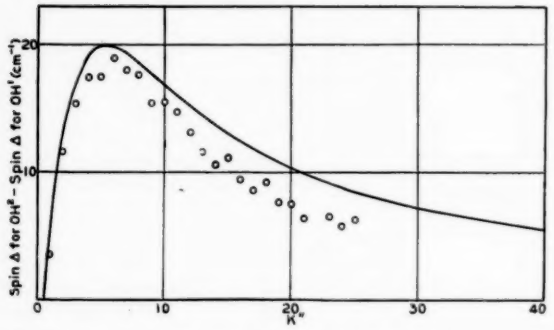

FIG. 2. Isotope effect in the width of the $^2\Pi$-components of OH. Full line, theoretical curve; circles, observed values (unpublished data of Johnston and Dawson).

of the isotope effect, plotted as circles, are calculated from the data of Jenkins and McKellar,[3] for BO, and from the unpublished data of Johnston and Dawson, for $O^{16}H^2$.[4] The continuous curves in Figs. 1 and 2 are the theoretical values for the isotope effect and were constructed through the use of Eq. (9) of Dawson and Johnston,[5] which is a convenient way of expressing the Hill and Van Vleck relationship.[6] Attention is called to the fact that this equation does not accurately reproduce the spin doublet spacing of either isotopic molecule, for either BO or OH, although the disagreement in this respect is much less for BO. Hence the perfect agreement with the experimental values for BO and the near agreement with OH is more than we could have expected. As the curves (together with the theoretical equation) show, the spin doublet isotope effect is zero at the band origin, rises rapidly to a maximum and again approaches zero asymptotically at high quantum numbers.

Figs. 3 and 4 show the presence of the large Λ-coupling electronic isotope effect, in the $^2\Pi_{3/2}$-state (Fig. 3) and in the $^2\Pi_{1/2}$-state (Fig. 4). In these figures the upper curves, with the black circles to represent the experimental data, give the full Λ-widths for $O^{16}H^1$ while the white circles represent the experimental data for $O^{16}H^2$. The experimental points along the upper curves are average values for the (2,0), (1,0) and (0,0) levels while the white circles, as in Fig. 2, are based on the (1,0) band.

Van Vleck[7] gives a theoretical expression for Λ-doubling but his equation fails to fit, for OH, by quite a large factor.[5] It also fails to give the proper *differences* between the Λ-doublets of $O^{16}H^1$ and $O^{16}H^2$. However, we find that Van Vleck's equation for a case "*b*" molecule will give nearly the correct *ratios* of the Λ-doublets, for a common value of the rotational quantum number. This ratio, which reduces to the inverse square of the ratio of the moments of inertia of the isotopic molecules, is about 0.284 for OH.

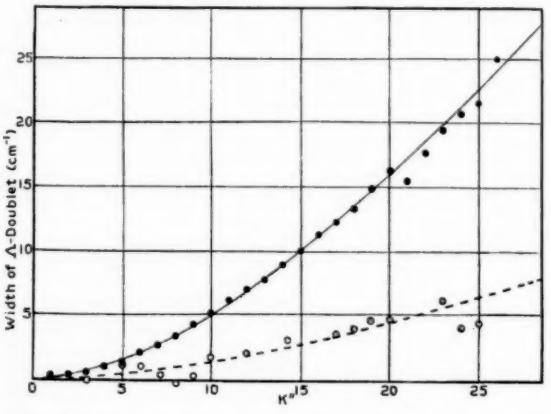

FIG. 3. Isotope effect in the Λ-doublets of the $^2\Pi_{3/2}$-level of OH. Black circles, observed Λ-doublets in $O^{16}H^1$ [averages of the (2,0), (1,0) and (0,0) bands]; full line, smooth curve through the data; open circles, observed Λ-doublets in $O^{16}H^2$ [from the (1,0) band]; dotted line, constructed from the data for $O^{16}H^1$ by using the B_0^2 ratio.

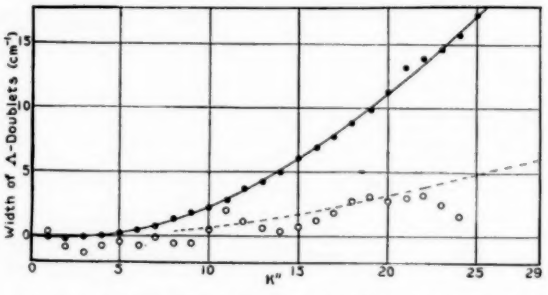

FIG. 4. Isotope effect in the Λ-doublets of the $^2\Pi_{1/2}$-level of OH. Black circles, observed Λ-doublets in $O^{16}H^1$ (averages); full line, smooth curve through the data; open circles, observed Λ-doublets in $O^{16}H^2$ (1′,0″) band; dotted line, constructed from the data for $O^{16}H^1$ by means of the B ratios.

[3] Jenkins and McKellar, Phys. Rev. **42**, 464 (1932).

[4] We employ the data of the (1, 0) band, of OH, because the lines of that band fall in a good region for measurement and are not often obliterated. We have similar data from several other bands which agree well with that from the (1, 0) band.

[5] Dawson and Johnston, Phys. Rev. **43**, 980 (1933).

[6] Hili and Van Vleck, Phys. Rev. **32**, 250 (1928).

[7] Van Vleck, Phys. Rev. **33**, 467 (1929).

The curves with broken lines were constructed from the smoothed data for $O^{16}H^{1}$ (represented in the continuous curves) by reducing the latter by the factor 0.284.

The isotope shifts in the spectrum lines are one-half of the isotope effects on the doublets width since the separate components of the doublets are each shifted nearly symmetrically from their common center of gravity. The shifts in the spectrum lines may be either positive or negative in sign, depending upon the arrangement of the levels involved in the transition.

No appreciable isotope effect was observed in the separation of the components of the $^{2}\Sigma$-level.

The Spectrum of Fluorine, F II, F III, F IV

I. S. BOWEN, *Norman Bridge Laboratory of Physics, California Institute of Technology*

(Received September 27, 1933)

The spectrum of fluorine extending from 125A to 620A has been obtained by using a two-meter grazing-incidence spectrograph. A large number of these lines, including nearly all of the stronger ones, have been classified as transitions in the F II, F III and F IV ions. This has made possible the classification of additional lines measured by Dingle in the longer wave-length regions. These analyses yield the following ionization potentials: F II 34.81 volts, F III 62.35 volts, F IV 87.34 volts.

IN the present investigation new plates of the fluorine spectrum were obtained extending over the range from 125A to 620A. The source was a vacuum spark between hollow aluminum electrodes into which LiF had been fused. The spectrograph was of the grazing-incidence type using a two-meter radius glass grating which was ruled with 960 lines per mm on an engine built and operated by Mr. Julius Pearson of the California Institute shop. The various stages of ionization were partially differentiated by the introduction of self-induction into the spark circuit. Oxygen and aluminum wave-lengths determined by Edlén were used as standards.

The observed lines that it has been possible to classify in the present investigation as transitions between terms of F IV, F III and F II are listed in Tables I, III and V, respectively. Tables II, IV and VI give the term values obtained from the analyses of the spectra of these ions. For the sake of completeness terms located by earlier authors have been included with, however, some minor changes in the absolute values as discussed below. These analyses account for nearly all of the strong extreme ultraviolet lines.

In Table II the values of the triplet terms of F IV were fixed by extrapolating the values of the terms of the s^2p3d configuration from the corresponding terms in C I, N II and O III. The value thus obtained should be correct to a very few thousand frequency units. The singlet terms were somewhat less accurately obtained by an extrapolation of the relative positions of the singlet and triplet terms of the s^2p^2 configuration of these same ions.

TABLE I. *Classified lines of F IV.*

Int.	λ(Vac.)	ν	Classification	Int.	λ(Vac.)	ν	Classification
1	199.763	500593	$s^2p^2\ ^3P_{1,0}-s^2p3d\ ^3P_{0,1}$	4	251.026	398365	$s^2p^2\ ^1D-s^2p3s\ ^1P$
1	199.836	500410	$s^2p^2\ ^3P_1-s^2p3d\ ^3P_1$	3	270.222	370066	$s^2p^2\ ^1S-s^2p3s\ ^1P$
1	199.923	500193	$s^2p^2\ ^3P_1-s^2p3d\ ^3P_2$	6	419.662	238287	$s^2p^2\ ^3P_0-sp^3\ ^3S$
1	199.996	500010	$s^2p^2\ ^3P_2-s^2p3d\ ^3P_1$	7	420.061*	238061	$s^2p^2\ ^3P_1-sp^3\ ^3S$
3	200.086	499785	$s^2p^2\ ^3P_2-s^2p3d\ ^3P_2$	8	420.743*	237675	$s^2p^2\ ^3P_2-sp^3\ ^3S$
2	201.008	497493	$s^2p^2\ ^3P_0-s^2p3d\ ^3D_1$	7	430.742	232158	$s^2p^2\ ^1D-sp^3\ ^1P$
3	201.066	497349	$s^2p^2\ ^3P_1-s^2p3d\ ^3D_2$	4	490.607	203829	$s^2p^2\ ^1S-sp^3\ ^1P$
4	201.160	497117	$s^2p^2\ ^3P_2-s^2p3d\ ^3D_3$	8	491.048	203646	$s^2p^2\ ^1D-sp^3\ ^1D$
1	201.232	496939	$s^2p^2\ ^3P_2-s^2p3d\ ^3D_2$	5	570.643*	175241	$s^2p^2\ ^3P_0-sp^3\ ^3P$
3	239.864	416903	$s^2p^2\ ^3P_1-s^2p3s\ ^3P_2$	7	571.357*	175022	$s^2p^2\ ^3P_1-sp^3\ ^3P$
3	240.016	416639	$s^2p^2\ ^3P_0-s^2p3s\ ^3P_1$	7	572.640*	174630	$s^2p^2\ ^3P_2-sp^3\ ^3P$
5	240.094	416504	$s^2p^2\ ^3P_2-s^2p3s\ ^3P_2$	4	676.06*	147916	$s^2p^2\ ^3P_0-sp^3\ ^3D_1$
2	240.163	416384	$s^2p^2\ ^3P_1-s^2p3s\ ^3P_1$	5	677.17*	147643	$s^2p^2\ ^3P_1-sp^3\ ^3D_2$
3	240.280	416181	$s^2p^2\ ^3P_1-s^2p3s\ ^3P_0$	5	679.19*	147234	$s^2p^2\ ^3P_2-sp^3\ ^3D_3$
3	240.384	416001	$s^2p^2\ ^3P_2-s^2p3s\ ^3P_1$				

* Previously classified by Bowen (reference 2).

TABLE II. *Term values in F IV.*

		$s^2p^2\ ^3P_0$	708000	$sp^3\ ^3D_3$	560154
		$s^2p^2\ ^3P_1$	707774	$sp^3\ ^3D_2$	560101
		$s^2p^2\ ^3P_2$	707388	$sp^3\ ^3D_1$	560084
		$s^2p^2\ ^1D$	683200	$sp^3\ ^3P$	532756
		$s^2p^2\ ^1S$	654881	$sp^3\ ^1D$	479554
				$sp^3\ ^3S$	469713
				$sp^3\ ^1P$	451042
$s^2p3s\ ^3P_0$	291593			$s^2p3d\ ^3D_1$	210507
$s^2p3s\ ^3P_1$	291379			$s^2p3d\ ^3D_2$	210433
$s^2p3s\ ^3P_2$	290878			$s^2p3d\ ^3D_3$	210271
$s^2p3s\ ^1P$	284835			$s^2p3d\ ^3P_2$	207592
				$s^2p3d\ ^3P_1$	207371
				$s^2p3d\ ^3P_0$	207181

In F III, Dingle[1] had classified a large number of lines as transitions between terms arising from the addition of a $3s$, a $3p$ or a $3d$ electron to the ^3P state of the core and Bowen[2] had identified a group of strong lines involving the s^2p^3 and sp^4 configurations. In the present analyses a large number of extreme ultraviolet lines have been identified as transitions to these low levels of the s^2p^3 configuration from the high levels found by Dingle and also from a large group of additional high levels that had not previously been located. Among others, all of the terms caused by the addition of a $3s$, $3p$ or $3d$ electron to the ^1D state of the core were found. The location of these terms made it possible to classify many of the strong unclassified lines in Dingle's list as

TABLE III. *Classified lines in F III.*

Int.	λ(Vac.)	ν	Classification		Int.	λ(Vac.)	ν	Classification	
2	214.788	465575	$s^2p^3\ ^4S$	$-s^2p^2(^3P)5d\ ^4P_{\frac{1}{2}, 1\frac{1}{2}}$	8	656.86*	152239	$s^2p^3\ ^4S$	$-sp^4\ ^4P_{1\frac{1}{2}}$
2	214.857	465426	$s^2p^3\ ^4S$	$-s^2p^2(^3P)5d\ ^4P_{2\frac{1}{2}}$	8	658.34*	151897	$s^2p^3\ ^4S$	$-sp^4\ ^4P_{2\frac{1}{2}}$
3	226.083	442315	$s^2p^3\ ^4S$	$-s^2p^2(^3P)4d\ ^4P_{\frac{1}{2}, 1\frac{1}{2}}$	0	1071.66	93313	$s^2p^2(^3P)3p\ ^4D_{\frac{1}{2}}$	$-s^2p^2(^3P)4d\ ^4P_{1\frac{1}{2}}$
3	226.169	442147	$s^2p^3\ ^4S$	$-s^2p^2(^3P)4d\ ^4P_{2\frac{1}{2}}$	0	1099.10	90984	$s^2p^2(^3P)3p\ ^4P_{1\frac{1}{2}}$	$-s^2p^2(^3P)4d\ ^4P_{1\frac{1}{2}}$
0	243.397	410851	$s^2p^3\ ^2D$	$-s^2p^2(^3P)4d\ ^2D$	0	1101.55	90781	$s^2p^2(^3P)3p\ ^4P_{1\frac{1}{2}, 2\frac{1}{2}}$	$-s^2p^2(^3P)4d\ ^4P_{2\frac{1}{2}, 1\frac{1}{2}}$
3	244.786	408520	$s^2p^3\ ^2D_{2\frac{1}{2}}$	$-s^2p^2(^3P)4d\ ^2F_{3\frac{1}{2}}$	0	1103.64	90609	$s^2p^2(^3P)3p\ ^4P_{2\frac{1}{2}}$	$-s^2p^2(^3P)4d\ ^4P_{2\frac{1}{2}}$
3	245.020	408130	$s^2p^3\ ^2D_{1\frac{1}{2}}$	$-s^2p^2(^3P)4d\ ^2F_{2\frac{1}{2}}$		λ(Air)			
0	245.876	406709	$s^2p^3\ ^2D$	$-s^2p^2(^1D)4s\ ^2D$	$\frac{1}{2}$	2455.81	40707.4	$s^2p^2(^3P)3p\ ^4D_{1\frac{1}{2}}$	$-s^2p^2(^3P)3d\ ^4P_{1\frac{1}{2}}$
4	254.178	393425	$s^2p^3\ ^2P$	$-s^2p^2(^3P)4d\ ^2D$	7	2470.279	40469.02	$s^2p^2(^1D)3s\ ^2D_{2\frac{1}{2}}$	$-s^2p^2(^1D)3p\ ^2P_{1\frac{1}{2}}$
4	255.718	391056	$s^2p^3\ ^4S$	$-s^2p^2(^3P)3d\ ^4P_{\frac{1}{2}}$	2	2470.48	40465.8	$s^2p^2(^1D)3s\ ^2D_{1\frac{1}{2}}$	$-s^2p^2(^1D)3p\ ^2P_{1\frac{1}{2}}$
5	255.775	390969	$s^2p^3\ ^4S$	$-s^2p^2(^3P)3d\ ^4P_{1\frac{1}{2}}$	6	2478.709	40331.40	$s^2p^2(^1D)3s\ ^2D_{1\frac{1}{2}}$	$-s^2p^2(^1D)3p\ ^2P_{\frac{1}{2}}$
6	255.866	390830	$s^2p^3\ ^4S$	$-s^2p^2(^3P)3d\ ^4P_{2\frac{1}{2}}$	0	2492.58	40107.0	$s^2p^2(^3P)3p\ ^4P_{2\frac{1}{2}}$	$-s^2p^2(^3P)3d\ ^2F_{2\frac{1}{2}}$
5	256.358	390079	$s^2p^3\ ^4S$	$-s^2p^2(^3P)3d\ ^4D_{\frac{1}{2}, 1\frac{1}{2}, 2\frac{1}{2}}$	1	2543.4	39305.7	$s^2p^2(^1D)3p\ ^2F_{3\frac{1}{2}}$	$-s^2p^2(^1D)3d\ ^2D_{2\frac{1}{2}}$
1	256.892	389269	$s^2p^3\ ^2P$	$-s^2p^2(^1D)4s\ ^2D$	1	2596.5	38501.9	$s^2p^2(^3P)3p\ ^4P_{\frac{1}{2}}$	$-s^2p^2(^3P)3d\ ^2P_{\frac{1}{2}}$
3	260.312	384154	$s^2p^3\ ^2D_{2\frac{1}{2}}$	$-s^2p^2(^1D)3d\ ^2P_{1\frac{1}{2}}$	0	2602.9	38407.2	$s^2p^2(^3P)3p\ ^4P_{1\frac{1}{2}}$	$-s^2p^2(^3P)3d\ ^2P_{\frac{1}{2}}$
3	260.387	384044	$s^2p^3\ ^2D_{1\frac{1}{2}}$	$-s^2p^2(^1D)3d\ ^2P_{\frac{1}{2}}$	$\frac{1}{2}$	2610.8	38291.0	$s^2p^2(^3P)3p\ ^4P_{\frac{1}{2}}$	$-s^2p^2(^3P)3d\ ^2P_{1\frac{1}{2}}$
2	260.500	383877	$s^2p^3\ ^2D$	$-s^2p^2(^3P)4s\ ^2P$	1	2617.3	38195.9	$s^2p^2(^3P)3p\ ^4P_{1\frac{1}{2}}$	$-s^2p^2(^3P)3d\ ^2P_{1\frac{1}{2}}$
6	261.729	382075	$s^2p^3\ ^2D$	$-s^2p^2(^1D)3d\ ^2D$	7	2625.000	38083.89	$s^2p^2(^1D)3p\ ^2F_{3\frac{1}{2}}$	$-s^2p^2(^1D)3d\ ^2G_{4\frac{1}{2}}$
6	263.809	379062	$s^2p^3\ ^2D$	$-s^2p^2(^1D)3d\ ^2F$	8	2629.686	38016.03	$s^2p^2(^1D)3p\ ^2F_{3\frac{1}{2}}$	$-s^2p^2(^1D)3d\ ^2G_{4\frac{1}{2}}$
3	270.670	369454	$s^2p^3\ ^2P$	$-s^2p^2(^1D)3d\ ^2S$	1	2630.93	37998.1	$s^2p^2(^1D)3p\ ^2D_{2\frac{1}{2}}$	$-s^2p^2(^3D)3d\ ^2P_{1\frac{1}{2}}$
2	272.701	366702	$s^2p^3\ ^2P$	$-s^2p^2(^1D)3d\ ^2P_{1\frac{1}{2}}$	$\frac{1}{2}$	2634.8	37942.2	$s^2p^2(^1D)3p\ ^2D_{1\frac{1}{2}}$	$-s^2p^2(^1D)3d\ ^2P_{1\frac{1}{2}}$
1	272.755	366629	$s^2p^3\ ^2P$	$-s^2p^2(^1D)3d\ ^2P_{\frac{1}{2}}$	4	2639.05	37881.1	$s^2p^2(^1D)3p\ ^2D_{1\frac{1}{2}}$	$-s^2p^2(^1D)3d\ ^2P_{\frac{1}{2}}$
2	272.910	366421	$s^2p^3\ ^2P$	$-s^2p^2(^3P)4s\ ^2P$	0	2645.5	37788.8	$s^2p^2(^3P)3p\ ^4S$	$-s^2p^2(^3P)3d\ ^2D_{1\frac{1}{2}}$
4	274.254	364625	$s^2p^3\ ^2P$	$-s^2p^2(^1D)3d\ ^2D$	2	2727.93	36646.9	$s^2p^2(^1D)3p\ ^2P_{\frac{1}{2}}$	$-s^2p^2(^1D)3d\ ^2S$
4	276.776	361303	$s^2p^3\ ^2D_{2\frac{1}{2}}$	$-s^2p^2(^3P)3d\ ^2D_{2\frac{1}{2}}$	4	2737.954	36512.84	$s^2p^2(^1D)3p\ ^2P_{1\frac{1}{2}}$	$-s^2p^2(^1D)3d\ ^2S$
3	276.887	361158	$s^2p^3\ ^2D_{1\frac{1}{2}}$	$-s^2p^2(^3P)3d\ ^2D_{1\frac{1}{2}}$	5	2747.870	36381.08	$s^2p^2(^1D)3p\ ^2F_{3\frac{1}{2}}$	$-s^2p^2(^1D)3d\ ^2F_{3\frac{1}{2}}$
7	279.685	357545	$s^2p^3\ ^2D_{2\frac{1}{2}}$	$-s^2p^2\ (^3P)3d\ ^2F_{3\frac{1}{2}}$	1	2751.8	36329.1	$s^2p^2(^1D)3p\ ^2F_{2\frac{1}{2}}$	$-s^2p^2(^1D)3d\ ^2F_{2\frac{1}{2}}$
7	280.002	357140	$s^2p^3\ ^2D_{1\frac{1}{2}}$	$-s^2p^2(^3P)3d\ ^2F_{2\frac{1}{2}}$	1	2752.8	36315.9	$s^2p^2(^1D)3p\ ^2F_{3\frac{1}{2}}$	$-s^2p^2(^1D)3d\ ^2F_{3\frac{1}{2}}$
1	280.804	356120	$s^2p^3\ ^2D_{2\frac{1}{2}}$	$-s^2p^2(^3P)3d\ ^4D_{3\frac{1}{2}}$	4	2755.307	36282.89	$s^2p^2(^1D)3s\ ^2D_{2\frac{1}{2}}$	$-s^2p^2(^1D)3p\ ^2D_{1\frac{1}{2}}$
1	280.897	356002	$s^2p^3\ ^2D$	$-s^2p^2(^3P)3d\ ^4D_{\frac{1}{2}, 1\frac{1}{2}, 2\frac{1}{2}}$	7	2755.556	36279.61	$s^2p^2(^1D)3s\ ^2D_{1\frac{1}{2}}$	$-s^2p^2(^1D)3p\ ^2D_{1\frac{1}{2}}$
2	281.199	355620	$s^2p^3\ ^2D_{1\frac{1}{2}}$	$-s^2p^2(^3P)3d\ ^2P_{\frac{1}{2}}$	5	2756.664	36265.02	$s^2p^2(^1D)3p\ ^2F_{3\frac{1}{2}}$	$-s^2p^2(^1D)3d\ ^2F_{3\frac{1}{2}}$
3	281.343	355438	$s^2p^3\ ^2D_{2\frac{1}{2}}$	$-s^2p^2(^3P)3d\ ^2P_{1\frac{1}{2}}$	10	2759.589	36226.60	$s^2p^2(^1D)3s\ ^2D_{2\frac{1}{2}}$	$-s^2p^2(^1D)3p\ ^2D_{2\frac{1}{2}}$
4	290.838	343834	$s^2p^3\ ^2P$	$-s^2p^2(^3P)3d\ ^2D_{2\frac{1}{2}}$	3	2759.81	36223.7	$s^2p^2(^1D)3s\ ^2D_{1\frac{1}{2}}$	$-s^2p^2(^1D)3d\ ^2D_{2\frac{1}{2}}$
3	290.941	343712	$s^2p^3\ ^2P$	$-s^2p^2(^3P)3d\ ^2D_{1\frac{1}{2}}$	4	2781.956	35935.35	$s^2p^2(^1D)3p\ ^2D_{2\frac{1}{2}}$	$-s^2p^2(^1D)3d\ ^2D_{2\frac{1}{2}}$
1	295.366	338563	$s^2p^3\ ^2P$	$-s^2p^2(^3P)3d\ ^4D_{\frac{1}{2}, 1\frac{1}{2}, 2\frac{1}{2}}$	$1\frac{1}{2}$	2949.91	33889.5	$s^2p^2(^1D)3p\ ^2P_{\frac{1}{2}}$	$-s^2p^2(^1D)3d\ ^2P_{1\frac{1}{2}}$
3	295.708	338171	$s^2p^3\ ^2P$	$-s^2p^2(^3P)3d\ ^2P_{\frac{1}{2}}$	2	2955.13	33829.6	$s^2p^2(^1D)3p\ ^2P_{\frac{1}{2}}$	$-s^2p^2(^1D)3d\ ^2P_{\frac{1}{2}}$
3	295.880	337975	$s^2p^3\ ^2P$	$-s^2p^2(^3P)3d\ ^2P_{1\frac{1}{2}}$	2	2959.666	33777.76	$s^2p^2(^3P)3p\ ^4S$	$-s^2p^2(^3P)3d\ ^2F_{2\frac{1}{2}}$
8	315.227	317232	$s^2p^3\ ^4S$	$-s^2p^2(^3P)3s\ ^4P_{2\frac{1}{2}}$	5	2961.596	33755.74	$s^2p^2(^1D)3p\ ^2P_{1\frac{1}{2}}$	$-s^2p^2(^1D)3d\ ^2P_{1\frac{1}{2}}$
7	315.545	316912	$s^2p^3\ ^4S$	$-s^2p^2(^3P)3s\ ^4P_{1\frac{1}{2}}$	1	2966.89	33695.5	$s^2p^2(^1D)3p\ ^2P_{1\frac{1}{2}}$	$-s^2p^2(^1D)3d\ ^2P_{\frac{1}{2}}$
6	315.759	316697	$s^2p^3\ ^4S$	$-s^2p^2(^3P)3s\ ^4P_{\frac{1}{2}}$	$1\frac{1}{2}$	3034.54	32944.3	$s^2p^2(^1D)3p\ ^2D_{2\frac{1}{2}}$	$-s^2p^2(^1D)3d\ ^2F_{2\frac{1}{2}}$
7D	322.657	309927	$s^2p^3\ ^2D$	$-s^2p^2(^1D)3s\ ^2D$	7	3039.254	32893.26	$s^2p^2(^1D)3p\ ^2D_{2\frac{1}{2}}$	$-s^2p^2(^1D)3d\ ^2F_{3\frac{1}{2}}$
4	341.926	292461	$s^2p^3\ ^2P$	$-s^2p^2(^1D)3s\ ^2D$	6	3039.746	32887.94	$s^2p^2(^1D)3p\ ^2D_{1\frac{1}{2}}$	$-s^2p^2(^1D)3d\ ^2F_{2\frac{1}{2}}$
5	343.895	290786	$s^2p^3\ ^2D_{2\frac{1}{2}}$	$-s^2p^2(^3P)3s\ ^2P_{1\frac{1}{2}}$	10	3042.808	32854.85	$s^2p^2(^1D)3s\ ^2D_{2\frac{1}{2}}$	$-s^2p^2(^1D)3p\ ^2F_{3\frac{1}{2}}$
4	344.387	290371	$s^2p^3\ ^2D_{1\frac{1}{2}}$	$-s^2p^2(^3P)3s\ ^2P_{\frac{1}{2}}$	2	3048.80	32790.3	$s^2p^2(^1D)3s\ ^2D_{2\frac{1}{2}}$	$-s^2p^2(^1D)3p\ ^2F_{2\frac{1}{2}}$
5	365.864	273326	$s^2p^3\ ^2P$	$-s^2p^2(^3P)3s\ ^2P_{1\frac{1}{2}}$	8	3049.139	32786.64	$s^2p^2(^1D)3s\ ^2D_{1\frac{1}{2}}$	$-s^2p^2(^1D)3p\ ^2F_{2\frac{1}{2}}$
4	366.384	272938	$s^2p^3\ ^2P$	$-s^2p^2(^3P)3s\ ^2P_{\frac{1}{2}}$	4	3154.387	31692.74	$s^2p^2(^1D)3p\ ^2P_{1\frac{1}{2}}$	$-s^2p^2(^1D)3d\ ^2D_{2\frac{1}{2}}$
9	429.496*	232831	$s^2p^3\ ^2D_{1\frac{1}{2}}$	$-sp^4\ ^2P_{\frac{1}{2}}$	1	3357.82	29772.7	$s^2p^2(^3P)3p\ ^2P_{\frac{1}{2}}$	$-s^2p^2(^3P)3d\ ^4D_{\frac{1}{2}}$
10D	430.173*	232465	$s^2p^3\ ^2D_{1\frac{1}{2}, 2\frac{1}{2}}$	$-sp^4\ ^2P_{1\frac{1}{2}}$	1	3367.65	29685.8	$s^2p^2(^3P)3p\ ^2P_{1\frac{1}{2}}$	$-s^2p^2(^3P)3d\ ^4D_{\frac{1}{2}}$
6	464.302*	215377	$s^2p^3\ ^2P$	$-sp^4\ ^2P_{\frac{1}{2}}$	1	3372.24	29645.3	$s^2p^2(^3P)3p\ ^2P_{1\frac{1}{2}}$	$-s^2p^2(^3P)3d\ ^4D_{1\frac{1}{2}}$
8	465.132*	214993	$s^2p^3\ ^2P$	$-sp^4\ ^2P_{1\frac{1}{2}}$	2	3401.62	29389.4	$s^2p^2(^3P)3p\ ^2P_{\frac{1}{2}}$	$-s^2p^2(^3P)3d\ ^2P_{\frac{1}{2}}$
10D	567.712*	176146	$s^2p^3\ ^2D$	$-sp^4\ ^2D$	3	3411.66	29302.8	$s^2p^2(^3P)3p\ ^2P_{1\frac{1}{2}}$	$-s^2p^2(^3P)3d\ ^2P_{\frac{1}{2}}$
4	630.17*	158687	$s^2p^3\ ^2P$	$-sp^4\ ^2D$	2	3426.34	29177.3	$s^2p^2(^3P)3p\ ^2P_{\frac{1}{2}}$	$-s^2p^2(^3P)3d\ ^2P_{1\frac{1}{2}}$
7	656.10*	152416	$s^2p^3\ ^4S$	$-sp^4\ ^4P_{\frac{1}{2}}$	4	3436.57	29090.5	$s^2p^2(^3P)3p\ ^2P_{1\frac{1}{2}}$	$-s^2p^2(^1P)3d\ ^2P_{1\frac{1}{2}}$

* Previously classified by Bowen (reference 2). Wave-lengths above 2000A are taken from Dingle's list of unclassified lines (references 1 and 3).

[1] H. Dingle, Proc. Roy. Soc. **A122**, 144 (1929).

[2] I. S. Bowen, Phys. Rev. **29**, 245 (1927).

TABLE IV. *Term values in F III.*

		$s^2p^3\ ^4S$	505404	$sp^4\ ^4P_{2\frac{1}{2}}$	353507
		$s^2p^3\ ^2D_{2\frac{1}{2}}$	471329	$sp^4\ ^4P_{1\frac{1}{2}}$	353165
		$s^2p^3\ ^2D_{1\frac{1}{2}}$	471298	$sp^4\ ^4P_{\frac{1}{2}}$	352988
		$s^2p^3\ ^2P$	453857	$sp^4\ ^2D$	295169
				$sp^4\ ^2P_{1\frac{1}{2}}$	238864
				$sp^4\ ^2P_{\frac{1}{2}}$	238474
$s^2p^2(^3P)3s\ ^4P_{\frac{1}{2}}$	188702.7	$s^2p^2(^3P)3p\ ^2S$	160971.6	$s^2p^2(^3P)3d\ ^4F_{1\frac{1}{2}}$	118152.7
$s^2p^2(^3P)3s\ ^4P_{1\frac{1}{2}}$	188491.4	$s^2p^2(^3P)3p\ ^4D_{\frac{1}{2}}$	156709.5	$s^2p^2(^3P)3d\ ^4F_{2\frac{1}{2}}$	118043.8
$s^2p^2(^3P)3s\ ^4P_{2\frac{1}{2}}$	188172.5	$s^2p^2(^3P)3p\ ^4D_{1\frac{1}{2}}$	156594.6	$s^2p^2(^3P)3d\ ^4F_{3\frac{1}{2}}$	117888.2
$s^2p^2(^3P)3s\ ^2P_{\frac{1}{2}}$	180920.1	$s^2p^2(^3P)3p\ ^4D_{2\frac{1}{2}}$	156404.9	$s^2p^2(^3P)3d\ ^4F_{4\frac{1}{2}}$	117684.5
$s^2p^2(^3P)3s\ ^2P_{1\frac{1}{2}}$	180535.6	$s^2p^2(^3P)3p\ ^4D_{3\frac{1}{2}}$	156146.0	$s^2p^2(^3P)3d\ ^2P_{1\frac{1}{2}}$	115886.5
$s^2p^2(^1D)3s\ ^2D_{2\frac{1}{2}}$	161393.8	$s^2p^2(^3P)3p\ ^4P_{\frac{1}{2}}$	154175.9	$s^2p^2(^3P)3d\ ^2P_{\frac{1}{2}}$	115674.3
$s^2p^2(^1D)3s\ ^2D_{1\frac{1}{2}}$	161390.5	$s^2p^2(^3P)3p\ ^4P_{1\frac{1}{2}}$	154081.6	$s^2p^2(^3P)3d\ ^4D_{2\frac{1}{2}}$	115334.3
		$s^2p^2(^3P)3p\ ^4P_{2\frac{1}{2}}$	153892.9	$s^2p^2(^3P)3d\ ^4D_{1\frac{1}{2}}$	115331.7
		$s^2p^2(^3P)3p\ ^2D_{1\frac{1}{2}}$	149430.4	$s^2p^2(^3P)3d\ ^4D_{\frac{1}{2}}$	115291.6
		$s^2p^2(^3P)3p\ ^2D_{2\frac{1}{2}}$	149040.0	$s^2p^2(^3P)3d\ ^4D_{3\frac{1}{2}}$	115201.6
		$s^2p^2(^3P)3p\ ^4S$	147933.0	$s^2p^2(^3P)3d\ ^4P_{2\frac{1}{2}}$	114577.7
		$s^2p^2(^3P)3p\ ^2P_{\frac{1}{2}}$	145063.8	$s^2p^2(^3P)3d\ ^4P_{1\frac{1}{2}}$	114436.0
		$s^2p^2(^3P)3p\ ^2P_{1\frac{1}{2}}$	144976.9	$s^2p^2(^3P)3d\ ^4P_{\frac{1}{2}}$	114364.8
		$s^2p^2(^1D)3p\ ^2F_{2\frac{1}{2}}$	128603.8	$s^2p^2(^3P)3d\ ^2F_{2\frac{1}{2}}$	114154.4
		$s^2p^2(^1D)3p\ ^2F_{3\frac{1}{2}}$	128539.0	$s^2p^2(^3P)3d\ ^2F_{3\frac{1}{2}}$	113784.5
		$s^2p^2(^1D)3p\ ^2D_{2\frac{1}{2}}$	125167.1	$s^2p^2(^3P)3d\ ^2D_{1\frac{1}{2}}$	110143.9
		$s^2p^2(^1D)3p\ ^2D_{1\frac{1}{2}}$	125110.9	$s^2p^2(^3P)3d\ ^2D_{2\frac{1}{2}}$	110025.9
		$s^2p^2(^1D)3p\ ^2P_{\frac{1}{2}}$	121059.1	$s^2p^2(^1D)3d\ ^2F_{3\frac{1}{2}}$	92273.9
		$s^2p^2(^1D)3p\ ^2P_{1\frac{1}{2}}$	120924.8	$s^2p^2(^1D)3d\ ^2F_{2\frac{1}{2}}$	92222.9
				$s^2p^2(^1D)3d\ ^2G_{4\frac{1}{2}}$	90523.0
				$s^2p^2(^1D)3d\ ^2G_{3\frac{1}{2}}$	90519.9
				$s^2p^2(^1D)3d\ ^2D_{2\frac{1}{2}}$	89231.9
				$s^2p^2(^1D)3d\ ^2P_{\frac{1}{2}}$	87229.4
				$s^2p^2(^1D)3d\ ^2P_{1\frac{1}{2}}$	87169.1
				$s^2p^2(^1D)3d\ ^2S$	84412.1
$s^2p^2(^3P)4s\ ^2P$	87436			$s^2p^2(^3P)4d\ ^4P_{2\frac{1}{2}}$	63284
$s^2p^2(^1D)4s\ ^2D$	64596			$s^2p^2(^3P)4d\ ^2F_{2\frac{1}{2}}$	63168
				$s^2p^2(^3P)4d\ ^4P_{1\frac{1}{2}}$	63095
				$s^2p^2(^3P)4d\ ^2F_{3\frac{1}{2}}$	62809
				$s^2p^2(^3P)4d\ ^2D$	60447
				$s^2p^2(^3P)5d\ ^4P_{2\frac{1}{2}}$	39978
				$s^2p^2(^3P)5d\ ^4P_{1\frac{1}{2},\frac{1}{2}}$	39829

TABLE V. *Classified lines in F II.*

Int.	λ(Vac.)	ν	Classification	Int.	λ(Vac.)	ν	Classification
0	353.452	282924	$s^2p^4\ ^3P_2 - s^2p^3(^2P)3d\ ^3P_2$	3	436.288	229206	$s^2p^4\ ^3P_1 - s^2p^3(^2P)3s\ ^3P$
2	375.300	266454	$s^2p^4\ ^3P_2 - s^2p^3(^2D)3d\ ^3P_2$	1	436.578	229054	$s^2p^4\ ^3P_0 - s^2p^3(^2P)3s\ ^3P$
1	375.434	266358	$s^2p^4\ ^3P_2 - s^2p^3(^2D)3d\ ^3S$	6	457.183	218731	$s^2p^4\ ^1D - sp^5\ ^1P$
1	375.718	266157	$s^2p^4\ ^3P_1 - s^2p^3(^2D)3d\ ^3P_{0,1}$	6	471.990	211869	$s^2p^4\ ^3P_2 - s^2p^3(^2D)3s\ ^3D_3$
1	375.793	266104	$s^2p^4\ ^3P_1 - s^2p^3(^2D)3d\ ^3P_2$	5	472.710	211546	$s^2p^4\ ^3P_1 - s^2p^3(^2D)3s\ ^3D_2$
1*D*	375.928	266008	$s^2p^4\ ^3P_{1,0} - s^2p^3(^2D)3d\ ^3S, P_1$	3	473.021	211407	$s^2p^4\ ^3P_0 - s^2p^3(^2D)3s\ ^3D_1$
1	376.686	265473	$s^2p^4\ ^3P_2 - s^2p^3(^2D)3d\ ^3D_3$	8	484.650	206334	$s^2p^4\ ^1D - s^2p^3(^2P)3s\ ^1P$
0	377.140	265154	$s^2p^4\ ^3P_1 - s^2p^3(^2D)3d\ ^3D_2$	4	513.637	194690	$s^2p^4\ ^1S - sp^5\ ^1P$
2	380.902	262535	$s^2p^4\ ^1D - s^2p^3(^2P)3d\ ^1D$	6	514.942	194197	$s^2p^4\ ^1D - s^2p^3(^2D)3s\ ^1D$
1	393.664	254024	$s^2p^4\ ^3P_2 - s^2p^3(^4S)4d\ ^3D$	6	546.846*	182867	$s^2p^4\ ^3P_2 - s^2p^3(^4S)3s\ ^3S$
0	394.194	253682	$s^2p^4\ ^3P_1 - s^2p^3(^4S)4d\ ^3D$	4	547.873*	182524	$s^2p^4\ ^3P_1 - s^2p^3(^4S)3s\ ^3S$
1	400.579	249639	$s^2p^4\ ^1D - s^2p^3(^2D)4s\ ^1D$	3	548.324*	182374	$s^2p^4\ ^3P_0 - s^2p^3(^4S)3s\ ^3S$
4	405.644	246522	$s^2p^4\ ^1D - s^2p^3(^2D)3d\ ^1F$	3	548.511	182312	$s^2p^4\ ^1S - s^2p^3(^2P)3s\ ^1P$
5	407.053	245668	$s^2p^4\ ^1D - s^2p^3(^2D)3d\ ^1P$	8	605.67*	165106	$s^2p^4\ ^3P_2 - sp^5\ ^3P_1$
4	407.511	245392	$s^2p^4\ ^1D - s^2p^3(^2D)3d\ ^1D$	7	606.27*	164943	$s^2p^4\ ^3P_1 - sp^5\ ^3P_0$
1	417.891	239297	$s^2p^4\ ^1S - s^2p^3(^2P)3d\ ^1P$	9	606.81*	164796	$s^2p^4\ ^3P_2 - sp^5\ ^3P_2$
1	422.012	236960	$s^2p^4\ ^3P_2 - s^2p^3(^4S)4s\ ^3S$	4	606.95*	164758	$s^2p^4\ ^3P_1 - sp^5\ ^3P_1$
0	422.650	236602	$s^2p^4\ ^3P_1 - s^2p^3(^4S)4s\ ^3S$	7	607.48*	164614	$s^2p^4\ ^3P_0 - sp^5\ ^3P_1$
5	430.905	232070	$s^2p^4\ ^3P_2 - s^2p^3(^4S)3d\ ^3D_3$	8	608.06*	164457	$s^2p^4\ ^3P_1 - sp^5\ ^3P_2$
5	431.541	231728	$s^2p^4\ ^3P_1 - s^2p^3(^4S)3d\ ^3D_2$		λ(Air)		
3	431.812	231582	$s^2p^4\ ^3P_0 - s^2p^3(^4S)3d\ ^3D_1$	4	3739.60	26733.2	$sp^5\ ^1P - s^2p^3(^2P)3p\ ^1D$
4	435.640	229547	$s^2p^4\ ^3P_2 - s^2p^3(^2P)3s\ ^3P$	6	4083.919	24479.39	$s^2p^3(^2P)3p\ ^1P - s^2p^3(^2P)3d\ ^1D$
				2	5173.16	19325.2	$sp^5\ ^1P - s^2p^3(^2P)3p\ ^1P$

* Previously classified by Bowen (reference 2). Wave-lengths above 2000A are taken from Dingle's list of unclassified lines (reference 3).

TABLE VI. *Term values in F II.*

		$s^2p^4\ ^3P_2$	282193	$sp^5\ ^3P_2$	117395
		$s^2p^4\ ^3P_1$	281850	$sp^5\ ^3P_1$	117089
		$s^2p^4\ ^3P_0$	281701	$sp^5\ ^3P_0$	116907
		$s^2p^4\ ^1D$	260393	$sp^5\ ^1P$	41668.4
		$s^2p^4\ ^1S$	236355		
$s^2p^3(^4S)3s\ ^5S$	105536.00	$s^2p^3(^4S)3p\ ^5P_1$	79580.55	$s^2p^3(^4S)3d\ ^5D_4$	51032.12
$s^2p^3(^4S)3s\ ^3S$	99325.0	$s^2p^3(^4S)3p\ ^5P_2$	79569.22	$s^2p^3(^4S)3d\ ^5D_3$	51031.21
$s^2p^3(^2D)3s\ ^3D_3$	70323.58	$s^2p^3(^4S)3p\ ^5P_3$	79549.67	$s^2p^3(^4S)3d\ ^5D_2$	51030.01
$s^2p^3(^2D)3s\ ^3D_2$	70302.51	$s^2p^3(^4S)3p\ ^3P_1$	74490.29	$s^2p^3(^4S)3d\ ^5D_1$	51029.33
$s^2p^3(^2D)3s\ ^3D_1$	70289.48	$s^2p^3(^4S)3p\ ^3P_0$	74487.29	$s^2p^3(^4S)3d\ ^5D_0$	51028.81
$s^2p^3(^2D)3s\ ^1D$	66200.4	$s^2p^3(^4S)3p\ ^3P_2$	74485.59	$s^2p^3(^4S)3d\ ^3D_1$	50126.02
$s^2p^3(^2P)3s\ ^1P$	54045.2	$s^2p^3(^2D)3p\ ^3D_1$	46019.85	$s^2p^3(^4S)3d\ ^3D_2$	50125.22
$s^2p^3(^2P)3s\ ^3P_2$	52648.37	$s^2p^3(^2D)3p\ ^3D_2$	46017.13	$s^2p^3(^4S)3d\ ^3D_3$	50123.14
$s^2p^3(^2P)3s\ ^3P_1$	52646.76	$s^2p^3(^2D)3p\ ^3D_3$	45994.63	$s^2p^3(^2D)3d\ ^3G$	17695.5
$s^2p^3(^2P)3s\ ^3P_0$	52644.10	$s^2p^3(^2D)3p\ ^1F$	45627.1	$s^2p^3(^2D)3d\ ^3F_2$	17237.08
		$s^2p^3(^2D)3p\ ^3F_4$	44682.29	$s^2p^3(^2D)3d\ ^3F_3$	17231.57
		$s^2p^3(^2D)3p\ ^3F_3$	44681.48	$s^2p^3(^2D)3d\ ^3F_4$	17224.29
		$s^2p^3(^2D)3p\ ^3F_2$	44680.83	$s^2p^3(^2D)3d\ ^3D_3$	16717.50
		$s^2p^3(^2D)3p\ ^1P$	42946.6	$s^2p^3(^2D)3d\ ^3D_2$	16691.46
		$s^2p^3(^2D)3p\ ^3P_2$	42097.10	$s^2p^3(^2D)3d\ ^3D_1$	16673.06
		$s^2p^3(^2D)3p\ ^3P_1$	42036.86	$s^2p^3(^2D)3d\ ^3S$	15829.51
		$s^2p^3(^2D)3p\ ^3P_0$	42010.29	$s^2p^3(^2D)3d\ ^3P_2$	15735.93
		$s^2p^3(^2D)3p\ ^1D$	34986.3	$s^2p^3(^2D)3d\ ^3P_1$	15691.08
		$s^2p^3(^2P)3p\ ^3S$	28886.0	$s^2p^3(^2D)3d\ ^3P_0$	15673.85
		$s^2p^3(^2P)3p\ ^3D_3$	27496.90	$s^2p^3(^2D)3d\ ^1D$	15000.0
		$s^2p^3(^2P)3p\ ^3D_2$	27481.84	$s^2p^3(^2D)3d\ ^1P$	14721.5
		$s^2p^3(^2P)3p\ ^3D_1$	27475.24	$s^2p^3(^2D)3d\ ^1F$	13869.9
		$s^2p^3(^2P)3p\ ^1S$	25667.4	$s^2p^3(^2P)3d\ ^3F$	4111.4
		$s^2p^3(^2P)3p\ ^3P_0$	24945.3	$s^2p^3(^2P)3d\ ^3P_0$	−697.8
		$s^2p^3(^2P)3p\ ^3P_1$	24930.4	$s^2p^3(^2P)3d\ ^3P_1$	−714.2
		$s^2p^3(^2P)3p\ ^3P_2$	24906.5	$s^2p^3(^2P)3d\ ^3P_2$	−748.7
		$s^2p^3(^2P)3p\ ^1P$	22343.4	$s^2p^3(^2P)3d\ ^1D$	−2136.0
		$s^2p^3(^2P)3p\ ^1D$	14935.0	$s^2p^3(^2P)3d\ ^1P$	−2951.4
				$s^2p^3(^2P)3d\ ^3D_3$	−4502.7
				$s^2p^3(^2P)3d\ ^3D_2$	−4507.4
				$s^2p^3(^2P)3d\ ^3D_1$	−4508.1
$s^2p^3(^4S)4s\ ^5S$	46879.05			$s^2p^3(^4S)3d\ ^3D$	28169.
$s^2p^3(^4S)4s\ ^3S$	45228.57				
$s^2p^3(^2D)4s\ ^1D$	10761.8			$s^2p^3(^4S)4f\ ^3F$	27642.9
				$s^2p^3(^4S)4f\ ^5F$	27487.1

transitions between them. As in several cases these high terms included two or three members of a series, it was possible to fix the absolute values of the terms with a much greater accuracy than had hitherto been possible. Furthermore, the identification of fourteen intercombination lines made it possible to fix the relative positions of the doublets and quartets. These results called for a shift of +6300 frequency units in Dingle's quartet term values and of +5534.5 units in his doublets. The relative positions of the terms based on the ^1D and on the ^3P term of the core may be in error by as much as ten frequency units as the only connections between them involve lines of about 300A wave-length.

For the sake of completeness the term values found by Dingle, corrected as mentioned above, are included in Table IV. The positions of the $s^2p^2(^3P)3d\,^2P$ terms, tentatively fixed by Dingle on rather meager evidence, were not confirmed by lines connecting them with the ^2P and ^2D states of the s^2p^3 configuration. The extreme ultraviolet lines, listed in Table III, point to another position, namely that indicated in Table IV. Unfortunately the lines that should connect the terms in this new position with $s^2p^2(^3P)3p\ ^2P$ fall outside the range of the Table of F III lines given by Dingle. In his Table of F II lines,[3] however, there are a group of four lines, listed at the end of Table III of this article, at exactly the right position and having the correct relative intensity. The separation of the $s^2p^2(^3P)3d\ ^2P$ terms found in this way is the same as that adopted by Dingle, thus indicating that his identifications of $s^2p^2(^3P)3p\ ^2S - s^2p^2(^3P)3d\ ^2P$ were correct but those of

[3] H. Dingle, Proc. Roy. Soc. **A128**, 600 (1930).

$s^2p^2(^3P)3s\ ^2P - s^2p^2(^3P)3p\ ^2S$ were not. If this rearrangement is valid the latter lines should fall in the green where they may have failed to appear because of lack of plate sensitivity. The new arrangement is supported by the fact that it makes the relative position of the terms of both the $s^2p^2(^3P)3p$ and $s^2p^2(^3P)3d$ configurations very similar to that of the corresponding terms in O II.

Dingle[3] has also classified a large number of visible and near ultraviolet lines in F II. By utilizing the present data it has been possible to identify many of the extreme ultraviolet lines as transitions between high level terms, including those found by Dingle and the terms of the s^2p^4 configuration. These new lines connect all of Dingle's triplet levels together and also all of his singlet levels, although no intercombinations between the two systems have been found. These connections and other relationships in the newly identified lines indicate that Dingle's levels should be shifted as follows: triplets of families A and B should be increased by $+2000$ cm^{-1}, of family C by $+2530$ cm^{-1}; singlets of family B by $+1000$ cm^{-1}, and of family C by $+3610$ cm^{-1}. The quintets remain unchanged. One or two minor changes in Dingle's identification of lines were made on the basis of additional evidence now available. Table VI includes all levels that have been fixed, those taken from Dingle's list being shifted as indicated above.

These analyses indicate that the ionization potential of F II is 34.81 volts, of F III, 62.35 volts and of F IV, 87.34 volts.

The Effect of Crystalline Electric Fields on the Paramagnetic Susceptibility of Cupric Salts

O. M. JORDAHL, *Department of Physics, University of Wisconsin*

(Received December 6, 1933)

The paramagnetic susceptibility of the cupric ion in the hexahydrate sulphates $Cu(NH_4)_2(SO_4)_2 : 6H_2O$ and $CuK_2(SO_4)_2 : 6H_2O$ has been computed on the assumption that the crystalline field has monoclinic symmetry but deviates only slightly from cubic symmetry. The computed variation of the *magnitudes* of the principal susceptibilities with temperature agrees with the data over the limited range of experimental measurements. The mean susceptibility should follow quite closely the simple formula $\chi = A/T + B$, even if the individual susceptibilities do not. This agrees very well with the observations of de Haas and Gorter on the mean susceptibility of $CuSO_4 : 5H_2O$ for the temperature range 14°K to 290°K. In a rhombic field, such as was previously used by Schlapp and Penney for calculations on Co^{++} and Ni^{++}, the directions of the principal magnetic axes are independent of temperature, while the more general monoclinic field gives a rotation of the magnetic axes as the temperature is varied. The calculated variation of the *direction* of the principal axes with temperature in Cu^{++} is in qualitative accord with the observations of Bartlett, but the numerical agreement is not very good. The introduction of an exceedingly asymmetrical diamagnetic correction greatly improves the agreement for the potassium salt, but more likely, the large rotations observed by Bartlett are due to allotropic changes, since the temperature range is not far below the temperatures at which dehydration and decomposition take place. From the choice of parameters which give agreement with the magnetic data, conclusions are drawn about the structures of these crystals.

INTRODUCTION

THE paramagnetic susceptibility of the ions of the iron group has recently received considerable theoretical attention. The general theory of the quenching of the magnetic contribution of the orbit by crystalline fields of the Bethe-Kramers type has been outlined by Van Vleck in his recent book,[1] confirming the hypothesis of Stoner and Bose. Detailed calculations have been carried out for Co, Ni and Cr by Schlapp and Penney[2] with very good results. This paper gives the results of calculations on Cu. Schlapp and Penney assumed that the potential field in the crystal could be represented by a predominant field of cubic symmetry upon which was superposed a small field of rhombic symmetry. The axes of the two fields were assumed to coincide so that the resulting field had rhombic symmetry. Our procedure is more general as we assume the axes of the rhombic field to be rotated about the common z-axis through an angle α away from the axes of the cubic field. This gives a resultant field of monoclinic symmetry which agrees better with the crystallographic symmetry, and allows the principal magnetic axes to vary in direction with temperature.

The assumed Hamiltonian is therefore:

$$H = D(x^4+y^4+z^4) + \{Ax'^2+By'^2-(A+B)z'^2\} + A'(\mathbf{L}\cdot\mathbf{S}) + \beta\mathfrak{H}\cdot(\mathbf{L}+2\mathbf{S}). \quad (1)$$

The first two terms are respectively the contributions of the cubic and rhombic fields, the respective axes being orientated so that $\cos(x, x') = \cos(y, y') = \cos\alpha$, and $\cos(z, z') = 1$. These two terms will be designated as the cubic and rhombic terms. The third term is the orbit-spin interaction and the last is the Zeeman term due to the external magnetic field $\mathfrak{H}$. Also, β is the Bohr magneton $eh/4\pi mc$, and A' is the orbit-spin coupling coefficient which, according to Laporte,[3] has the value -852 cm^{-1} for Cu^{++}. $\mathbf{L}$ and

[1] J. H. Van Vleck, *Electric and Magnetic Susceptibilities*, Oxford Press (1932). See especially Chapter XI.

[2] R. Schlapp and W. G. Penney, Phys. Rev. **42**, 666 (1932). For Co, Ni and Cr, as well as for Cu, the affix $^{++}$ is to be understood whenever the ion is mentioned.

[3] O. Laporte, Zeits. f. Physik **47**, 761 (1928). He gives the multiplet separation of the lowest term as 2130 cm^{-1}, which gives A' the value -852 cm^{-1}.

S are angular momentum vectors associated with the quantum numbers L and S of the orbit and spin, which have the values 2 and $\frac{1}{2}$, respectively. The rhombic term of the Hamiltonian may be expressed as follows in terms of the axes of the cubic field and the angle α:

$$(A\cos^2\alpha+B\sin^2\alpha)x^2+(A\sin^2\alpha+B\cos^2\alpha)y^2 -(A+B)z^2+(A-B)xy\sin 2\alpha. \quad (2)$$

We may first consider the problem qualitatively. The cubic field is assumed so large that its effect is predominant. Bethe[4] has shown by group theory, that under the influence of an electric field of cubic symmetry, the fivefold degenerate representation of the orbital rotation group for $L=2$ divides into two irreducible representations Γ_3 and Γ_5 which are respectively doubly and triply degenerate. In order to obtain agreement with experiment it is necessary to assume that the lowest energy level belongs to the representation Γ_3. This also agrees with the conclusions of Van Vleck.[5]

The introduction of the electron spin of course complicates the problem, doubling the number of states. Even after the introduction of the orbit-spin forces many of the states coincide, for a well-known theorem of Kramers tells us that, in a system with an odd number of electrons, there is always at least a twofold degeneracy. Fig. 1 shows how the energy levels arising from a ^2D configuration behave in the presence of the various fields. The right half of the diagram is labelled with Bethe's notation, while on the left the notation corresponds to that of Mulliken.[6] It is particularly to be noted that when the twofold level, Γ_3, is increased to a fourfold one by the introduction of the spin, none of the four components separate until rhombic or magnetic field terms are included. In the language of group theory, $D_{\frac{1}{2}}\times\Gamma_3=\Gamma_8$, where $D_{\frac{1}{2}}$ is the rotation group for the spin, Γ_3 is a doubly degenerate representation of the single-valued cubic group, and Γ_8 is a fourfold degenerate representation of the double-valued cubic group which is characteristic of half-integral quantum numbers.[7] The degeneracy is completely removed only by the simultaneous application of an electric field of rhombic (or monoclinic) symmetry and a magnetic field, the latter removing the Kramers degeneracy. Without the magnetic field, but including the electric field terms, the whole problem has a twofold degeneracy. The components which are due to the magnetic field may be distinguished by the superscripts + or −, while the five levels in the absence of the field are designated by Roman or Arabic numerals without the superscript.

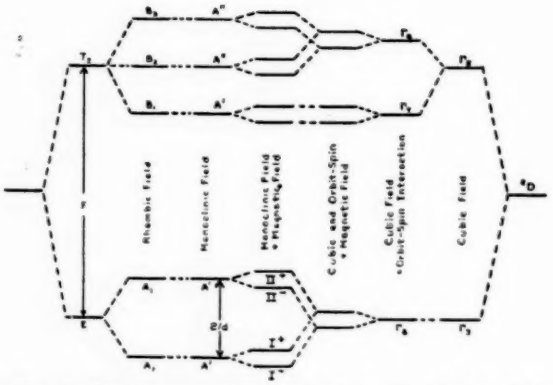

FIG. 1. The diagram shows how the energy levels arising from a ^2D configuration are influenced by the various fields. At either side of the diagram, the large separation produced by the cubic field is shown. At the left side, the rhombic field is superposed to give a resulting field of rhombic or monoclinic symmetry which removes the orbital degeneracy and yields five states. The inclusion of the spin produces no additional splitting until an external magnetic field is applied. Then all degeneracy is removed and the number of states is doubled. Proceeding now from the right side of the figure, the superposition of the orbit-spin forces on the cubic field removes only part of the degeneracy, and there are only six states even after the application of the magnetic field. The complete solution considers the combination of these two effects. Only the states branching from Γ_3 are normal states.

For the calculation of the magnetic susceptibility, we must know the energies of the lowest states (I and II in Fig. 1) and how these energies are affected by the magnetic field. The contribution of each state to the susceptibility is proportional to the population of that state, which, in turn, is proportional to the appropriate Boltzmann factor $\exp(-W_i/kT)$. Therefore the three upper states, having negligible population, will affect the susceptibility only as they modify the energies of the lower states.

[4] H. Bethe, Ann. d. Physik **3**, 133 (1929).
[5] J. H. Van Vleck, Phys. Rev. **41**, 208 (1932).
[6] R. S. Mulliken, Phys. Rev. **43**, 288 (1933).
[7] This relation is the analog of Eq. (1) of Schlapp and Penney's paper, reference 2.

The Matrix Elements

The matrix elements of the electric field may be determined for a one-electron system by direct quadrature using central wave functions. Since it is sufficient to consider only elements that are diagonal in L, the radial factor enters merely as a constant. Cu^{++} has a $d^9\ ^2D$ configuration, and considerations similar to those underlying the Pauli reciprocity theorem tell us that it is equivalent to a one-electron system with the sign of the proportionality factors changed.[8] Most of the matrix elements which we need for the crystalline potential have been given by Schlapp and Penney.[9] However, we also need the elements of xy, *viz.:*

$$\left.\begin{aligned}&[xy](M_L\pm 2,\ M_L)=\pm\tfrac{1}{4}i\tau[(L\pm M_L+2)(L\pm M_L+1)(L\mp M_L)(L\mp M_L-1)],\\&[xy](M_L',\ M_L)=0,\qquad M_L'\neq M_L\pm 2,\qquad \tau=-2r^2/(2L+3)(2L-1).\end{aligned}\right\}\tag{3}$$

Then the nonvanishing matrix elements of the rhombic term (2) are:

$$\left.\begin{aligned}&[Ax'^2+By'^2-(A+B)z'^2](M_L,\ M_L)=[Ax^2+By^2-(A+B)z^2](M_L,\ M_L)\\&\qquad=\tfrac{1}{2}\tau(A+B)(3M_L^2-L^2-L),\\&[Ax'^2+By'^2-(A+B)z'^2](M_L\pm 2,\ M_L)=[(A-B)(x^2\cos 2\alpha+xy\sin 2\alpha)](M_L\pm 2,\ M_L)\\&\qquad=-\tfrac{1}{4}\tau(A-B)[(L\pm M_L+2)(L\pm M_L+1)(L\mp M_L)(L\mp M_L-1)]^{\frac{1}{2}}\exp(\pm 2i\alpha).\end{aligned}\right\}\tag{4}$$

The matrix elements of $(\mathbf{L}\cdot\mathbf{S})$ are also given by Schlapp and Penney. We need only add the matrix elements of the Zeeman term. Introducing the definitions:

$$\mu\equiv\beta(\mathbf{L}+2\mathbf{S});\qquad \mathfrak{K}\equiv\beta\mathfrak{H}_z,\qquad \mathfrak{K}_x\equiv\beta\mathfrak{H}_x,\qquad \mathfrak{K}_y=\beta\mathfrak{H}_y,\tag{5}$$

one finds

$$\left.\begin{aligned}&\beta\mathfrak{H}\cdot(\mathbf{L}+2\mathbf{S})=\mathfrak{H}_x\mu_x+\mathfrak{H}_y\mu_y+\mathfrak{H}_z\mu_z,\\&[\beta\mathfrak{H}\cdot(\mathbf{L}+2\mathbf{S})](M_LM_S;\ M_LM_S)=\mathfrak{K}(M_L+2M_S),\\&[\beta\mathfrak{H}\cdot(\mathbf{L}+2\mathbf{S})](M_L\pm 1,\ M_S;\ M_LM_S)=\tfrac{1}{2}(\mathfrak{K}_x\mp i\mathfrak{K}_y)[L(L+1)-M_L(M_L\pm 1)]^{\frac{1}{2}},\\&[\beta\mathfrak{H}\cdot(\mathbf{L}+2\mathbf{S})](M_L,\ M_S\pm 1;\ M_LM_S)=(\mathfrak{K}_x\mp i\mathfrak{K}_y)[S(S+1)-M_S(M_S\pm 1)]^{\frac{1}{2}}.\end{aligned}\right\}\tag{6}$$

The Secular Matrix

The secular matrix $\mathbf{H}$, shown in Fig. 2, is diagonal in the elements of the cubic field. This results from the choice of the system of representation in which the Φ part of the orbital wave functions are proportional[10] to $\sin M_L\Phi$ and $\cos M_L\Phi$ rather than to $\exp(iM_L\Phi)$. It should perhaps be pointed out here that the matrix elements defined above are those appropriate to the exponential form of the wave function.[11] The following definitions have been introduced in

[8] This change in sign accounts for the minus sign in our definitions of τ and q' in (3) and (7). For a general discussion of the sign of q' see reference 5.

[9] See reference 2, p. 672. Their a corresponds to our τ. In their first statement on p. 673, we may note the following minor correction: q and a should be replaced by q'/k_1 and a/c_1, respectively, where k_1 and c_1 are the constants computed for a one-electron system. For Cu^{++} the ratios are negative. The value of c_1 is the same as $-\tau$, while

$$k_1=[3r^4/2(2L+5)(4L^2-9)(2L-1)];$$

cf. the last equation on p. 201 of Penney and Schlapp, Phys. Rev. **41** (1932).

[10] This is not a general statement but is true for the case $L=2$, as was demonstrated by Bethe.

[11] The secular matrix $\mathbf{H}$ is easily obtained from the matrix elements given above by first setting up the matrix $\mathbf{H}_z$ in the M_LM_S system of quantization. Then the unitary transformation $\mathbf{S}^{-1}\mathbf{H}_z\mathbf{S}$ gives the matrix $\mathbf{H}$ which is diagonal in the cubic field if $\mathbf{S}$ contains factors of the form

$$2^{-\frac{1}{2}}\begin{vmatrix}1 & -1\\ 1 & 1\end{vmatrix}$$

for each pair of values $|M_L|$ and $-|M_L|$. We retain the spin matrices which are appropriate to the exponential form.

Λ^+									
Γ_3^+		Γ_5^+			Γ_5^-			Γ_3^-	
$2, \frac{1}{2}$	$0, \frac{1}{2}$	$-2, \frac{1}{2}$	$1, -\frac{1}{2}$	$-1, -\frac{1}{2}$	$1, \frac{1}{2}$	$-1, \frac{1}{2}$	$2, -\frac{1}{2}$	$0, -\frac{1}{2}$	$-2, -\frac{1}{2}$
$-6a+\mathfrak{R}$	η	$-A'-2\mathfrak{R}$	$A'/2$	$A'/2$	$-i\mathfrak{R}_y$	$\mathfrak{R}_x$	0	0	$\mathfrak{R}_x-i\mathfrak{R}_y$
η	$6a+\mathfrak{R}$	$-i\xi$	$3^{\frac{1}{2}}A'/2$	$-3^{\frac{1}{2}}A'/2$	$3^{\frac{1}{2}}i\mathfrak{R}_y$	$3^{\frac{1}{2}}\mathfrak{R}_x$	0	$\mathfrak{R}_x-i\mathfrak{R}_y$	0
$-A'-2\mathfrak{R}$	$i\xi$	$-F+\beta_5+\mathfrak{R}$	$A'/2$	$A'/2$	$-\mathfrak{R}_x$	$i\mathfrak{R}_y$	$-\mathfrak{R}_x+i\mathfrak{R}_y$	0	0
$A'/2$	$3^{\frac{1}{2}}A'/2$	$A'/2$	$-F+\beta_4-\mathfrak{R}$	$\frac{1}{2}A'-i\zeta-\mathfrak{R}$	0	$\mathfrak{R}_x+i\mathfrak{R}_y$	$i\mathfrak{R}_y$	$3^{\frac{1}{2}}\mathfrak{R}_x$	$\mathfrak{R}_x$
$A'/2$	$-3^{\frac{1}{2}}A'/2$	$A'/2$	$\frac{1}{2}A'+i\zeta-\mathfrak{R}$	$-F+\beta_5-\mathfrak{R}$	$-\mathfrak{R}_x-i\mathfrak{R}_y$	0	$-\mathfrak{R}_x$	$3^{\frac{1}{2}}i\mathfrak{R}_y$	$-i\mathfrak{R}_y$
$i\mathfrak{R}_y$	$-3^{\frac{1}{2}}i\mathfrak{R}_y$	$-\mathfrak{R}_x$	0	$-\mathfrak{R}_x+i\mathfrak{R}_y$	$-F+\beta_5+\mathfrak{R}$	$\frac{1}{2}A'-i\zeta+\mathfrak{R}$	$A'/2$	$-3^{\frac{1}{2}}A'/2$	$A'/2$
$\mathfrak{R}_x$	$3^{\frac{1}{2}}\mathfrak{R}_x$	$-i\mathfrak{R}_y$	$\mathfrak{R}_x-i\mathfrak{R}_y$	0	$\frac{1}{2}A'+i\zeta+\mathfrak{R}$	$-F+\beta_4+\mathfrak{R}$	$A'/2$	$3^{\frac{1}{2}}A'/2$	$A'/2$
0	0	$-\mathfrak{R}_x-i\mathfrak{R}_y$	$-i\mathfrak{R}_y$	$-\mathfrak{R}_x$	$A'/2$	$A'/2$	$-F+\beta_3-\mathfrak{R}$	$-i\xi$	$-A'+2\mathfrak{R}$
0	$\mathfrak{R}_x+i\mathfrak{R}_y$	0	$3^{\frac{1}{2}}\mathfrak{R}_x$	$-3^{\frac{1}{2}}i\mathfrak{R}_y$	$-3^{\frac{1}{2}}A'/2$	$3^{\frac{1}{2}}A'/2$	$i\xi$	$6a-\mathfrak{R}$	η
$\mathfrak{R}_x+i\mathfrak{R}_y$	0	0	$\mathfrak{R}_x$	$i\mathfrak{R}_y$	$A'/2$	$A'/2$	$-A'+2\mathfrak{R}$	η	$-6a-\mathfrak{R}$

FIG. 2. The **H** matrix. The terms in F are due to the cubic field, those in A' to the orbit-spin forces, and those in $\mathfrak{H}$ to the magnetic field. The other terms arise from the generalized rhombic term (2). The various symbols used are all defined in (6) and (7).

setting up the matrix in Fig. 2.

$$\left.\begin{aligned} &a=-\tau(A+B)/2; \quad b=-\tau(A-B)/2;\\ &F=24q'D; \qquad\quad q'=-\overline{r^4}/126;\\ &\eta=2\cdot 3^{\frac{1}{2}}b\cos 2\alpha; \quad \xi=2\cdot 3^{\frac{1}{2}}b\sin 2\alpha;\\ &\zeta=3b\sin 2\alpha; \qquad \beta_3=-6a;\\ &\beta_4=3a+3^{\frac{1}{2}}\eta/2; \quad \beta_5=3a-3^{\frac{1}{2}}\eta/2. \end{aligned}\right\} \quad (7)$$

In the matrix **H**, the terms in A' arise from the orbit-spin forces, those in $\mathfrak{R}$ from the magnetic field, and those in F from the cubic field. The other terms are due to the rhombic term in the crystalline field. Above the matrix we have indicated the relations between the matrix elements and the various group representations previously discussed. At the head of each column, are given the values of M_L and M_S appropriate to the exponential representation from which **H** was derived. These numbers serve to identify the matrix elements, but it must be remembered that, after the transformation to the trigonometric system of representation, M_L is no longer a good quantum number as regards sign.

When we proceed to the reduction of **H**, we note first that in the absence of the magnetic field the tenth degree matrix factors into two identical quintics. If a magnetic field is applied along the z-axis, the matrix still factors into two quintics (Λ^+ and Λ^-) which now differ in the sign of terms involving $\mathfrak{R}$. This simplifies matters greatly in the case $\alpha=0$, i.e., if the axes of the rhombic and cubic terms coincide, so that the resultant field has rhombic symmetry. Then it is possible to solve a quintic and obtain the principal susceptibility which corresponds to the application of the magnetic field along the z-axis. The other two principal susceptibilities are readily obtained from the first result by the cyclic permutation of the rhombic field parameters A, B and $-(A+B)$. In the general case that $\alpha\neq 0$, i.e., that the resultant field is monoclinic, this procedure fails, as the direction of the moment induced by the magnetic field directed along the coordinate axes may not agree with the direction of the applied field. That is, the magnetic axes (for which the direction of the induced moment is the same as that of the applied field) will not agree either with the axes of the cubic field or with those of the rhombic field but will lie in some intermediate position. When the magnetic field is applied in the xy plane, the secular matrix no longer factors. We then have to use a procedure somewhat similar

to that developed by Kramers[12] in his most recent calculations on tysonite.

As we have already pointed out, we shall be satisfied to know the energy values of the states arising from only the configuration Γ_3. The effect on these states of the levels arising from Γ_5 may be computed by perturbation theory. However, since there are matrix elements between nearly degenerate states, the energy values cannot be obtained by the direct application of standard series perturbation technique. The procedure which we shall use and the derivation of the third order perturbation formulas for off-diagonal elements are given in the next section.

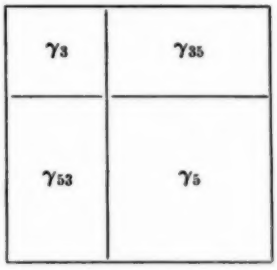

FIG. 3.

PERTURBATION TECHNIQUE

The $\mathbf{H}$ matrix is of the form $\mathbf{H}=\mathbf{H}_0+\lambda\mathbf{H}_1$, where $\mathbf{H}_0$ (the matrix of the cubic field) is diagonal and degenerate. The matrix $\mathbf{H}_1$, which contains the elements of the rhombic term, the orbit-spin interaction, and the magnetic field, has elements also on the main diagonal. In the zeroth approximation ($\lambda=0$), $\mathbf{H}$ factors into two parts γ_3 and γ_5 (Fig. 3) each of which has several equal roots. Referring to Fig. 1, we see that γ_3 should have four roots corresponding to the four levels arising from Γ_3, and Γ_5 should represent the six levels arising from Γ_5. We wish to know the roots of γ_3 to the order λ^3. Let m and n (with or without primes) refer to the elements of γ_3 and γ_5, respectively. We seek a unitary transformation matrix $\mathbf{S}=1+\lambda\mathbf{S}_1+\lambda^2\mathbf{S}_2$ such that $\mathbf{H}_2=\mathbf{S}^{-1}\mathbf{H}\mathbf{S}$ has no elements of the form $\mathbf{H}_2(m, n)$ to the order λ^2. This is a sufficiently good approximation unless we want the energy to the order λ^4. We require that $\mathbf{S}_1$ shall be of the form $\mathbf{S}_1(m, n)$ and that the elements of $\mathbf{S}_2$ be chosen to make $\mathbf{S}$ unitary. Then it is not difficult to show that[13]

$$S_1(m,n)=-\frac{H_1(mn)}{H_0(mm)-H_0(nn)}=\frac{H_1(mn)}{h\nu(mn)},\qquad S_2(mm')=-\tfrac{1}{2}\sum_n\frac{H_1(mn)H_1(nm')}{h\nu(mn)h\nu(m'n)},\tag{8}$$

$$H_2(mm')=H_0(mm')\delta_m{}^{m'}+H_1(mm')+H_2''(mm')+H_2'''(mm'),\tag{9}$$

where

$$H_2''(mm')=\sum_n\frac{H_1(mn)H_1(nm')}{h\nu(m'n)}\tag{10}$$

and

$$H_2'''(mm')=-\tfrac{1}{2}\sum_{m'',\,n}\frac{H_1(mm'')H_1(m''n)H_1(nm')}{h\nu(mn)\cdot h\nu(m'n)}-\tfrac{1}{2}\sum_{n,\,m''}\frac{H_1(mn)H_1(nm'')H_1(m''m')}{h\nu(mn)\cdot h\nu(m''n)}+\sum_{n,n'}\frac{H_1(mn)H_1(nn')H_1(n'm')}{h\nu(mn)h\nu(m'n')}.\tag{11}$$

DETERMINATION OF THE ENERGY VALUES

By means of the perturbation formulas given above the tenth degree matrix is reduced to one of the fourth degree representing the states I^* and II^* of Fig. 1. The result, $\mathbf{H}_2$, is shown schematically in Fig. 4, where the terms which vanish with the magnetic field have been designated by the letter h.

[12] H. A. Kramers, Proc. Amst. Acad. Sci. **35**, 1272 (1932).

[13] The matrix elements of $\mathbf{S}_2$ are not uniquely defined until we impose an additional condition. It is convenient, but not necessary, to require that the $\mathbf{S}_2$ be Hermitian; $\mathbf{S}_1$ is never Hermitian.

$$\begin{array}{cccc} f(1,1)+h(1,1) & f(1,2)+h(1,2) & h(1,2^-) & h(1,1^-) \\ f(2,1)+h(2,1) & f(2,2)+h(2,2) & h(2,2^-) & h(2,1^-) \\ h(2^-,1) & h(2^-,2) & f(2,2)+h(2^-,2^-) & f(1,2)+h(2^-,1^-) \\ h(1^-,1) & h(1^-,2) & f(2,1)+h(1^-,2^-) & f(1,1)+h(1^-,1^-). \end{array}$$

FIG. 4. The $\mathbf{H}_2$ matrix.

We now apply a unitary transformation $\mathbf{S}_2^{-1}\mathbf{H}_2\mathbf{S}_2=\mathbf{H}_3$, such that $\mathbf{H}_3$ is diagonal in the absence of a magnetic field. The transformation $\mathbf{S}_2$ is easily found as, in the absence of a magnetic field, $\mathbf{H}_2$ factors into two identical quadratics. Let the resulting matrix elements be represented by $f'(i,j)\delta_j^i$ and $h'(i,j)$. Another transformation (essentially the application of Eq. (10)) eliminates all elements of the form $h'(1,2)$ and $h'(1,2^-)$ and gives us a new matrix $\mathbf{H}_4$ with elements only along the two main diagonals. The final energy values are obtained by the solution of two quadratics of the form:

$$\begin{vmatrix} f''(i,i)+h''(i,i)-W & h''(i,i^-) \\ h''(i^-,i) & f''(i,i)+h''(i^-,i^-)-W \end{vmatrix}=0. \qquad i=1,2. \quad (12)$$

The two roots of either determinant differ only in the sign of $\mathfrak{H}$. The energy values have such a form that they may conveniently be expressed as follows in terms of the direction cosines l, m and n, of the magnetic field:

$$W_1=-(1/d)\pm\mathfrak{H}\beta V_1+\mathfrak{H}^2\beta^2 w_1, \qquad W_2=+(1/d)\pm\mathfrak{H}\beta V_2+\mathfrak{H}^2\beta^2 w_2, \quad (13)$$

where

$$\left.\begin{aligned} V_i&=\{\boldsymbol{A}_i(l^2+m^2)+\boldsymbol{B}_i(l^2-m^2)+\boldsymbol{C}_i lm+\boldsymbol{E}_i n^2\}^{\frac{1}{2}}, \\ w_i&=\boldsymbol{A}_i^{(2)}(l^2+m^2)+\boldsymbol{B}_i^{(2)}(l^2-m^2)+\boldsymbol{C}_i^{(2)}lm+\boldsymbol{E}_i^{(2)}n^2. \end{aligned}\right\} \quad (14)$$

The coefficients which appear in V_1 and w_1 are defined by:

$$\left.\begin{aligned} \boldsymbol{A}_1&=1+2R(2-ud)+R^2\{2-3ud-2u^2d^2-\eta d^2\tan^2 2\alpha+\sigma(1+2u^2d^2)\}, \\ \boldsymbol{B}_1&=-3^{\frac{1}{2}}R\eta d\{2+R(3-2ud+2\sigma ud)\}, \\ \boldsymbol{C}_1&=-2\cdot 3^{\frac{1}{2}}R^2\xi d\{2ud-\sigma(3-4ud)\}, \\ \boldsymbol{E}_1&=1+4R(1+ud)+R^2\{-1+6ud+4u^2d^2+4\sigma\eta^2d^2(1-\tan^2 2\alpha)\}, \\ \boldsymbol{A}_1^{(2)}&=Rd\{\sigma(2-ud)+\tfrac{1}{2}R(1+2u^2d^2)(\sigma^2-1)-\tfrac{1}{2}R\eta^2d^2\tan^2 2\alpha\}, \\ \boldsymbol{B}_1^{(2)}&=-3^{\frac{1}{2}}R\eta d^2\{\sigma-Rud(1-\sigma^2)\}, \\ \boldsymbol{C}_1^{(2)}&=-3^{\frac{1}{2}}R^2\xi d^2\{2ud-\sigma^2(3-4ud)\}, \\ \boldsymbol{E}_1^{(2)}&=2Rd\{\sigma(1+ud)+R\sigma^2\eta^2d^2(1-\tan^2 2\alpha)-R\eta^2d^2\}, \end{aligned}\right\} \quad (15)$$

where $2/d$ is the final separation of the states I and II produced by the rhombic field; $2u$ is the difference between the diagonal elements of $\mathbf{H}_2$, i.e., $2u$ equals $f(1,1)-f(2,2)$, and is approximately equal to $12a$; F is the separation of Γ_3 and Γ_5 produced by the cubic field; $R=A'/F$, and $\sigma=1/dA'$. The coefficients which appear in V_2 and w_2 may be obtained from (15) by changing the sign of d (and consequently of σ) throughout.

CALCULATION OF THE PRINCIPAL SUSCEPTIBILITIES

The components of the magnetic moment vector may be calculated by the relation:

$$M_q=NkT(\partial/\partial\mathfrak{H}_q)\textstyle\sum_i e^{-W_i/kT}/\sum_i e^{-W_i/kT}. \qquad q=x,y,z. \quad (16)$$

Here we have supposed the energy expressed in terms of the x, y and z components of the magnetic field, whereas previously we have written the energy values in terms of the absolute value of the magnetic field and its direction cosines referred to the cubic field axes. This should cause no confusion, as we may replace the derivative $\partial/\partial\mathfrak{H}_q$ of (16) by its equivalent $(1/\mathfrak{H})(\partial/\partial s)$, where s has the values l, m, n, according as $q=x$, y, z, respectively. The magnetic axes, along which the principal susceptibilities are defined, are those for which the direction of the induced moment is the same as the direction of the applied field. With the notation $\theta=1/dkT$, the partition function for our problem is:

$$\sum_i e^{-W_i/kT}=2e^{\theta}\{1+(\mathfrak{H}^2\beta^2/2kT)[(V_1^2/kT)-2w_1]\}+2e^{-\theta}\{1+(\mathfrak{H}^2\beta^2/2kT)[(V_2^2/kT)-2w_2]\}. \quad (17)$$

In the denominator of (16) it is sufficient to consider only that portion of the energy which is independent of $\mathfrak{H}$, so that the sum (17) reduces to $2(e^{\theta}+e^{-\theta})$. For the numerator of (16) we may drop from the partition function the terms independent of $\mathfrak{H}$ and define a new quantity Z which is a homogeneous quadratic function of $\mathfrak{H}$, and may be written in the form:

$$Z\equiv(\mathfrak{H}\beta/kT)^2\{\boldsymbol{A}(l^2+m^2)+\boldsymbol{B}(l^2-m^2)+\boldsymbol{C}lm+\boldsymbol{E}n^2\}, \quad (18)$$

where

$$\boldsymbol{A}=\{\boldsymbol{A}_1-2kT\boldsymbol{A}_1^{(2)}\}e^{\theta}+\{\boldsymbol{A}_2-2kT\boldsymbol{A}_2^{(2)}\}e^{-\theta} \quad (19)$$

and similar expressions for $\boldsymbol{B}$, $\boldsymbol{C}$ and $\boldsymbol{E}$.

Let us choose a new set of coordinates, x'', y'', z, for which the direction cosines of the magnetic field are l'', m'' and n, and $\cos(x, x'')=\cos\phi$. If we require the term in $l''m''$ to vanish when Z is referred to the new axes, the angle ϕ will be defined by the relation $\tan 2\phi\equiv\boldsymbol{C}/2\boldsymbol{B}$ and then

$$Z'=(\mathfrak{H}\beta/kT)^2\{(\boldsymbol{A}+[\boldsymbol{B}^2+\boldsymbol{C}^2/4]^{\frac{1}{2}})l''^2+(\boldsymbol{A}-[\boldsymbol{B}^2+\boldsymbol{C}^2/4]^{\frac{1}{2}})m''^2+\boldsymbol{E}n^2\}. \quad (20)$$

The magnetic axes will coincide with the coordinate axes x'', y'', z, and, by (16), the principal susceptibilities will be given by the expression:[14]

$$\chi_i kT/N\beta^2\equiv M_i=\{k^2T^2/2\mathfrak{H}_i\beta^2(e^{\theta}+e^{-\theta})\}\partial Z'/\partial\mathfrak{H}_i. \qquad i=x'', y'', z. \quad (21)$$

By knowing the experimental values for the principal susceptibilities, it is possible to determine the parameters $1/d$, R, ud and α which appear in (20), and thus obtain some information about the magnitude and type of symmetry of the crystalline fields.

Temperature Rotation of the Magnetic Axes

Since the coefficients $\boldsymbol{C}$ and $\boldsymbol{B}$, whose ratio determines the direction of the principal magnetic moment, are functions of temperature, it follows that the direction of the principal moment in the crystal is also a function of temperature. The angle which the direction of maximum susceptibility makes with the axis of the cubic field is given by the relation $\tan 2\phi=\boldsymbol{C}/2\boldsymbol{B}$.

Experiments on magnetic susceptibility always furnish the resultant susceptibility, and the total paramagnetism of the metal ion is obtained by adding a correction equal to the diamagnetism of the anion and the water of hydration. In the case of the cupric hexahydrate sulphates, this diamagnetic correction is about ten percent of the total value at room temperature. For want of any information to the contrary, the diamagnetic correction is usually assumed to be the same for each of the three principal subsceptibilities, but there is no inherent reason why this must be true.

---

[14] We find it convenient to discuss our results for the susceptibilities in terms of the quantity $M=\chi kT/N\beta^2$, which is 1/3 of the "effective magneton number." If Curie's law is obeyed M is a constant, and if the "spin-only" formula of Bose and Stoner is valid, the value of this constant is unity. The difference $M-1$ is a measure of the magnetic contribution of the orbit, and the variation of M with temperature measures the deviation from Curie's law.

Let us instead assume that one of the diamagnetic axes coincides with the z-axis of the crystalline fields, and that the other two diamagnetic axes lie in the xy plane with no particular correlation to the paramagnetic axes. Then we may introduce into the energy expression (13) a term

$$\mathfrak{H}^2\beta^2 G=\mathfrak{H}^2\beta^2[G_1(l^2+m^2+n^2)+G_2(l^2-m^2)+G_3lm], \tag{22}$$

which is the same for both states. G_1 is the mean diamagnetic correction and may be neglected if we use the experimental results which have been corrected in the usual way. The quantities G_2 and G_3 may be included in the sum (18) by redefining the coefficients:

$$\begin{aligned} \boldsymbol{B}&=\{\boldsymbol{B}_1-2kT(\boldsymbol{B}_1^{(2)}+G_2)\}e^{\theta}+\{\boldsymbol{B}_2-2kT(\boldsymbol{B}_2^{(2)}+G_2)\}e^{-\theta},\\ \boldsymbol{C}&=\{\boldsymbol{C}_1-2kT(\boldsymbol{C}_1^{(2)}+G_3)\}e^{\theta}+\{\boldsymbol{C}_2-2kT(\boldsymbol{C}_2^{(2)}+G_3)\}e^{-\theta}. \end{aligned} \tag{23}$$

The addition of these diamagnetic terms will modify both the formulas for the principal susceptibilities and the formula for the direction of the principal moment, for the resulting magnetic axes will be different from the axes of either the diamagnetic or paramagnetic parts alone. It is conceivable that reasonably small values of G_2 and G_3 may have an appreciable effect on the variation of the magnetic axes with temperature without greatly changing the values for the principal susceptibilities. If we write

$$G_2=6g_2Rbd/A' \quad \text{and} \quad G_3=-6g_3R^2bd/A', \tag{24}$$

the explicit formula for the direction of the magnetic axis is:

$$\tan 2\phi=\tfrac{1}{2}R\frac{\sin 2\alpha\{2ud(1-\tanh\theta/\theta)-3\sigma(1-kT/A')+4\sigma ud(1-kT/A')\tanh\theta\}-g_3kT/A'}{\cos 2\alpha(1-kT/A')\tanh\theta+g_2kT/A'}. \tag{25}$$

In general, then, there should be some variation of the direction of the magnetic axes with temperature. The direction of the magnetic axes will be constant in two particular cases: (1) when the axes of the rhombic and cubic terms coincide with the diamagnetic axes, i.e., when $g_3=\alpha=\xi=0$, the magnetic axes will coincide with the axes of the cubic field; (2) when the axes of the rhombic term make an angle of 45° with the cubic axes, and there is no diamagnetic asymmetry ($\eta=g_2=0$), the magnetic axes will make a constant angle of 45° with the axes of the cubic field.

It will be shown in the next section, that the above formula for the rotation of the magnetic axes with temperature is not entirely satisfactory. We have therefore repeated the calculations so as to ascertain the effect of a still more general rhombic term with components of higher degree in the crystalline potential. One finds that, after the addition of a fourth degree term of the form $\boldsymbol{D}x'^4+\boldsymbol{F}y'^4$, no further generality is secured by the addition of still higher order terms since the secular matrix then has as many independent arbitrary constants as is possible for a field of monoclinic symmetry. The calculations, therefore, were made by modifying the fourth degree terms, but the results are appropriate to the most general monoclinic field. The calculations are not included here because the results differ so slightly from those which we have described, but we will gladly furnish details to interested readers. It will suffice to point out the changes produced by the inclusion of the higher order rhombic terms. The **H** matrix would look like Fig. 2 except that the term $H(2,\frac{1}{2};-2,\frac{1}{2})$ would be $(-A'-2\mathfrak{R}-i\rho)$ where ρ is a new constant, and the constants η, ξ, ζ, and the β_i would have slightly different definitions from those given in (7); in particular, ξ and ζ would now be independent of each other. The solution proceeds as before but results in the addition of higher order terms in the coefficients defined in (15). These higher order terms have only negligible effect on the principal susceptibilities, but one of these terms becomes important in Eq. (25) in the limiting case when $\eta=g_2=0$, as it may not vanish. Thus Φ may be a function of T, not constant, even in this limiting case. We conclude, however, that the rhombic term (2) is sufficiently general for all practical purposes.

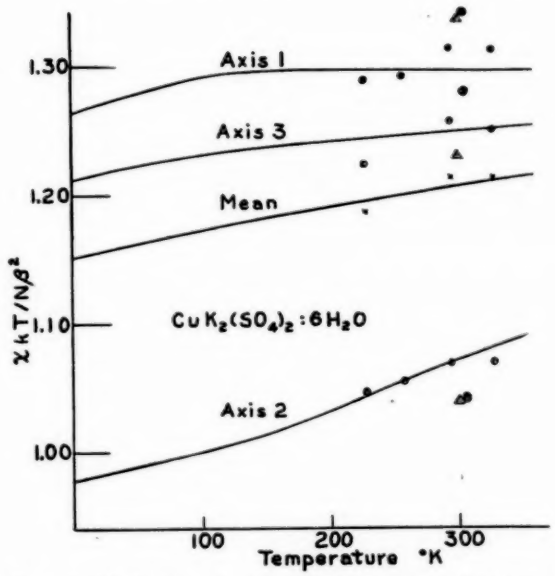

FIG. 5. Variation of the principal susceptibilities of $CuK_2(SO_4)_2 \cdot 6H_2O$ with temperature. Solid lines are computed curves. Experimental values: circles by Bartlett, triangles by Rabi, crossed circles by Krishnan and colleagues; crosses are means of Bartlett's values.

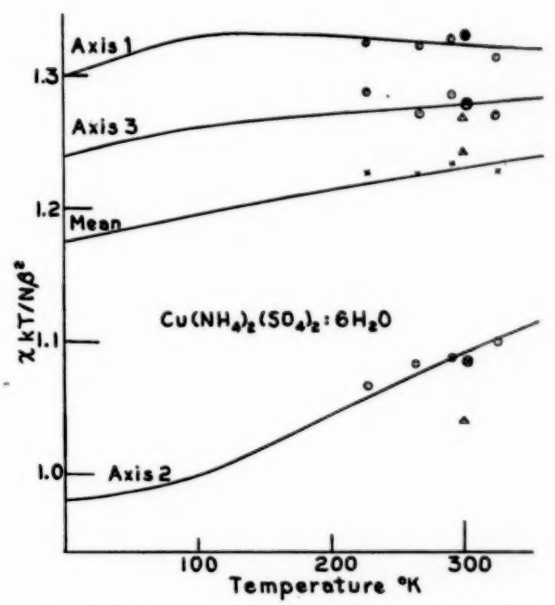

FIG. 6. Variation of the principal susceptibilities of $Cu(NH_4)_2(SO_4)_2 \cdot 6H_2O$ with temperature. Solid lines are computed curves. Experimental values: circles by Bartlett, triangles by Rabi, crossed circles by Krishnan and colleagues; crosses are means of Bartlett's values.

COMPARISON WITH EXPERIMENT

Experimental data on the principal susceptibilities and the temperature rotation of the magnetic axes, have been obtained by Bartlett[15] for the two cupric hexahydrate sulphates: $Cu(NH_4)_2(SO_4)_2 : 6H_2O$ and $CuK_2(SO_4)_2 : 6H_2O$. The primary experimental results are the volume susceptibilities and these are probably accurate to about one percent. However, because the change in volume of the crystal with temperature was neglected, for lack of accurate data, and because of uncertainties in the diamagnetic correction, the final result for the molar susceptibilities of the metal ion may be in error by as much as two percent. The relative values are, of course, much better.

We have computed the variation of the principal susceptibilities with temperature, for these two substances, by adjusting the parameters to fit Bartlett's data. Figs. 5 and 6 show the computed curves and the experimental points of Bartlett. Note that we have plotted, as ordinate, the quantity $\chi kT/N\beta^2$ which should be independent of temperature if Curie's law is accurately obeyed. In each case we have included our curve for the mean susceptibility, averaged over the three axes, together with the means of Bartlett's points. The data of Rabi[16] and of Krishnan and his colleagues[17] for the principal susceptibilities at room temperature are also indicated, but we have disregarded these points entirely in choosing the parameters for our computed curves. The data for the potassium salt especially illustrate the diversity of the experimental results.

Agreement with Bartlett's data has been obtained for $CuK_2(SO_4)_2 : 6H_2O$ by assuming that the separations produced by the rhombic and cubic fields are respectively 360 and 21,300 wave numbers, that $\tan 2\alpha = -4$, and that $ud = 0.2$, which corresponds to choosing the coefficients of the rhombic term in the ratio: $A : B : C = 18 : -17 : -1$. For $Cu(NH_4)_2(SO_4)_2 : 6H_2O$, we find that the cubic and rhombic fields produce energy separations of 18,930 and 340 wave numbers, respectively, that $\tan 2\alpha = +3$, and that $ud = 0.25$, which corresponds to $A : B : C = 11 : -10 : -1$. In both cases the rhombic

[15] B. W. Bartlett, Phys. Rev. **41**, 818 (1932); errata, Phys. Rev. **44**, 687 (1933).

[16] I. Rabi, Phys. Rev. **29**, 174 (1927).

[17] K. S. Krishnan, N. C. Chakravorty and S. Banerjee, Phil. Trans. **A232**, 99 (1933).

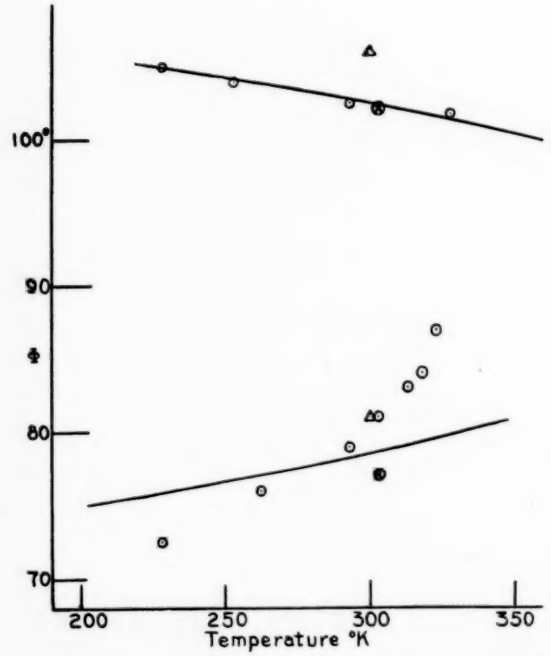

FIG. 7. Direction of the axis of maximum susceptibility as a function of temperature for crystals of $CuK_2(SO_4)_2 \cdot 6H_2O$ (upper curve) and for $Cu(NH_4)_2(SO_2)_2 \cdot 6H_2O$ (lower curve). The angles are referred to the crystallographic c-axis. Solid lines are computed curves. Experimental values: circles by Bartlett, triangles by Rabi, crossed circles by Krishnan and colleagues.

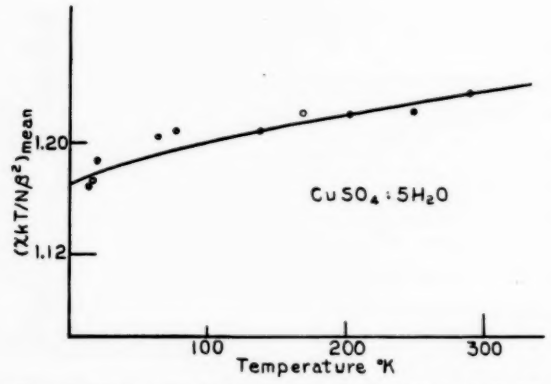

FIG. 8. Variation of the mean susceptibility of $CuSO_4 \cdot 5H_2O$ with temperature. Experimental points by de Haas and Gorter.

term turns out to be approximately of the form $A(x'^2 - y'^2)$.

Fig. 7 shows the agreement between the computed and observed values for the direction of the principal magnetic axes as a function of temperature. The experimental angles are referred to the crystallographic c-axis. Good agreement is obtained for the potassium salt by assuming: that the axis of the cubic field makes an angle of 110° 45′ with the crystallographic axis, that $g_2 = 0.15$, and that $g_3 = -7.5$, with the other crystal field parameters given above. This corresponds to a diamagnetic asymmetry of about 40 percent of the mean diamagnetic correction. Even this large diamagnetic asymmetry does not give a rotation of the magnetic axes of the magnitude observed for the ammonium compound. Of course, it is possible to choose parameters which will give the desired rotation if we do not try to fit the susceptibility data at the same time. It seems quite evident that some additional factor must be introduced to account for the large rotation of magnetic axes with temperature.

Fig. 8 shows that the assumption of a crystalline field of predominantly cubic symmetry is also consistent with the mean susceptibility of $CuSO_4 : 5H_2O$. The experimental points are due to de Haas and Gorter[18] and the computed curve assumes that the rhombic and cubic fields produce energy separations of 212 and 18,500 wave numbers, respectively, with $\tan 2\alpha = 4$ and $ud = 0.3$.

CONCLUSION

The method outlined above is capable of giving good agreement with the experimental results on the variation of the principal susceptibilities with temperature. It also furnishes us some information about the type and magnitude of the electric field within the crystal. This information may be used to supplement the x-ray data to obtain more information about the actual crystal structure than can be obtained by x-ray analysis alone. This is particularly true in the case of crystals of low symmetry, where the x-ray data are difficult to interpret.

The two cupric hexahydrate sulphates which we have studied belong to the class called the Tutton salts. X-ray data on the cupric Tutton salts appear to be lacking, but the analysis of $Mg(NH_4)_2(SO_4)_2 : 6H_2O$ by Hofmann[19] shows that the six molecules of water are located at the vertices of a regular octahedron with the metal ion, Mg^{++}, at the center. Incidentally, this arrangement of the water molecules in the Tutton

[18] W. J. de Haas and C. J. Gorter, Leiden Comm. 210d (1930).

[19] W. Hofmann, Z. Krist. **78**, 319 (1931).

salts is consistent with that deduced for $NiSnCl_6 : 6H_2O$ by Pauling[20] and for $NiSO_4 : 6H_2O$ by Beevers and Lipson.[21] The sulphate groups and the alkali or ammonium cations are situated at greater distances. It therefore seems logical to associate the predominant cubic field with the six water molecules, and to assume that the other groups produce the rhombic field which, when superposed on the cubic field, gives a resulting field of monoclinic symmetry. Our choice of parameters for the rhombic term, $A \backsimeq -B$ and $\alpha \backsimeq 45°$, suggests the location of the ionic groups, $SO_4^=$ and K^+ or NH_4^+, on two nearly orthogonal axes orientated at approximately 45° to the axes of the cubic field. However, the actual arrangement is probably not as simple as this.

It is a surprising fact that the mean susceptibility of $CuSO_4 : 5H_2O$ may be approximated over a wide range of temperature on the assumption that the crystalline field has predominantly cubic symmetry. Here the source of the cubic field is not obvious. However, one may suppose that some of the water molecules are shared in such a way as to give the octahedral arrangement around each metal ion. Of course, the agreement between the calculated and observed mean susceptibility may be only a coincidence, but the fact that the color of the blue vitriol is the same as that of the hexahydrates is another indication of similar group structures within the crystals. Furthermore, Gorter[22] has shown that, while D (the coefficient of the cubic term in (1)) is positive for an octahedral arrangement of six water dipoles, it would be negative for a tetrahedral or cubic arrangement of four or eight water dipoles, necessitating an inversion of Fig. 1. This would, presumably, alter the calculated dependence of the susceptibility on temperature and thus spoil the agreement with experiment. Data on the principal susceptibilities of this salt would be very welcome. Since the copper sulphate, pentahydrate, crystallizes in the triclinic form, the x-ray analysis is extremely difficult, and the magnetic analysis may point the way to a solution.

The important discovery by Bartlett,[15] that the direction of the principal magnetic axis is a function of temperature, is of considerable interest, and we have attempted to give an explanation for this result. We have shown that the changes of population of the various states with temperature does cause a rotation of the principal axis provided that the crystalline field has less than rhombic (e.g., monoclinic) symmetry. Unfortunately, the rotation of axes which we calculate using reasonable values of the crystal parameters is much too small in the case of the ammonium salt, and agreement is obtained in the case of the potassium salt only by assuming a large asymmetry in the diamagnetic correction. It is necessary to look for other or additional causes for the large rotation in the case of the ammonium salt. However, it may well be that the rotation of axes due to the repopulation of states is the important factor in other materials which have only feeble rotation.

A factor which has been entirely neglected is the thermal expansion of the crystal. Again experimental data are lacking, but it seems reasonable to expect asymmetrical thermal expansion in monoclinic crystals which are known to exhibit asymmetrical optical and magnetic properties. It is conceivable that, for certain critical arrangements, a slight asymmetric expansion might modify considerably the symmetry of the crystalline field, and thus cause the direction of the magnetic axes to change. For example (cf. Eq. (25)) suppose that α were very nearly 45°; then a slight asymmetrical expansion which would cause α to approach 45° would thereby produce a rapid rotation of the magnetic axes. The observed rotation (Fig. 8) for the ammonium salt suggests an approach to such a critical position. Even symmetrical thermal expansion will cause the crystal parameters to vary with temperature. We hope to have some data on the principal coefficients of thermal expansion of these cupric sulphates in the near future so that we may estimate the importance of this effect.

I wish to express my sincere thanks to Professor J. H. Van Vleck for his invaluable advice and constant encouragement during the course of this work. It is also a pleasure to acknowledge a grant from the Wisconsin Alumni Research Foundation which made the latter part of this work possible.

[20] L. Pauling, Z. Krist. **72**, 482 (1930).
[21] C. A. Beevers and H. Lipson, Z. Krist. **83**, 123 (1932).
[22] C. J. Gorter, Phys. Rev. **42**. 437 (1932).

The Rotation-Vibration Coupling in Diatomic Molecules

C. L. PEKERIS, *Harvard College Observatory and Massachusetts Institute of Technology*

(Received September 29, 1933)

A solution of the wave equation for the nuclear motion of a diatomic molecule with a Morse potential function and the rotational term included is given. The wave functions are found to have the same form as the functions obtained when the rotational term is neglected. The constants D_e and α_e in the equations

$$B_v = B_e - \alpha_e(v+\tfrac{1}{2}),$$
$$D_v = D_e + \beta_e(v+\tfrac{1}{2}),$$

are found to be given by the relations

$$D_e = -4B_e^3/\omega_e^2 \quad (1)$$

$$\alpha_e = 2x_eB_e(3[B_e/x_e\omega_e]^{\frac{1}{2}} - 3B_e/x_e\omega_e), \quad (2)$$

a result which can also be derived from Dunham's formulas. Eq. (2) differs from the corresponding relation in Kratzer's formula by the term in parenthesis. This term is fairly constant for a number of molecules and has an average value of 0.7 ± 0.1 as was found empirically by Birge. The values of α_e given by (2) show satisfactory agreement with experimental values for many molecules.

INTRODUCTION

FOR the purposes of a program of study of molecular spectra in astrophysical work, we have found it necessary to examine the effect of the rotational motion on the vibrational levels of a diatomic molecule in which the internuclear potential is of the Morse form. The rotational modification of the vibrational wave functions and the resulting modification of the probabilities of transition is of special importance in astrophysical work since at the high temperatures involved the recorded band-head maximum intensities occur at high j-values.

This question is also of interest in examining to what extent the potential function for a diatomic molecule is determinable from band spectrum data[1] as it has been found that quite different potential functions give practically the same vibrational levels. It is only when the coupling between vibration and rotation is considered that the adequacy of a given potential function can be tested.

If we write the wave function in the usual approximate form

$$\psi = \Phi(x, r)(R(r)/r)\Theta(\theta, \varphi) \quad (1)$$

then R satisfies the equation

$$d^2R/dr^2 - j(j+1)R/r^2 + (8\pi^2\mu/h^2)[E - U(r)]R = 0, \quad (2)$$

j being the rotational quantum number, $\mu = M_1M_2/(M_1+M_2)$. If we now assume a definite form for $U(r)$ and solve Eq. (2) with the second term left out, we find that up to a certain vibrational quantum number, the allowed vibrational levels are of the empirical form

$$E = E_{el} + hc[\omega_e(v+\tfrac{1}{2}) - x_e\omega_e(v+\tfrac{1}{2})^2 + y_e\omega_e(v+\tfrac{1}{2})^3\cdots] + hc\{B_v[(j+\tfrac{1}{2})^2 + \text{const.}] + D_v(j+\tfrac{1}{2})^4 + \cdots\} \quad (3)$$

with

$$B_v = B_e - \alpha_e(v+\tfrac{1}{2}) + \gamma_e(v+\tfrac{1}{2})^2 + \cdots, \quad (4)$$

$$D_v = D_e + \beta_e(v+\tfrac{1}{2}) + \cdots \quad (5)$$

for a variety of functions $U(r)$, different functions giving, however, different values for B_v, D_v, and especially for α_e when the complete Eq. (2) is solved. It is evident then that the value of α_e, though small, is of decisive importance in choosing the correct function $U(r)$.

[1] P. M. Davidson, Proc. Roy. Soc. **A135**, 459 (1932). G. Pöschl and E. Teller, Zeits. f. Physik **83**, 143 (1933). R. S. Mulliken, Rev. Mod. Phys. **4**, 77 (1932).

Morse[2] has shown that with his form of the potential energy

$$U(r)=E_{el}+D[1-e^{-a(r-r_e)}]^2 \tag{6}$$

containing two disposable constants D and a, and omitting the second term in Eq. (2), one obtains

$$\alpha_e=2B_e x_e, \tag{7}$$

$$D_e=-4B_e^3/\omega_e^2, \tag{8}$$

just as for the simple Kratzer potential function.[3] Of these Eq. (8) has been verified for a number of molecules[4] while Birge has found that the value of α_e as given by Eq. (7) is, on the average, too large by a factor of about 1.4.

We shall show, however, that if one includes the second term in Eq. (2), and uses the Morse function, one obtains a modified expression for α_e more in accord with the experimental values. It is to be noted that this formula can be derived readily from the general results of Dunham,[5] but the present analysis yields us also the modified *wave functions* which cannot be found directly by Dunham's procedure, but which are desired for later work.

We can take care of the rotational term in the following way. Substitute Eq. (6) in Eq. (2)

$$\frac{d^2R}{dr^2}-\frac{j(j+1)R}{r^2}+\frac{8\pi^2\mu}{h^2}[W-D^{-2a(r-r_e)}+2D^{-a(r-r_e)}]R=0, \tag{9}$$

$$W=E-E_{el}-D.$$

Following Morse, we let $y=e^{-a(r-r_e)}$ and (9) becomes

$$\frac{d^2R}{dy^2}+\frac{1}{y}\frac{dR}{dy}+\frac{8\pi^2\mu}{a^2h^2}\left[\frac{W}{y^2}+\frac{2D}{y}-D-\frac{Ar_e^2}{y^2r^2}\right]R=0, \tag{10}$$

$$A=j(j+1)h^2/8\pi^2\mu r_e^2.$$

Now

$$\frac{r_e^2}{r^2}=\frac{1}{(1-\ln y/r_e a)^2}=1+\frac{2}{ar_e}(y-1)+\left[-\frac{1}{ar_e}+\frac{3}{a^2r_e^2}\right](y-1)^2+\left[\frac{2}{3ar_e}-\frac{3}{a^2r_e^2}+\frac{4}{a^3r^3}\right](y-1)^3+\cdots. \tag{11}$$

We substitute the first three terms of (11) in (10) and leave the other terms to be treated later as a perturbation:

$$\frac{d^2R}{dy^2}+\frac{1}{y}\frac{dR}{dy}+\frac{8\pi^2\mu}{a^2h^2}\left[\frac{W-c}{y^2}+\frac{2D-c_1}{y}-D-c_2\right]R=0, \tag{12}$$

$$c=A\left(1-\frac{3}{ar_e}+\frac{3}{a^2r_e^2}\right),\qquad c_1=A\left(\frac{4}{ar_e}-\frac{6}{a^2r_e^2}\right),\qquad c_2=A\left(-\frac{1}{ar_e}+\frac{3}{a^2r_e^2}\right). \tag{13}$$

Now assume that $R(y)=Ne^{-z/2}z^{b/2}F(z),\qquad z=2dy,$

$$d^2=8\pi^2\mu(D+c_2)/a^2h^2,\qquad b^2=-32\pi^2\mu(W-c)/a^2h^2. \tag{14}$$

Then (12) becomes:

$$d^2F/dz^2+F(b+1-z)/z+vF/z=0, \tag{15}$$

---

[2] P. M. Morse, Phys. Rev. **34**, 57 (1929).

[3] A. Kratzer, Zeits. f. Physik **3**, 289 (1920).

[4] Cf. W. Weizel, *Bandenspektren*, Handbuch der Experimentalphysik Ergänzungsband **1**, p. 70.

[5] J. L. Dunham, Phys. Rev. **41**, 721 (1932). Cf. also P. M. Davidson, reference 1. I am indebted to the referee of the Physical Review for having pointed out this fact to me.

$$v=[4\pi^2\mu(2D-c_1)]/a^2h^2d-(b+1)/2=(k-b-1)/2; \qquad b=k-1-2v. \tag{16}$$

The polynomial-condition for (15) requires v to be an integer. Substituting (16) into (14), we get

$$W=E_{el}-D=c-(D-c_1/2)^2/(D+c_2)+(D-c_1/2)ah(v+\tfrac{1}{2})/\pi[2\mu(D+c_2)]^{\frac{1}{2}}-a^2h^2(v+\tfrac{1}{2})^2/8\pi^2\mu. \tag{17}$$

Upon developing the coefficients in (17) and neglecting all powers of c_1/D beyond the second, we finally get

$$E=E_{el}+hc[\omega_e(v+\tfrac{1}{2})-x_e\omega_e(v+\tfrac{1}{2})^2]+hc\{j(j+1)B_e[1-(v+\tfrac{1}{2})[3(B_e/x_e\omega_e)^{\frac{1}{2}}-3(B_e/x_e\omega_e)]2x_e+\cdots]\}$$
$$-hc(4B_e^3/\omega_e^2)[j(j+1)]^2+\cdots. \tag{18}$$

On comparing (18) with (3), it is seen that

$$\alpha_e=2x_eB_e[3(B_e/x_e\omega_e)^{\frac{1}{2}}-3(B_e/x_e\omega_e)], \tag{19}$$

$$D_e=-4B_e^3/\omega_e^2. \tag{20}$$

We shall now compute by the perturbation method the contribution to the energy by the neglected part of the rotational term. Turning to Eq. (9) in the form

$$\frac{d^2R}{dr^2}+\frac{8\pi^2\mu}{h^2}\left[W-D^{-2a(r-r_e)}+2D^{-a(r-r_e)}-A\frac{r_e^2}{r^2}\right]R,$$

we see that the correction ϵ_1 for the energy will be given by

$$\epsilon_1=A\int_{-\infty}^{+\infty}R^2(r)\,V_1(r)dr=(A/a)\int_0^{\infty}R^2(y)\,V_1(y)y^{-1}dy=(A/a)\int_0^{\infty}R^2(z)\,V_1(z)z^{-1}dz, \tag{21}$$

where $V_1(y)$ stands for the terms after $(y-1)^2$ in (11). We can obtain $F(z)$ of Eq. (15) in a closed form by applying the Laplace[6] transformation

$$F(z)=\int e^{-zt}f(t)dt. \tag{22}$$

On substituting in (15) and integrating once partially, we obtain a linear differential equation for $f(t)$, which is easily integrated. We thus get

$$F(z)=(c/2\pi i)\oint e^{-zt}t^{-(1+v)}(1+t)^{(b+v)}dt, \tag{23}$$

where the path of integration is a circle—of an eventually vanishing radius—around the origin.[7] We have for the normalization condition,

$$\int_{-\infty}^{+\infty}R(r)^2dr=1=(N^2/a)\int_0^{\infty}R^2(z)z^{-1}dz$$
$$=(1/2\pi i)^2(N^2/a)\oint t^{-(1+v)}(1+t)^{v+b}dt\oint s^{-(1+v)}(1+s)^{v+b}ds\int_0^{\infty}z^{b-1}e^{-z(1+s+t)}dz.$$

$$\int_0^{\infty}z^{b-1}e^{-z(1+s+t)}dz=(1+s+t)^{-b}\Gamma(b)=\left[\sum_{i=0}^{\infty}\binom{-b}{i}(1+s)^{-b-i}t^i\right]\Gamma(b).$$

---

[6] R. Courant and D. Hilbert, *Methoden der Mathematischen Physik I*, Chapter 7.

[7] This is the correct path only when v is an integer.

$$\therefore \quad 1=(1/2\pi i)^2(N^2/a)\Gamma(b)\left[\sum_{i=0}^{\infty}\binom{-b}{i}\oint t^{-(1+v-i)}(1+t)^{v+b}dt\oint s^{-(1+v)}(1+s)^{v-i}ds\right]$$

$$=(1/2\pi i)(N^2/a)\Gamma(b)\left[\sum_{i=0}^{v}\binom{-b}{i}\binom{v+b}{v-i}\oint s^{-(1+v)}(1+s)^{v-i}ds\right]=(N^2/a)\Gamma(b)\cdot\binom{v+b}{v},$$

since $(1+s)^{v-i}$ has a power s^v only when $i=0$. It follows that

$$N_v=\left[a/\Gamma(b)\cdot\binom{v+b}{v}\right]^{\frac{1}{2}}. \tag{24}$$

Similarly:

$$\int_{-\infty}^{+\infty}R^2(r)z^k dr=(1/2\pi i)^2\left[\binom{b+v}{v}\cdot\Gamma(b)\right]^{-1}$$

$$\times\left[\oint t^{-(1+v)}(1+t)^{v+b}dt\oint s^{-(1+v)}(1+s)^{v+b}ds\int_0^{\infty}z^{b+k-1}e^{-z(1+s+t)}dz\right]$$

$$=(1/2\pi i)^2\left[\Gamma(b+k)/\Gamma(b)\binom{b+v}{v}\right]\left[\sum_{i=0}^{\infty}\binom{-b-k}{i}\oint t^{-(1+v-i)}(1+t)^{v+b}dt\oint s^{-(1+v)}(1+s)^{v-k-i}ds\right]$$

$$=(1/2\pi i)\left[\Gamma(b+k)/\Gamma(b)\binom{b+v}{v}\right]\left[\sum_{i=0}^{v}\binom{-b-k}{i}\binom{v+b}{v-i}\oint s^{-(1+v)}(1+s)^{v-k-i}ds\right]$$

$$=(1/2\pi i)\left[\Gamma(b+k)/\Gamma(b)\binom{b+v}{v}\right]\left[\sum_{i=0}^{v}\binom{-b-k}{v-i}\binom{v+b}{i}\oint s^{-(1+v)}(1+s)^{i-k}ds\right].$$

Now $(1+s)^{i-k}$ will have a power s^v only when $(i-k)$ is negative so that the last sum reduces to

$$\left[\Gamma(b+k)/\Gamma(b)\binom{b+v}{v}\right]\sum_{i=0}^{(k-1),\,v}\binom{-b-k}{v-i}\binom{v+b}{i}\binom{i-k}{v}=\int_{-\infty}^{+\infty}R^2(r)z^k dr, \tag{25}$$

where the summation is to be carried to the smaller one of the numbers $(k-1)$ and v. By writing out a few terms of the series it can be easily ascertained that

$$\sum_{i=0}^{k=1,\,v}\binom{-b-k}{v-i}\binom{v+b}{i}\binom{i-k}{v}=\binom{-b-k}{v}\binom{-k}{v}\left[1+\frac{(b+v)v(1-k)}{(-b-k-v+1)(-k-v+1)}\right.$$

$$\left.+\frac{(b+v)(b+v-1)v(v-1)(1-k)(2-k)}{2!(-b-k-v+1)(-b-k-v+2)(-k-v+1)(-k-v+2)}+\cdots\right]$$

$$=\binom{-b-k}{v}\binom{-k}{v}\mathbf{F}\left(\begin{matrix}-b-v,\ -v,\ 1-k\\ -b-k-v+1,\ -k-v+1\end{matrix};1\right). \tag{26}$$

The generalized hypergeometric function **F**, although of a simple form, is not one of either of the two types which can be summed in a closed form.[8] However, for the application in view its summation is not laborious. The first few polynomials of $\int R^2(r)z^k dr$ are given below:

[8] Hardy, Proc. Camb. Phil. Soc. **21**, 492 (1923).

$$k=0 \quad 1$$
$$k=1 \quad b$$
$$k=2 \quad b^2+2b(v+\tfrac{1}{2})$$
$$k=3 \quad b^3+6b^2(v+\tfrac{1}{2})+6b(v+\tfrac{1}{2})^2+\tfrac{1}{2}b$$
$$k=4 \quad b^4+12b^3(v+\tfrac{1}{2})+b^2[30(v+\tfrac{1}{2})^2+7/2]+20(v+\tfrac{1}{2})^3+7(v+\tfrac{1}{2}). \tag{27}$$

Carrying out now the integration of $[-\int R^2(r)(1-z/2d)^3dr]$ and $\int R^2(r)(1-z/2d)^4dr$, we find that the coefficients of $(v+\frac{1}{2})$ are $(-1/k^3)$ and $(-3/k^3)$, respectively. Since $(1/k)\backsimeq x_e$, it is clear that these terms are of a smaller order of magnitude than the terms for α_e in (19).

As a check on the above calculations, we compute the perturbation of the energy due to the first three terms in (11), using Morse's solution of (9), in which the rotational term was completely neglected. We find that

$$\epsilon_1=c_1+c_2+c-(2/k)(v+\tfrac{1}{2})(c_1+c_2)=A[1-6(v+\tfrac{1}{2})(ar_e-1)/ka^2r_e^2]. \tag{28}$$

This gives an expression for α_e which is identical with (19), but it does not contain the term $[j(j+1)]^2$ of (18). Now the smallness of the perturbation term for the energy shows that $R(z)$ is a close approximation to the wave function of a diatomic molecule whose energy equation conforms to (18).

Comparison with Experimental Results

Values of α_e were computed by (19) for the molecules for which the table of molecular constants in Jevons' *Report on Band Spectra of Diatomic Molecules* contains sufficient data. The ratio of these values to the observed values of α_e are given in the third column of Table I. The prefix H in this column signifies, in the notation of Jevons, that the vibrational coefficients are derived from band-spectra data; where there is no H, the coefficients are derived from band-origin data. The sign to the right in this column gives the sign of $y_e\omega_e$ when it is known. The agreement is generally good, the discrepancies being within the probable error in the data. Some of the molecules which contain a cubic term in the vibrational energy equation, and for which therefore the present theory is strictly not applicable, show considerable deviations of α_e from the computed values. In most cases of large discrepancies

Table I. *Comparison of experimental and computed values of α_e. Values of $3(B_e/x_e\omega_e)^{\frac{1}{2}}-3B_e/x_e\omega_e(\equiv F)$.*

Molecule	State	α_e comp. / α_e obs.	F	Molecule	State	α_e comp. / α_e obs.	F	Molecule	State	α_e comp. / α_e obs.	F	Molecule	State	α_e comp. / α_e obs.	F
CuH	A	0.96	0.72	CdH	B	0.8 +	0.72	Na_2	C	H 1.01 −	0.74	BO	X	0.93	0.71
	X	.89	.75		A	.74	.73		B	H 1.25	.75	AlO	B	.83	.72
AgH	A	1.11	.59		X	.85 −	.68		A	H 1.28 +	.75		X	1.01	.63
	X	0.91	.74	HgH^+	A	.92 −	.73	K_2	C	H 1.45	.68	CO	B	H 1.5	.48
AuH	A	1.05	.62	HgH	X	1.19 +	.53		A	H 1.41	.72		A	H 0.97	.64
	X	1.02	.73	AlH	A	0.87	.75	C_2	d	1.38	.53	SiO	$^1\Pi$	H .90 +	.65
BeH^+	$^1\Sigma^+$	0.67 −	.63	BiH	A	.71	.75		B	1.39	.63		X	H .97 +	.68
	$^1\Sigma^+$	.94 −	.75		X	.64	.72		b	0.97	.69	TiO	C	H .95	.66
BeH	$^2\Pi$	.92 −	.75	OH	$^2\Sigma^+$	.92	.73		A	1.10	.70		X	H 1.18	.68
	$^2\Sigma^+$	.96 −	.75	HF	$^1\Sigma$	.47	.69	CN	B	1.07 −	.64	PbO	D	H 1.3	.75
MgH^+	$^1\Sigma^+$	.96	.66	HCl	$^1\Sigma$	.90	.74		A	0.97	.69		A	H 1.0	.60
	$^1\Sigma^+$	1.02	.74	BeF	A	.95	.72		X	.99	.71		X	H 1.0	.61
MgH	A	1.0	.73		X	.92	.72	SiN	B	1.12 +	.49	NO	B	0.64	.72
	X	1.0	.74	Cl_2	O	H 1.0	.43		X	0.98	.67		B	.94	.71
CaH	D	7	.60		$^1\Sigma^+$	H 1.1	.56	N_2^+	B	.94 −	.64		A	1.2	.68
	B	1.1	.75	Br_2	B	H 0.86 −	.47		X	1.0 −	.68		X	0.95	.68
	A	1.0	.75		X	H 1.2	.68	N_2	B	H 0.81	.67		X	.97	.68
	X	0.95	.75	ICl	A	H 0.8	.45		A	H 1.4	.65	O_2^+	A	H 1.4	.60
ZnH^+	$^1\Sigma^+$	H .9	.71		X	H .54	.59	P_2	a	H 0.83 −	.68		X	H 2.	.64
	$^1\Sigma^+$	H .89 −	.74	I_2	B	H 1.0	.46		X	H .93 −	.67	O_2	B	1.1	.58
CdH^+	$^1\Sigma^+$	H .37	.47		X	H 1.0	.56	BeO	C	H .83	.74		A	0.94 −	.65
	$^1\Sigma^+$	H 1.0 −	.73	Li_2	C	H 1.05 −	.74		B	H .93	.72		X	.91	.69
					B	H 1	.73		A	H 1.00	.70	SO	B	H .91	.63
					A	H 1.00 −	.75						X	.93	.67

there is also considerable deviation of the factor in brackets of Eq. (19) from its mean value. This factor has for the 93 tabulated molecules a mean value of 0.67 with a mean deviation of 0.06.

We may therefore expect that the wave functions of Morse, as presently modified, give a satisfactory representation of vibration and rotation states of a diatomic molecule whose energy equation does not contain any appreciable cubic term in $(v+\frac{1}{2})$. With these functions it should be possible to determine the probabilities of transition between a state (j', v') of one electronic state to a state $(j'' v'')$ of another electronic state of the molecule. We shall have occasion to return to this matter in another communication.

The author wishes to express his appreciation and gratitude to Professor D. H. Menzel and to Professor P. M. Morse for advice and helpful suggestions.

The Value of e/m from the Zeeman Effect

L. E. KINSLER AND W. V. HOUSTON, *Norman Bridge Laboratory of Physics, California Institute of Technology*
(Received November 7, 1933)

The measurement of e/m from the Zeeman effect of the red singlet lines of Cd and Zn has been repeated with careful attention to all of the sources of experimental uncertainty. The magnetic field has been measured, under the actual conditions of operation, with an uncertainty of about one part in three thousand. The final result is

$$e/m = 1.7570 \pm 0.0010.$$

IN the report published about two years ago on the determination of e/m from the Zeeman effect,[1] the value was given as $e/m = 1.7579 \pm 0.0025$ e.m.u. This work confirmed the "spectroscopic value" in being much lower than the older "deflection values" but was considerably lower than the spectroscopic values previously reported.[2] The precision was not great enough, however, to make sure whether this new discrepancy was real or not. The present paper is a report of the continuance of this work in the effort to reduce the uncertainty of the result. The apparatus and the methods have not been essentially changed so the reader is referred to the previous paper for details of the experimental arrangement.

The major cause of uncertainty in the published value was the uncertainty in the magnetic field. The two methods used in its determination gave slightly different results and so a large part of the present work has been directed toward the removal of this source of uncertainty. We have given especial attention to the following points: (a) the duplication and interchange of all standards and instruments, resistances, standard solenoids, potentiometers, etc., to locate constant errors in the individual pieces; (b) the use of standard resistances and cells recently measured at the Bureau of Standards; (c) careful measurement and control of temperature, both because of its effect on resistance and its effect in causing expansion of solenoids; (d) the calibration of the solenoid both before and after its use in making spectroscopic measurements.

The equation for determining e/m by this method is

$$e/m = (4\pi c/K)(\Delta\nu/I)(1/\bar{a}).$$

We shall take up successively the determination of K, $\Delta\nu/I$, and $\bar{a}$.

Measurement of the Magnetic Field

The intensity of the magnetic field in absolute gauss was determined from the equation $H = KI$, where K is a constant to be determined experimentally and I is the current. The current was measured by a potentiometer and a standard resistance. The determination of K for weak fields and its use for strong fields is not satisfactory, because the rise of temperature and the mechanical stresses in the solenoid may affect this constant. It has therefore been necessary to determine K under the actual conditions of operation. This determination was made by comparison with long single-layer solenoids, whose constants could be computed from their dimensions.

a. The standard solenoids

Four different solenoids were used in the calibration. Two of these consisted of a single layer of No. 12 bare copper wire wound on linen Bakelite tubes which had been threaded to take ten turns per inch. The other two were wound with No. 20 enameled wire on tubes threaded for 28 turns per inch. One of these

[1] J. S. Campbell and W. V. Houston, Phys. Rev. **39**, 601 (1932).

[2] R. T. Birge, Phys. Rev. Supplement **1**, 1 (1929).

was wound on linen Bakelite and the other on a brass tube. All of these solenoids were slipped inside the large solenoid and were insulated from it, as was described in the previous paper.

The numbers of turns per centimeter were determined by measurement with a glass cathetometer scale used in such a way that coincidences were observed between the edges of turns and marks on the scale. This scale was calibrated against a Gaertner type M 1001 standard meter at Pomona College and also against a glass decimeter scale which belongs to the Mt. Wilson Observatory and which had been calibrated at the Bureau of Standards. Both calibrations led to the result that our glass scale is uniformly 0.032 percent too long at 21°C.

The Bakelite solenoids have the advantage that it is easy to avoid leaks between the winding and the tube but they also change in dimensions with the season of the year. This is presumably due to the change in humidity and the corresponding change in the moisture content of the Bakelite. This explanation is supported by the fact that all three Bakelite solenoids seem to change together at about the same rate. The turn density of the brass solenoid showed no measurable change at all and after careful winding it was not possible to detect any leak between the winding and the core.

These standard solenoids were usually used at a temperature slightly different from that at which they were measured. Consequently, it was necessary actually to measure the temperature and to hold it fairly constant during a series of readings. A temperature coefficient of 2×10^{-5} was applied to all of the solenoids. This coefficient is near to those of brass, copper and Bakelite. The validity of this correction is apparent from the greater coherence of measurements, made over a temperature range of 30°, when it is applied. Table I gives the data on the solenoids. The constants K_s of these solenoids are determined from the relation

$$K_s = 0.4\pi n \cos\alpha \cos\phi,$$

where n is the number of turns per cm, α is the angle subtended at the center by the radius of the end of the winding and ϕ is the pitch of the winding.

TABLE I. a. *Data on the standard solenoids.*

Solenoid	Effective diameter in cm	Length	$0.4\pi \cos\alpha \cos\phi$
Bakelite No. 1	6.00	89.7	1.25371±3
Bakelite No. 2	5.97	89.5	1.25374±1.5
Bakelite No. 3	5.92	90.4	1.25395±2
Brass	5.86	90.0	1.25397±2

b. *Measurement of Turn Density*

Solenoid	Date	Readings	Turns per cm	K_s
Bakelite No. 1	12/21/31	40	3.9326±4	4.9303±5
	1/29/32	30	3.9340±3	4.9321±4
Bakelite No. 2	12/21/31	50	3.9389±2	4.9384±3
	1/10/32	44	3.9403±7	4.9401±9
	6/20/32	60	3.9353±2	4.9338±3
	3/3/33	18	3.9406±3	4.9405±4
Bakelite No. 3	12/23/31	30	11.0295±15	13.8304±19
	2/4/32	34	11.0322±8	13.8338±11
Brass	12/23/31	30	11.0220±10	
	2/4/32	30	11.0232±5	13.8224±10
	2/1/33	30	11.0235±10	

b. Other measuring apparatus

All currents were measured with standard resistances and potentiometers. Four different potentiometers were used and these were checked against each other. In some cases deflection potentiometers were used but usually the ordinary type was preferred because of their greater sensitivity.

The one and ten ohm shunts were new ones, with certificates from the Bureau of Standards and negligible temperature coefficients. The other shunts were calibrated by the Bureau for several different currents. The same Weston standard cell was used for all measurements. It was compared at various times with new cells from the Bureau and found to be sufficiently constant. A final determination was made in comparison with two new cells kept in a thermostat. Over a three weeks' period the maximum deviation from the mean value was 0.008 percent and the mean value was 1.01857±0.00004 volts.

c. The null method calibration

The methods of making the calibration were described in detail in the previous paper. The null method consists in balancing the field of the large solenoid against that of a standard solenoid which is placed inside of it. The balance

is determined from the deflection of a ballistic galvanometer when a flip coil is turned over in the center of the solenoids. If I is the current in the large solenoid when the balance is obtained, and I_s is the current in the standard, then

$$K = K_s I_s / I.$$

Three flip coils were used. One contained 50,000 turns while the others contained 4000 and 7000 turns, respectively. The chief purpose of the null method was to test the reliability of the apparatus, the coherence of the standard solenoids and the constancy of the large solenoid with time. The results are summarized in Table II.

TABLE II. *Null method calibration.*

Solenoid	Date	No. values	Mean I_s/I	K_s	K
Bakelite No. 1	12/23/31	10	7.4768±10	4.9303	36.863±5
Bakelite No. 2	12/23/31	10	7.4665±11	4.9384	36.873±6
	6/28/32	8	7.4728±5	4.9338	36.869±3
Bakelite No. 3	12/24/31	10	2.6659±3	13.8304	36.870±6
Brass	12/25/31	8	2.6679±4	13.8224	36.877±6
	12/5/32	8	2.6677±2	13.8224	36.874±4
			Mean		36.871±5

d. The mutual inductance calibration

The essential point of this method is to compare the throw of a ballistic galvanometer when the flip coil is turned over with its throw when the current is reversed in the primary of a mutual inductance. In this way it is possible to obtain a relation between the strength of the magnetic field and the magnitude of the mutual inductance. By doing this both with the large solenoid and with the standards, K can be determined from the relation $K = K_s(I_s'/I_m')(I_m/I)$. I_s' is the current in the standard solenoid for which the throw is equal to that with I_m' in the primary of the mutual, while I is the current in the large solenoid which gives the same throw as the current I_m in the mutual. The accuracy and reliability of this method depend upon the following factors:

(1) The constant of the galvanometer must not change during the calibration of any one solenoid against the mutual inductance. The effects of all the solenoids on the galvanometer were eliminated by removing it to a room some 40 feet distant. The stray magnetic field at this distance was negligible. Deflections of about constant magnitude and the same direction were always used. With these precautions the galvanometer readings showed the required consistency.

(2) The method also requires that the mutual inductance shall have the same value for a wide range of currents in its primary. It was necessary to change the current by a factor of 200. Two different mutual inductances were used. The first was described in the previous paper. The second was larger and was used in a different location. Both were made without any trace of ferromagnetic material and were placed as far as possible from the floor and ceiling which might have contained steel reinforcement. Both coils led to the same result, as can be seen from Table III. As a further check upon this constancy, the deflection due to the reversal of different currents in the primary was compared with the steady deflection due to constant currents through the galvanometer. This showed that the mutual inductance was constant with an uncertainty of less than 0.03 percent.

TABLE III. a. *Calibration of the mutual inductances with standard solenoids.*

Solenoid	I_s/I_m	K_s	$K_s I_s/I_m$	Mean
Mutual inductance No. 1 in January, 1932				
Bakelite No. 1	95516±14	4.9321	47109±8	
Bakelite No. 2	95341±15	4.9401	47099±11	47098±11
Bakelite No. 3	34048±7	13.8338	47101±11	
Brass	34063±9	13.8224	47083±13	
Mutual inductance No. 2 in March, 1933				
Bakelite No. 2	27089±3	4.9405	133833±18	133843±21
Brass	96840±17	13.8224	133856±25	

b. *Calibration of the large solenoid in terms of the mutual inductances*

Current amp.	Mutual No. 1 January, 1932 I_m/I	K	Mutual No. 2 March, 1933 I_m/I	K
1	78266±16	36.862±9	27546±8	36.868±11
5			27549±4	36.872±7
15	78266±32	36.862±15		
150	78251±17	36.855±9		
190	78236±33	36.848±15	27529±6	36.846±9
Adopted value of K under operating conditions				36.835±12

(3) To be sure of the constancy of the flip coils two different ones were used. These gave internally consistent readings and agreed with each other. The flip coils were insulated from the surrounding solenoid by a glass tube.

(4) A fourth and very important factor in this method is the resistance of the galvanometer circuit. If this should change in any way, the deflection would change correspondingly. The two points at which heating could take place are the flip coil and the secondary of the mutual inductance. The flip coil might be expected to absorb heat from the surrounding solenoid, especially when a heavy current is being used. This was avoided by blowing a current of air around the glass tube which enclosed the flip coil. With this arrangement, temperature equilibrium was attained in about ten minutes and was maintained indefinitely. Some heating was found to occur in the secondary of the mutual inductance due to the current passing through it. This was reduced to a negligible amount by immersing the whole mutual inductance in a bath of transformer oil. These precautions kept the change of resistance to less than 0.02 percent during the time of a series of measurements.

Table III gives the results of the calibration with the mutual inductances. The values at the low currents are in good agreement with those obtained by the null method. At the higher currents the constant decreases somewhat. This may be attributed to two causes. In the first place, the mechanical stresses caused by the large currents may distort the winding enough to affect the constant. This effect would tend to lower the constant. In addition to this, the correction for the increase in temperature may be inadequate. All of the values in the table have been reduced to 22°C. The temperature of the solenoid was measured by measuring the temperature of the outside of the brass case and this was probably somewhat lower than the effective temperature in the winding. The measured temperature averaged around 40° for the heavy currents. Since, however, the Zeeman effect measurements and the calibration measurements were made under identical conditions, an error in this correction will have no effect upon the final result. The adopted value of K given in Table III differs from that tabulated for 190 amp. by the amount of this temperature correction and by 0.005 percent to change from international to absolute gauss. This adopted value, then, represents the constant of the solenoid as determined under the actual conditions of operation.

e. The measurement of the current

The other essential factor in the measurement of the magnetic field is the measurement of the current. This was measured by a potentiometer connected across the terminals of a 0.001 ohm resistance. This resistance was calibrated by the Bureau of Standards for two different currents. It showed a change of 9 parts in 10,000 between 60 amp. and 300 amp. This was evidently due to heating and so care was taken always to permit this shunt to attain approximate temperature equilibrium before use. By measuring the temperature changes, it was found that this procedure assured a constancy of this shunt to within 0.01 percent. The actual value of this shunt is of no importance in the final result, since it was used in the same way both for the calibration and for the spectroscopic work.

The constancy of the current was maintained within 0.015 percent by manual control of the current in the field coils of the motor-generator set.

Spectroscopic Measurements

The same interferometer and method was used as was described previously. The source of light was changed in that a stop was placed at the back of the constriction, so that no light could reach the spectrograph except that from the center of the magnetic field. It was also operated at a considerably lower temperature which made the lines somewhat sharper.

Photographs were taken for a range of currents at each separation of the interferometer plates. These currents were so selected as to be more or less evenly divided between those which gave too wide a separation of the components for even spacing in the interferometer pattern and those which gave too narrow a separation. In this way errors due to overlapping of the components were eliminated from the average. The currents used ranged from 175 amp. to 195 amp., while the interferometer separations

TABLE IV. *Spectroscopic measurements.*

Order difference	Cadmium λ6438 Number of plates	$2\Delta\nu/I$	Zinc λ6362 Number of plates	$2\Delta\nu/I$
1.5	2	34356±5		
3.5	12	34350±14	9	34352±22
4.5	18	34346±16	12	34355±19
Means		34348±15		34354±20
$\bar{a}$		0.99978		0.99996
$2\Delta\nu/Ia$		34356±15		34355±20
$2\pi c/K$		51141±17		51141±17
e/m				1.7570±0.0010

were such as to separate the Zeeman effect components from 1.5 to 4.5 orders of interference. Table IV shows the results of these measurements. These results appear to be lower than those previously given by about 0.1 percent. This is due to an error discovered in one of the potentiometers. This error also gives K close to the value previously reported, but, in fact, the difference in the final result should really be attributed to the magnetic measurements. The indicated uncertainties in $\Delta\nu/I$ represent the mean deviations of the values of this quantity from different plates. The uncertainty is essentially that in $\Delta\nu$, although there may be a little due to the uncertainty in the reading of the potentiometer and the control of the current.

The quantity $\bar{a}$ was determined theoretically in exactly the manner previously described. It involves the g factors of the levels involved. The uncertainty ascribed to the value of e/m is only that indicated by the spread of the experimental values and takes no account of the possible uncertainty in the theory of the Zeeman effect. The uncertainty indicated throughout is the mean deviation. Had probable errors been used their values would have been approximately one-half of the given deviations. In all of the tabulated data the agreement between various mean values is very close to that to be expected from the mean deviations.

The value we have obtained is in good agreement with the recent value of Dunnington[3] by a deflection method, and is certainly lower than the previously accepted spectroscopic value. The uncertainty has been reduced as far as it seems practical to go with the present apparatus.

[3] F. G. Dunnington, Phys. Rev. **43**, 404 (1933).

Some Physical Properties of Compressed Gases. IV. The Entropies of Nitrogen, Carbon Monoxide and Hydrogen

W. EDWARDS DEMING AND LOLA S. DEMING, *Fertilizer Investigations, Bureau of Chemistry and Soils, U. S. Department of Agriculture, Washington, D. C.*

(Received December 1, 1933)

Previous work on these gases has yielded values for the expansion coefficients $(T/v)(dv/dT)_p$, $-(p/v)(dv/dp)_T$, and for $-T(d^2v/dT^2)_p$ at temperatures between $-70°$ and $400°$ or $500°$C and at pressures between 25 and 1200 atmospheres. The evaluation of such derivatives renders possible the calculation of many physical properties of the substance. To those properties that have been reported previously for nitrogen, carbon monoxide and hydrogen, the authors now add the change in entropy $\Delta S = -\int_1^p (dv/dT)_p dp$ along isotherms. The integral is evaluated by graphical quadrature from the previously determined expansion coefficient $(T/v)(dv/dT)_p$. The absolute entropy at various pressures along an isotherm is then obtained by adding ΔS to the entropy at one atmosphere. The calculated values of ΔS are shown in a table, and the absolute entropies are shown by isotherms at various temperatures between $-75°$ and 600°C to 1200 atmospheres. With an ideal gas, the integral $\Delta S = -\int_1^p (dv/dT)_p dp$ would be simply $-R \ln p$ along all isotherms. The authors' calculations show that ΔS is always greater in absolute value than $R \ln p$, the difference being more pronounced at low temperatures and high pressures as would be expected. At 1200 atmospheres and at ordinary temperatures, all three gases have lost roughly 15 units of entropy. When an actual gas is compressed along an isotherm, $(dv/dT)_p$ has at first the value that it would have if the gas were ideal, namely, R/p, but it gradually becomes greater than R/p. This disparity continues until with sufficient pressure a point is reached where $(dv/dT)_p$ again becomes equal to, and finally less than, R/p. Eventually $(dv/dT)_p$ must become so small that $|p^c(dv/dT)_p|$ with $c>1$ remains bounded, in order that ΔS may be finite when p is infinite. The authors find that $(dv/dT)_p$ for these gases becomes equal to R/p at about 1200 atmospheres. If $(dv/dT)_p \leqq R/p$ and $p>1000$, the pressure must be raised to 2×10^6 atmospheres or higher to extract an additional 15 units of entropy. Hence it would seem impossible ever to reduce one of these gases above the critical temperature to a state of near zero entropy by the application of pressure alone, unless the graph of $(dv/dT)_p$ against p has humps or infinite discontinuities (giving convergent integrals) beyond 1000 atmospheres.

THE authors' graphical method for evaluating the derivatives $(T/v)(dv/dT)_p$, $-(p/v)(dv/dp)_T$, and $-T(d^2v/dT^2)_p$ from p, v, T data of gases has made possible the calculation of a number of physical properties. This method is especially applicable when the p, v, T data are taken at a large number of points in the temperature and pressure ranges covered, as fortunately happens to be the case with the compressibility work done by Bartlett and his co-workers at this laboratory. Calculations of density, temperature and pressure expansion coefficients, heat capacities at constant volume and constant pressure, fugacity and the Joule-Thomson coefficient have been published for nitrogen,[1] carbon monoxide[2] and hydrogen.[3] At the suggestion of our colleague Dr. Oliver R. Wulf, we have now included entropy in the calculations, and we wish at this time to present the results for the three gases just named.

With the temperature coefficient $(T/v)(dv/dT)_p$ already computed it is a simple matter to evaluate

$$\Delta S = -\int_1^p (dv/dT)_p dp \qquad (31)^*$$

graphically along isotherms, except at the low pressure end below 50 atmospheres where the steepness and curvature of the plots of $(dv/dT)_p$ against p rendered the work difficult and inexact. The integrations from 1 to 25 and from 1 to 50 atmospheres were accordingly performed analytically by the following procedure.

[1] W. Edwards Deming and Lola E. Shupe, Phys. Rev. **37**, 638 (1931).

[2] W. Edwards Deming and Lola E. Shupe, Phys. Rev. **38**, 2245 (1931).

[3] W. Edwards Deming and Lola E. Shupe, Phys. Rev. **40**, 848 (1932).

* The equations, figures and tables in this article will be numbered as continuations from the previous ones.

The integrand can be written as the product of the two factors v/T and $(T/v)(dv/dT)_p$, and both of these factors can be expressed by a series in p. Examination of the published Tables I, II and III suggests that the expansion coefficients can probably be well represented along isotherms by the series

$$(T/v)(dv/dT)_p = 1 + a'p + b'p^2,$$
$$-(p/v)(dv/dp)_T = 1 + ap + bp^2,$$

up to about 100 atmospheres. The adjustable parameters in these series were determined by fitting them to the published values of the expansion coefficients along each isotherm. All four parameters would of course be zero if the gas were ideal.

By integration of the second series with the condition that $pv = RT$ at $p = 0$, it is easy to deduce that

$$v = (RT/p)e^{-(ap+\frac{1}{2}bp^2)}$$
$$\doteq (RT/p)[1 - ap + \tfrac{1}{2}(a^2 - b)p^2]$$

closely enough. Thence

$$\Delta S = -\int_1^p (dv/dT)_p dp = -(1/T)\int_1^p v(T/v)(dv/dT)_p dp$$
$$= -(1/T)\int_1^p (RT/p)[1 - ap + \tfrac{1}{2}(a^2 - b)p^2][1 + a'p + b'p^2]dp$$
$$= -R[\ln p/1 + (a' - a)(p - 1) + \tfrac{1}{2}(b' - aa' + \tfrac{1}{2}a^2 - \tfrac{1}{2}b)(p^2 - 1^2)].$$

In this manner the integrations along isotherms were performed up to 25, 50 and 75 atmospheres. The last limit was included to permit comparison of the analytical and graphical methods in the vicinity of 50 atmospheres, and to tie together the results of the upper and lower ranges.

In this paper we have used $R = 1.9869$ cal./mol·deg. as given by the I.C.T., so that our values with Johnston's (*vide infra*) will form a consistent set. The values of ΔS are shown in Table IV. The hydrogen is probably closely a 3 : 1 orthopara mixture at all the temperatures and pressures in Bartlett's compressibility work.

There seems to be no reliable way of estimating the probable errors of the entries in Table IV. Below 100 atmospheres and above -25°C, we venture to suggest 0.02 cal./mol·deg. as a conservative estimate of the probable error in ΔS. At lower temperatures and higher pressures the precision will be less. At 1000 atmospheres the probable error may be as high as 0.1. Values listed above 1000 atmospheres, and those above 400°C and below -70°C, were obtained by extrapolating p, v, T data on suitable charts, and may therefore have still lower precision. These estimates of probable errors apply as well to the absolute entropies obtained by adding ΔS to the absolute entropy at 1 atmosphere (*vide infra*), since values of the latter are subject to practically no experimental error. However, *relative* changes in entropy, obtained by subtracting one value from another not far removed on the same isotherm should be fairly exact, and for this reason two decimals are listed throughout Table IV.

To get absolute entropies, ΔS must be added to S', the entropy of the *actual* gas at one atmosphere. Absolute entropies at one atmosphere calculated from spectroscopic data are for the gas in the *ideal* state, and it is necessary to make proper correction. The difference between the entropy of the gas in the actual state and the entropy of the same gas in the ideal state is

$$S_{act} - S_{ideal} = -\int_0^p \{(dv/dT) - (dv/dT)_{id}\}dp$$
$$= -\int_0^p \{(dv/dT) - RT/p\}dp$$
$$= -\int_0^p \{(dv/dT) - v/T \doteq \alpha/T\}dp \qquad (32)$$
$$= -(1/T)\int_0^p \mu C_p dp + (1/T)\int_0^p \alpha dp,$$

TABLE IV. *The decrease in the entropies of nitrogen, carbon monoxide and hydrogen along isotherms, from their entropies at one atmosphere.* The units are calories per mol per degree.

		Pressure in Atmospheres													
t°C	Gas	25	50	75	100	150	200	300	400	500	600	800	1000	1100	1200
−75	H_2	6.43	7.84	8.69	9.28	10.14	10.75	11.63	12.25	12.73	13.13	13.74	14.21	14.41	14.59
−70	CO	6.67	8.32	9.44	10.31	11.61	12.51	13.65	14.31	14.81	15.24	15.89	16.40	16.62	16.81
	N_2	6.65	8.38	9.48	10.34	11.60	12.46	13.52	14.22	14.73	15.14	15.77	16.27	16.47	16.65
−50	H_2	6.42	7.82	8.66	9.25	10.10	10.70	11.56	12.17	12.66	13.05	13.66	14.12	14.32	14.49
	CO	6.65	8.18	9.24	10.04	11.23	12.07	13.17	13.87	14.39	14.80	15.46	15.96	16.17	16.36
	N_2	6.62	8.26	9.31	10.10	11.31	12.17	13.25	13.95	14.47	14.88	15.52	16.03	16.24	16.42
−25	H_2	6.42	7.81	8.64	9.23	10.05	10.65	11.49	12.10	12.57	12.95	13.56	14.02	14.22	14.39
	CO	6.59	8.12	9.11	9.87	10.96	11.75	12.82	13.54	14.07	14.48	15.14	15.64	15.85	16.04
	N_2	6.58	8.21	9.19	9.92	11.03	11.82	12.89	13.60	14.13	14.54	15.20	15.70	15.91	16.11
0	H_2	6.41	7.80	8.63	9.21	10.04	10.63	11.47	12.08	12.54	12.92	13.52	13.98	14.18	14.36
	CO	6.55	8.03	8.99	9.70	10.74	11.50	12.54	13.25	13.80	14.22	14.88	15.36	15.57	15.76
	N_2	6.53	8.14	9.08	9.78	10.82	11.57	12.63	13.35	13.89	14.32	14.98	15.49	15.71	15.91
20	N_2	6.51	8.02	8.94	9.62	10.62	11.37	12.40	13.12	13.66	14.10	14.76	15.28	15.50	15.71
25	H_2	6.41	7.77	8.60	9.19	10.02	10.62	11.46	12.06	12.53	12.91	13.50	13.96	14.16	14.33
	CO	6.53	7.98	8.92	9.60	10.61	11.34	12.38	13.09	13.63	14.06	14.71	15.21	15.42	15.62
50	H_2	6.41	7.79	8.60	9.18	10.01	10.60	11.43	12.03	12.49	12.86	13.45	13.91	14.10	14.27
	CO	6.51	7.94	8.85	9.52	10.51	11.22	12.22	12.94	13.48	13.91	14.57	15.07	15.29	15.48
	N_2	6.48	7.97	8.86	9.52	10.48	11.18	12.19	12.91	13.45	13.89	14.56	15.08	15.31	15.57
100	H_2	6.40	7.79	8.60	9.18	10.01	10.59	11.41	12.00	12.46	12.84	13.42	13.87	14.07	14.24
	CO	6.48	7.87	8.76	9.40	10.34	11.03	12.01	12.71	13.25	13.68	14.34	14.86	15.08	15.27
	N_2	6.46	7.91	8.77	9.40	10.32	10.99	11.94	12.64	13.17	13.61	14.28	14.81	15.03	15.24
150	CO	6.46	7.89	8.77	9.40	10.31	10.97	11.93	12.62	13.15	13.58	14.26	14.79	15.01	15.20
200	H_2	6.40	7.79	8.61	9.18	10.00	10.57	11.39	11.98	12.43	12.80	13.38	13.83	14.02	14.20
	CO	6.45	7.85	8.71	9.33	10.22	10.87	11.81	12.50	13.02	13.46	14.14	14.67	14.89	15.09
	N_2	6.44	7.90	8.74	9.35	10.22	10.85	11.75	12.40	12.91	13.33	13.98	14.49	14.70	14.90
300	H_2	6.40	7.78	8.59	9.17	9.98	10.55	11.36	11.95	12.40	12.77	13.35	13.79	13.99	14.16
	CO	6.43	7.81	8.65	9.26	10.13	10.76	11.67	12.32	12.84	13.26	13.92	14.44	14.66	14.86
	N_2	6.42	7.86	8.68	9.28	10.12	10.73	11.59	12.21	12.69	13.09	13.72	14.20	14.41	14.60
400	H_2	6.40	7.77	8.58	9.16	9.96	10.54	11.35	11.93	12.38	12.75	13.32	13.77	13.96	14.14
	CO	6.42	7.77	8.60	9.19	10.04	10.65	11.53	12.17	12.68	13.09	13.75	14.27	14.48	14.68
	N_2	6.40	7.80	8.62	9.21	10.05	10.64	11.49	12.09	12.56	12.95	13.56	14.04	14.24	14.43
500	H_2	6.40	7.76	8.58	9.16	9.96	10.54	11.35	11.93	12.38	12.75	13.32	13.77	13.96	14.14
	N_2	6.40	7.82	8.63	9.21	10.03	10.61	11.45	12.05	12.51	12.89	13.50	13.97	14.17	14.36
600	N_2	6.40	7.82	8.64	9.22	10.04	10.62	11.44	12.03	12.49	12.87	13.47	13.94	14.14	14.32
		For Comparison													
	Ideal	6.40	7.77	8.58	9.15	9.96	10.53	11.33	11.90	12.35	12.71	13.28	13.73	13.91	14.09

where $\alpha = RT/p - v = -v(RT/pv - 1)$, and μ and C_p denote the Joule-Thomson coefficient and the heat capacity at constant pressure. The derivatives (dv/dT) are understood to be taken at constant pressure, and refer to the actual gas unless written with the subscript "*id.*" If the upper limit is one atmosphere the integrands may be considered constant over the interval of integration, so at one atmosphere the last equation gives

$$S' - S^\circ = -\mu C_p/T + \alpha/T, \tag{33}$$

wherein μC_p and α are to be evaluated anywhere in the neighborhood of zero pressure. This can be done by means of the tables already published, remembering that $-\alpha$ at $p=0$ is the second virial coefficient. The corrections $S' - S^\circ$ vary

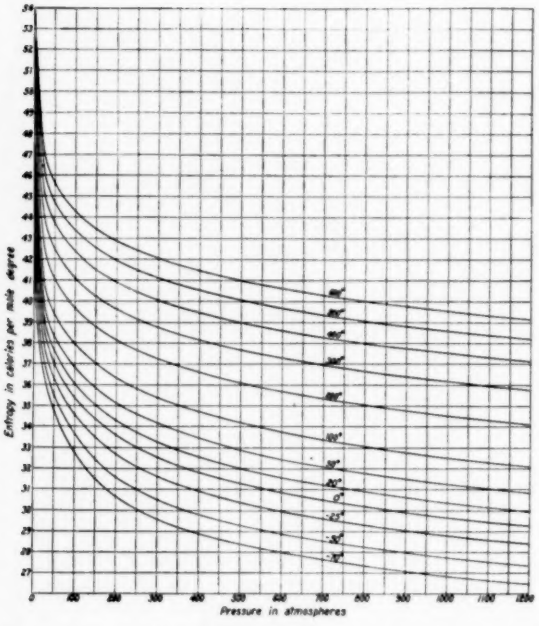

FIG. 25. The entropy of nitrogen along various isotherms as a function of pressure.

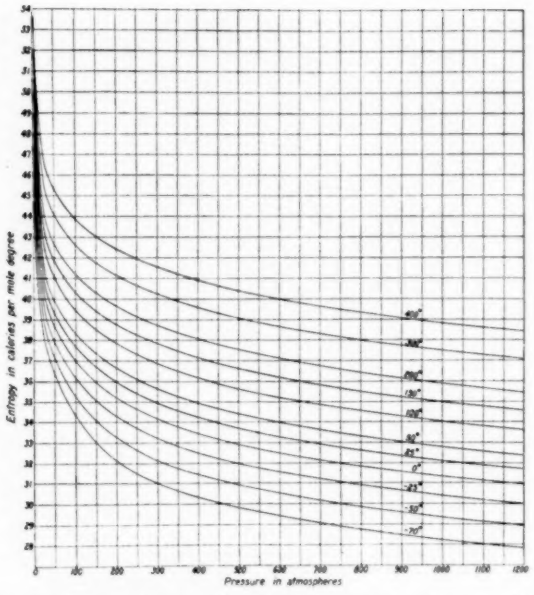

FIG. 26. The entropy of carbon monoxide along various isotherms as a function of pressure.

from negligible amounts up to several hundredths cal./mol·deg., as shown in Table V.

The values of $S°$ were kindly furnished by Professor H. L. Johnston and Mr. C. O. Davis of Ohio State University, who interpolated their data for us in advance of publication.[4]

The values of S found by adding ΔS to S' are shown by the isotherms of Figs. 25, 26 and 27.

TABLE V. *The absolute entropy $S°$ of ideal hydrogen, carbon monoxide and nitrogen at one atmosphere, furnished by H. L. Johnston and C. O. Davis.*

The difference $S'-S°$ between the entropy of the ideal gas and the actual gas at one atmosphere $S'-S°=\mu C_p/T-\alpha/T$. The units are calories per mol per degree. μC_p and α are found from previous publications, see footnotes 1, 2, 3. Nuclear spin excluded.

	Hydrogen (3 : 1)		Carbon Monoxide		Nitrogen	
t °C	$S°$	$S'-S°$	$S°$	$S'-S°$	$S°$	$S'-S°$
−75	28.474	−0.008				
−70			44.643	0.005	43.118	−0.019
−50	29.257	.008	45.296	.002	43.770	− .016
−25	29.970	.019	46.035	.000	44.507	− .013
0	30.624	.024	46.703	−.002	45.176	− .010
25	31.225	.027	47.313	−.003	45.786	− .007
50	31.782	.029	47.874	−.005	46.346	− .006
100	32.784	.059	48.878	−.005	47.352	− .004
150			49.760	−.006		
200	34.437	.027	50.549	−.006	49.012	− .002
300	35.779	.024	51.921	−.006	50.368	− .001
400	36.914	.022	53.097	−.006	51.536	.000
500	37.883	.020			52.559	.000
600					53.477	.000

[4] H. L. Johnston and C. O. Davis, J. Am. Chem. Soc., to appear.

DISCUSSION

If the gas were ideal, the values of $-\Delta S$ would be merely $R \ln p$ at all temperatures. Values of $R \ln p$ are shown at the bottom of Table IV for comparison with the values of $-\Delta S$ obtained for the actual gases. It will be noticed that the decrease in entropy of the actual gases

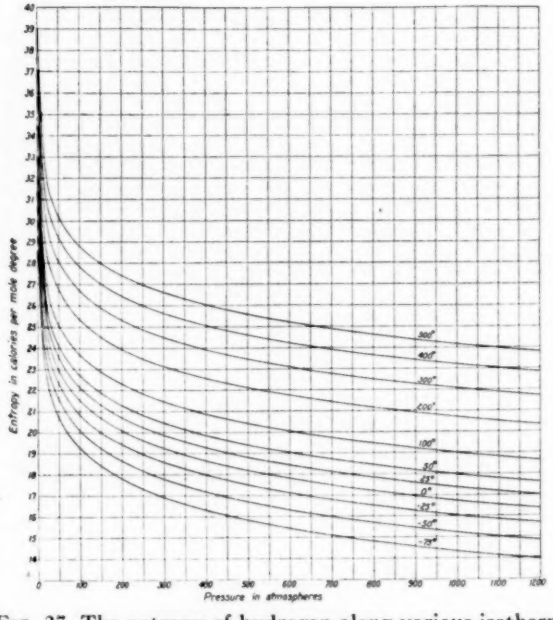

FIG. 27. The entropy of hydrogen along various isotherms as a function of pressure.

is in all cases greater than it would be for the ideal gas. This is to be expected at moderate pressures, for according to van der Waals' equation

$$(p+a/v^2)(v-b)=RT$$

we should have

$$(dv/dT)_p=R/(p-a/v^2+2ab/v^3)>R/p \quad (34)$$

and consequently

$$-\Delta S=\int_1^p (dv/dT)_p dp$$

$$=R\int_1^p (p-a/v^2+2ab/v^3)^{-1}dp>R\ln p. \quad (35)$$

This integral is divergent, as is easiest seen by transforming $(p-a/v^2+2ab/v^3)^{-1}dp$ into $d\ln(v-b)$. But if a substance be subjected to an ever increasing pressure at any temperature, its entropy must decrease to zero or possibly some finite amount,[5] so the integral for ΔS must be convergent and not divergent. Consequently van der Waals' equation must sooner or later break down. Indeed, for any actual gas, the integrand $(dv/dT)_p$ must at some pressure become and remain less than R/p, and in such a manner that

$$|p^c(dv/dT)_p| \text{ with } c>1$$

remains bounded, if the integral for ΔS is to be convergent.

Differences of ΔS from one pressure to another in Table IV indicate that for all three gases the integrand $(dv/dT)_p$ becomes equal to R/p at about 1200 atmospheres for all the isotherms here studied, because the changes in ΔS that accompany changes in pressure from 1000 to 1100 and from 1100 to 1200 atmospheres are about the same as those of the ideal gas.

If a substance had the same value of $(dv/dT)_p$ as the ideal gas, namely R/p, a change of pressure from 1000 to 2×10^6 atmospheres would be required to extract 15 more units of entropy. Hence, it would seem that if one of these gases is to be reduced to a state of zero entropy by the application of pressure, there must be humps or infinite discontinuities (giving convergent integrals) in the graph of $(dv/dT)_p$ against p, somewhere above 1000 atmospheres.

In conclusion the authors wish to express their indebtedness to Dr. Oliver R. Wulf for suggesting these calculations and for his continued interest and help. Professor H. L. Johnston and Mr. C. O. Davis furnished the values of $S°$.

[5] G. N. Lewis, Zeits. f. physik. Chemie **130**, 532 (1927).

LETTERS TO THE EDITOR

Prompt publication of brief reports of important discoveries in physics may be secured by addressing them to this department. Closing dates for this department are, for the first issue of the month, the twentieth of the preceding month; for the second issue, the fifth of the month. The Board of Editors does not hold itself responsible for the opinions expressed by the correspondents.

Note on the Repetition of the Michelson-Morley Experiment

In a very interesting report[1] on his ether-drift experiments, Mr. Miller compares his positive ether-drift effect with the negative results of other experimenters of whom I myself am one.[2] Mr. Miller finds the cause of the discrepancy in the fact that I enclosed the optical arrangement in a metal case and worked in a massive building, as did the other experimenters cited by Mr. Miller. I did so, of course, in order to eliminate disturbances caused by local and temporal variations of temperature. For if, assuming a length of the light path of 30 m, one calculates what difference in temperature of the two branches of the interferometer produces a displacement of 1/10 of a fringe (this is the order of magnitude observed). One gets the astonishing result that a difference of 1/500° is sufficient. The mere warmth of the body of the observer who, in Mr. Miller's experiments, stands near the interferometer can produce such an effect. But the question whether the ether penetrates the walls of a building, from the point of view of any ether theory, is decided by the fact that in the Sagnac and the Michelson-Gale experiments one gets the full displacement expected from the theory of a resting ether. To make use of this result in an experiment which, without the best protection against disturbances by temperature, is hardly performable, is but a natural chain of reasoning. As in general one cannot answer all questions of a physical complex by only one experiment, one must draw conclusions from the whole experimental material. Therefore I think that my experimental arrangement is apt to decide the question whether the ether drift exists or not and that it is not—as readers of the paper of Mr. Miller might be inclined to think—an arrangement adopted to prove a preconception.

GEORG JOOS
Physikalisches Institut der Universität, Jena,
November 11, 1933.

[1] D. C. Miller, Rev. Mod. Phys. **5**, 203 (1933).
[2] G. Joos, Ann. d. Physik **7**, 385 (1930).

Comments on Dr. Georg Joos's Criticism of the Ether-Drift Experiment

A small change in the temperature of the air in the entire light path of the interferometer of the order of magnitude given by Professor Joos would produce a displacement of the fringe system of 0.1 of a fringe width, the *entire* light path being uniformly heated. When Morley and Miller designed their interferometer in 1904, they were fully cognizant of this fact, and it has never since been neglected.[1] Elaborate tests have been made under natural conditions, and especially with artificial heating, for the development of methods which would be free from this effect.

It should be borne in mind that the ether-drift observation does not depend upon any absolute reading, nor even upon a simple displacement of the fringes; it depends upon a *regularly periodic variation* in the position of the entire fringe system, and the period is *twenty-five seconds throughout*. The temperature would have to increase and *decrease*, with periodic regularity in each twenty-five seconds! to produce the results. Any irregular fluctuation will be eliminated in the long series of turns. The observer maintains a constant relation to the apparatus and if the warmth of the observer's body is effective, it would be a continual heating effect which produces a *continuous* drift of the fringes, which is of no effect in the calculated results. The body cannot *cool and heat* the air, alternately every twenty-five seconds, and by variable amounts which depend upon the sidereal time.

The ether drift reported cannot be due to the heating of the house; elaborate analyses have been made to detect such effects. The effects are wholly independent of the sun's heat, of day and night, of summer and winter.

It seems quite sufficient that throughout the thousands of observations, the results are found to vary in both magnitude and azimuth in a systematic manner, depending upon sidereal time, and upon the varying combinations of cosmical and orbital motions, as is fully explained in the printed report.

DAYTON C. MILLER
Case School of Applied Science,
Cleveland, Ohio,
December 26, 1933.

[1] See D. C. Miller, Rev. Mod. Phys. **5**, 203 (1933), especially pages 212, 213, 215, 220, etc.

Large Artificial Crystals of Graphite

Professor Goetz and his collaborators[1, 2] have recently described a new method of producing "large artificial crystals of graphite." Chemically purified graphite particles, of more or less uniform size, are dispersed in a liquid gelatine solution, and the medium is placed in a strong magnetic field; there will naturally result a reorientation of the particles. If the medium is allowed to solidify in the presence of the magnetic field, the solidified mass will contain, embedded in it, a large number of graphite particles having the same orientations as were imposed on them by the field when the medium was still liquid. Professor Goetz assumes that the particles will then be crystallographically parallel to one another, and the medium will be similar to a large single crystal.

It appears to me that under the conditions of the above experiment, the graphite particles will not be parallel to one another. As is well known, a graphite crystal exhibits a large magnetic anisotropy, its diamagnetic susceptibility along its hexagonal axis, *viz.*, $\chi_{\|}$, being several times greater than the susceptibility, $\chi_{\perp}$, for directions in its basal plane. Because of this anisotropy, the magnetic field will exert a strong orienting couple on the particles (the couple due to the asymmetric *shape* of the particles will be much smaller in comparison, even in fields of strong inhomogeneity). The crystal flakes will therefore orient themselves in such manner as to bring their basal planes parallel to the direction of the field, i.e., parallel to a line, and therefore *not necessarily parallel to one another*. Indeed, if their orientations are determined solely by the magnetic field (the settling down of the particles under gravity being supposed to have no influence), the hexagonal axes of the different crystals will be oriented at random in the equatorial plane, i.e., in the plane normal to the direction of the field.

If this view is correct, the value $\chi_{\|}/\chi_{\perp}=28$, obtained by Goetz and Faessler[2] from measurements on such orientated graphite particles, on the assumption that the particles are crystallographically parallel. must be taken to correspond to

$$\tfrac{1}{2}(\chi_{\|}+\chi_{\perp})/\chi_{\perp}=28,$$

i.e.,

$$\chi_{\|}/\chi_{\perp}=55.$$

In connection with this high value for $\chi_{\|}/\chi_{\perp}$, the results of magnetic measurements[3] by Guha and Roy in this laboratory, on some well-developed natural crystals of graphite, may be of interest. Their results are

$$\chi_{\|}=-22.8\times10^{-6} \text{ per g},$$

$$\chi_{\perp}=-0.4\times10^{-6} \text{ per g},$$

and hence

$$\chi_{\|}/\chi_{\perp}=57.$$

Because of the extreme smallness of $\chi_{\perp}$, its value will be sensitive to any traces of impurities that might be present in the crystal, and the above value of $\chi_{\|}/\chi_{\perp}$ will be uncertain to that extent. Its closeness, however, to the value deduced from the results of Goetz and Faessler, deserves mention.

K. S. KRISHNAN

210 Bowbazar Street,
Calcutta, India,
November 27, 1933.

[1] Goetz, Focke and Faessler, Phys. Rev. **39**, 169, 553 (1932).

[2] Goetz and Faessler, Phys. Rev. **40**, 1053A (1932).

[3] Reported in a recent communication to Nature.

Concerning the Tensor Nature of the Dielectric Constant and Magnetic Permeability in Anisotropic Media

It is commonly assumed that in weak fields the components of the electric displacement D in a crystal are connected with those of the electric field E by linear relations of the form

$$D_x=\epsilon_{11}E_x+\epsilon_{12}E_y+\epsilon_{13}E_z, \qquad (\epsilon_{ji}=\epsilon_{ij}). \tag{1}$$

There are also analogous relations in the magnetic case, where B, H, μ replace D, E, ϵ and to which all our discussion applies equally well. It is perhaps not entirely trivial to give a proof of (1) by means of quantum mechanics. To be sure, once it is granted that D is a linear function of E, one can show from very general energy considerations[1] that $\epsilon_{ij}=\epsilon_{ji}$, and of course the ϵ_{ij} must transform like a tensor since E, H are vectors. However, it is illuminating to show how (1) is proved from modern atomic theory, since the linearity is not immediately obvious when the Stark or Zeeman levels depend on the components of E or H in a complicated, irrational fashion,[2] as is the case when there is a Paschen-Back effect, or when there is a crystalline field with very little (e.g., with triclinic or monoclinic) symmetry. The proof is founded upon the theorem of the invariance of the spur or diagonal sum of any matrix. The partition function $Z=\Sigma_a e^{-W_a/kT}$ may superficially appear to be very complicated in its dependence on E because the energies W of the individual states may involve E_x, E_y, E_z in a rather complex fashion, as already noted. However, after we perform the summation over all the states, Z depends on the components of E in the simple power form

$$Z=Z_0[1+\Sigma_i\alpha_iE_i+\Sigma_{ij}\beta_{ij}E_iE_j+\cdots], \quad (\beta_{ij}=\beta_{ji}) \tag{2}$$

devoid of irrationalities. This is proved by noting that Z

[1] Cf., for instance, J. H. Jeans, *Electricity and Magnetism*, Section 170. 4th Ed.

[2] For an example of energy formulas which involve the field strength under the radical sign, see Eq. (13) of Jordahl's paper in this issue. More generally, an nth rather than square root may be encountered.

is equal to the matrix invariant,[3] Spur $e^{-\mathbf{H}/kT}$. Now the Hamiltonian matrix $\mathbf{H}$ has the structure

$$\mathbf{H}=\mathbf{H}_0+\mathbf{p}_xE_x+\mathbf{p}_yE_y+\mathbf{p}_zE_z,$$

where $\mathbf{p}_x$, $\mathbf{p}_y$, $\mathbf{p}_z$ are the components of the electric moment matrices of the structural unit (atom, molecule or microcrystal) along the three coordinate axes. In the final system of representation which diagonalizes the total energy $\mathbf{H}$, the W_a's may be complicated functions of E_x, E_y, E_z but in the initial system, which is ordinarily used before application of the field, and which diagonalizes only $\mathbf{H}_0$, the elements of $\mathbf{H}_0$, $\mathbf{p}_x$, $\mathbf{p}_y$, $\mathbf{p}_z$ are all independent of E, so that the expansion of Z will take the form (2) when the matrices $e^{-\mathbf{H}/kT}$ are developed in a Taylor's series in E. Because of the invariance of the diagonal sum, the form (2) is, of course, also preserved in the final system. To prove Eqs. (1), we have only to note that the components of the polarization are given by formulas such as[4]

$$P_x=NkT\partial \log Z/\partial E_x. \tag{3}$$

The coefficients α_i in (2) vanish if there is no residual polarization, as we have tacitly assumed. Since $D_x=E_x+4\pi P_x$ we thus see that for small fields, Eqs. (1) are valid with $\epsilon_{ij}=\delta_{ij}+8\pi\beta_{ij}$. An analogous proof can, of course, also be constructed in classical theory. Classically, the partition function Z is an integral over phase space rather than the diagonal sum of a matrix, but still depends on E in the simple fashion (2).

Two incidental remarks about (1) are the following. (a) The coefficients ϵ_{ij} in (1) are functions of temperature due to changes in population of the different stationary states, as well as to changes in the constants of the crystalline structure. As O. M. Jordahl shows elsewhere in the present issue, the principal magnetic axes consequently may vary with temperature. (b) If a crystal has hexagonal symmetry two of the constants must be equal after the cross terms $\epsilon_{ij}(j\neq i)$ have been made to vanish by transformation to the principal magnetic axes. It is thus impossible to have different initial susceptibilities or Faraday rotations in different directions perpendicular to the "optic" axis in hexagonal crystals. This statement applies quite generally, even with Heisenberg exchange effects, interatomic valence forces, etc., provided only that saturation is neglected, since there is nothing in the above proof to prevent our taking the structural unit larger than a single atom or molecule. One thus must attribute to crystalline imperfections, or some other deviation from perfect hexagonality, the variations of the Verdet constant within a plane perpendicular to the optic axis which are reported by Becquerel[5] in his noteworthy investigations on tysonite at low temperatures.

J. H. Van Vleck

Physics Department,
University of Wisconsin,
November 30, 1933.

[3] The utility of considering the partition function as a matrix spur in systems of representation which do not diagonalize the total energy has been stressed by F. Bloch, Zeits. f. Physik **74**, 295 (1932); E. Wigner, Phys. Rev. **40**, 749 (1932), R. Serber, ibid. **43**, 1011 (1933). A development similar to (2) also has been utilized in Kramers' article on tysonite in Proc. Amsterdam Acad., 1933.

[4] For proof of (3) see J. H. Van Vleck, *The Theory of Electric and Magnetic Susceptibilities*, Eq. (46) of Chapter VI, and (3) of Chapter VII. The quantum mechanical proof of (46) given in Section 36 was intended only for isotropic media, but is extended to crystals without difficulty by regarding W as a function of E_x, E_y, E_z rather than of just E.

[5] J. Becquerel, Leiden Comm. 211c.

Quantum Statistics of Almost Classical Assemblies*

It is the object of the present note to call attention to a slight error in Eqs. (10), (20) and (21) of an article of the same title, which appeared in a recent number of this journal,[1] and to make a few supplementary remarks. The right-hand side of each of these equations should contain an extra factor, $1/N!$. The origin of this factor will be apparent from the following considerations.

The sum of states of a real gas, consisting of N molecules, may be expressed in the form,

$$\sigma=\int_{-\infty}^{+\infty}\cdots\int\sum_n\psi_n^*e^{-\beta H}\psi_n dq_1\cdots dq_{3N}, \tag{1}$$

where H is the Hamiltonian operator of the entire system, the ψ_n its characteristic functions, the q's are the configuration coordinates of the N molecules, and β is equal to $1/kT$. With the aid of the symmetric or the antisymmetric plane wave functions,

$$\Phi(p,q)=1/(N!)^{\frac{1}{2}}\sum_P(\pm1)^{|P|}\exp[(iP/h)\sum_{k=1}^{N}\mathbf{p}_k\cdot\mathbf{r}_k], \tag{2}$$

the orthogonal functions, ψ_n, may be expanded as Fourier integrals.

$$\psi_n(q)=\int_{-\infty}^{+\infty}\cdots\int S_n(p)\Phi(p,q)dp_1\cdots dp_{3N}. \tag{3}$$

When these expansions are substituted in Eq. (1), one obtains,

$$\sigma=\int_{-\infty}^{+\infty}\cdots\int\{\sum_n S_n^*(p')S_n(p)\}\{\Phi^*(p',q)e^{-\beta H}\Phi(p,q)\}dp'_1\cdots dp'_{3N}dp_1\cdots dp_{3N}dq_1\cdots dq_{3N}. \tag{4}$$

It may be shown without difficulty that functions, $S_n(p)$, which form a complete orthogonal set in momentum space, satisfy the following relation,

$$\sum_n S_n^*(p')S_n(p)=[1/N!(2\pi h)^N]\prod_{k=1}^{3N}\delta(p'_k-p_k), \tag{5}$$

where h is Planck's constant divided by 2π and $\delta(p'-p)$ is

* Contribution No. 322.

[1] J. G. Kirkwood, Phys. Rev. **44**, 31 (1933).

the Dirac delta-function. The error in the previous paper amounted to omitting the factor, $1/N!$, on the right-hand side of the above equation. The summation over the index, n, may be carried out with the aid of the completeness relation, Eq. (5), and the subsequent integrations over the $p'_1 \cdots p'_{3N}$, performed in the usual way.

$$\int_{-\infty}^{+\infty} F(p')\delta(p'-p)dp' = F(p). \quad (6)$$

Finally, one obtains,

$$\sigma = [1/N!(2\pi h)^N] \int_{-\infty}^{+\infty} \cdots \int \Phi^*(p, q) e^{-\beta H} \Phi(p, q) dp_1 \cdots dp_{3N} dq_1 \cdots dq_{3N}. \quad (7)$$

This equation becomes identical with Eq. (10) of the previous article, except for the extra factor $1/N!$, when the functions $\Phi(p, q)$, given by Eq. (2) are explicitly introduced. Since Eqs. (20) and (21) are merely modifications of Eq. (10), they must also contain this factor. The same result is obtained when the completeness relation for the configuration wave functions, $\psi_n(q)$, is employed, instead of that of the momentum wave functions, $S_n(p)$.

The additional factor, $1/N!$, while relatively trivial from a mathematical point of view, is of considerable physical importance. When the right side of Eq. (7) is expanded in powers of Planck's constant, and only the first term is retained, one obtains the following semiclassical expression for σ.

$$\sigma = [1/N!(2\pi h)^N] \int_{-\infty}^{+\infty} \cdots \int e^{-\beta H(p, q)} dp_1 \cdots dp_{3N} dq_1 \cdots dq_{3N}, \quad (8)$$

where $H(p, q)$ is the classical Hamiltonian function. The entropy of the system is given by the usual formula,

$$S = k[\log \sigma - \beta(\partial \log \sigma / \partial \beta)]. \quad (9)$$

Thus, the factor, $1/N!$, in σ provides the necessary term, $k(N - N \log N)$ in the entropy, after $\log N!$ has been approximated by Stirling's formula. In classical statistics, this factor, $1/N!$, has to be introduced somewhat arbitrarily. Gibbs accomplishes this by counting the group of $N!$ permutations or specific phases, included in each generic phase only once instead of $N!$ times. However, when classical statistics is treated as a limiting case of quantum statistics, the whole question is automatically taken care of by the symmetry restrictions imposed upon the wave functions by the Pauli exclusion principle.

JOHN G. KIRKWOOD
Research Laboratory of Physical Chemistry,
Massachusetts Institute of Technology,
December 7, 1933.

The Relative Abundance of the Lithium Isotopes

Although many attempts have been made to measure directly the relative abundance of the lithium isotopes the results so far reported are quite discordant. Bainbridge, in a paper describing his experiments on this problem,[1] has given a critical survey of the other work in this field. In this connection we thought it of interest to report the results of a set of experiments, extending over a period of several weeks, performed in connection with one of our laboratory courses.

A mass-spectrometer was constructed in the form of a glass tube bent in the shape of a semicircle having a filament and accelerating slit at one end and a slit and Faraday collector at the other. The walls of the tube were heavily silvered. The tube was surrounded by a solenoid capable of furnishing a magnetic field of 400 gauss. Lithium ions emitted by a spodumene coating on the filament described a semicircular path of 5.5 cm radius and those entering the collector were detected by means of an electrometer. The resolving power was sufficient to separate isotopes 6 and 7 quite well. The total emission from the filament was measured with a galvanometer. The conditions specified by Bainbridge,[1] that (1) the emission be not limited by space charge and (2) that ions reach the collector by identical paths, were fulfilled.

The results of a number of determinations for the current ratio Li^7/Li^6 all fell between 8 and 9 with an average value of 8.4. The results seemed to be independent of the current density within the errors of measurement and no change in the ratio with age of the filament was perceptible. Our results are in disagreement with those cited in reference (1) but agree with those of Wijk and Koeveringe[2] and Nakamura.[3] These authors found 7.2 and 8, respectively, from band spectra. All measured values are in bad agreement, however, with the abundance calculated from the masses of the isotopes and the atomic weight.

G. P. HARNWELL
WALKER BLEAKNEY
Palmer Physical Laboratory,
Princeton, N. J.,
December 12, 1933.

[1] K. T. Bainbridge, J. Frank. Inst. **212**, 317 (1931).
[2] v. Wijk and v. Koeveringe, Proc. Roy. Soc. **A132**, 98 (1931).
[3] G. Nakamura, Nature **128**, 759 (1931).

Multiple Laue Spots

Double Laue spots have been frequently observed when thick crystals composed of atoms of low atomic number were used. Cork[1] has described triple spots observed with crystals of quartz, calcite and Rochelle salt. A Laue photograph of a slab of crystalline quartz was recently made for the purpose of determining the directions of the

[1] Cork, Phys. Rev. **42**, 749 (1932).

crystallographic axes. The slab, 0.52 cm thick, was mounted so that the face upon which x-rays from a tungsten target tube operated at 55 kv were incident, was 5.0 cm from the photographic film. The spots observed were all either double or triple.

The occurrence of triple spots may be explained by assuming that the crystal is ideally perfect except near the two surfaces where it is more nearly ideally imperfect. Let λ be the wave-length of the x-rays reflected by the Bragg planes parallel to the direction *OC*. Because of the imperfection of the crystal at the point of incidence, *O*, the diffracted ray *OB* will have considerable angular width and will be correspondingly intense. However, because of the

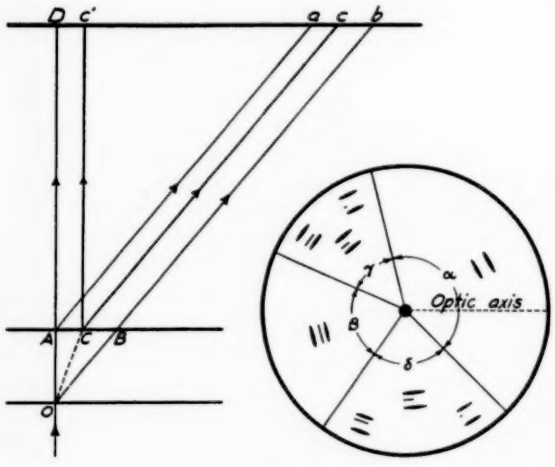

FIG. 1.

perfection of the interior of the crystal there will be a narrow angular range having approximately the direction, *OB*, within which rays of wave-length λ cannot proceed far without suffering total reflection after which their direction of propagation is approximately parallel to *OA*.[2] Similarly rays of wave-length λ having directions close to that of *OA* will suffer total reflection and assume a direction of propagation nearly parallel to *OB*. It follows that the x-rays lying in this narrow angular range will suffer successive total reflection as they proceed through the crystal. The direction of propagation will always be nearly parallel to either *OA* or *OB* but the path can never be far from the line *OC* and the energy will emerge from the crystal near the point *C* in two rays *Cc* and *Cc'*. The rays *OA* and *OB* will have relatively large angular width but will have no energy within a narrow range of angular width equal to that of the ray *Cc*. The imperfection of the crystal at *A* will give rise to a relatively strong diffracted ray *Aa*. Thus there should appear upon the photographic film three spots on a radial line, the outside spots, *a* and *b*, relatively intense with a less intense spot, *c*, between them. The triple spots observed are of this character.

If the body of the crystal is not ideally perfect, but is made up of small mosaic blocks within each of which primary extinction is effective, no spot will appear at *c* but instead a slight fogging of the film in a band extending from *a* to *b*. This is the character of the double spots observed.

The absolute position of the outside spot of each set was studied by making a gnomonic projection and the relative positions of the other spots were measured. The inside and outside spots of each set lie in positions *a* and *b* within the accuracy of observation. This confirms the conclusions of Colby and Harris[3] who studied the variation of the relative intensity of doublet spots when the crystal surfaces were treated. The intermediate spot was measured for 31 triplets; 21 of these spots lie accurately in position *c*; 8, slightly inside; and 2, slightly outside this position.

The circular insert shows typical drawings of the multiple spots as they appear on various parts of the photographic film. Note that in regions γ and δ the intermediate spot is cut off on the side toward the α-region, this being more pronounced as the boundary of the α-region is approached. This is the type of distribution to be expected if the incident ray *OA* traversed the slab close to the edge of a block of nearly perfect crystal.

It seems feasible by this method to locate large perfect blocks within a quartz crystal and to survey their boundaries. Laue photographs of several other specimens have been made in some of which triple spots occur. As yet no other specimen has been found in which such a block extends completely across the crystal.

CARLETON C. MURDOCK

Department of Physics,
Cornell University,
December 15, 1933.

[2] Darwin, Phil. Mag. **27**, 675 (1914).
[3] Colby and Harris, Phys. Rev. **43**, 562 (1933).

On the Magnetic and Gyromagnetic Properties of Pyrrhotite

The *g*-value and other magnetic properties of pyrrhotite (Fe_7S_8) may be obtained theoretically from the following simple model: We consider one *d*-electron (or several independent *d*-electrons) per atom, with fairly large spin-orbit interaction (but not as large as the interatomic exchange energies), in a hexagonal crystal which has the iron atoms in successive principal planes not directly opposite one another, but staggered, or else far apart. In the absence of x-ray data on the positions of the iron atoms in Fe_7S_8, this seems to be a reasonable assumption.

One effect of the large spin-orbit interaction is that, assuming ferromagnetic saturation and its large crystal spin, the lowest states will be those in which the orbital momenta are orientated antiparallel to the spins. Taking projections in the direction of the magnetization, each m_s is $-1/2$ and each m_l is 2. The *g*-value is then $(2m_s+m_l)/(m_s+m_l)=1/(3/2)=2/3$. Incomplete orientation of the orbit would make a deviation toward smaller *g*-values. For pyrrhotite, Coeterier[1] observes $g=0.63$.

[1] Coeterier, Helv. Phys. Acta **6**, 483 (1933).

Again, taking the properties of the lowest state as indicative of the properties of the crystal at moderate temperatures, we ask if the state of large crystal spin is lowest when the spin is in the principal plane, and when it is perpendicular to that plane (parallel to the principal axis). With the spin in the crystal plane, the states of lowest spin-orbit energy have charge distributions largely outside the principal plane, so that the overlapping of the wave functions is small near most of the next nuclei and the exchange integrals probably positive, making also the electrostatic energy low for the states of large total spin. In this direction, then, we expect ferromagnetism. With the spin perpendicular to this plane, the state with lowest spin-orbit energy has charge distribution in the plane of the nearest neighbors, so is apt to have negative exchange integrals; the state which probably has positive exchange integrals has orbital momenta in the principal plane and so high spin-orbit energy. It has energy lower than the state with spin in the principal plane only when the external field is extremely high; hence the difficulty of magnetization along the axis, as observed in pyrrhotite.

This is an example of the fact that ferromagnetic anisotropy, and consequently remanence and hysteresis, always seem to arise from the spin-orbit interaction within the atoms.

It will be noted that this type of ferromagnetism depends largely on the orientation of the orbits. The spins in this model are, as usual, coupled together by the electrostatic exchange effect consequent upon the exclusion principle. The orbits are coupled to one another through the medium of the spins, there being no direct exchange coupling of the orbits.

D. R. Inglis

Ohio State University,
December 15, 1933.

Photoelectric Properties and Electrical Resistance of Metallic Films

Recently completed experiments[1] show that a film of spectroscopically pure, outgassed cadmium deposited by evaporation on an oxidized iron plate in vacuum does not, at any stage in the formation of the film, exhibit a threshold wave-length longer than that characteristic of the cadmium in bulk. This is true for temperatures of the cathode between liquid air and room temperature. Similar results have been reported for mercury.[2] As is well known, thin films of the alkali metals show a marked dependence of the threshold wave-length and photoelectric emission on film thickness. Films of platinum, silver and gold also exhibit maxima in their total emission-thickness curves. Since these effects are observed for film thicknesses of less than about 20 molecular layers, the failure to observe them with cadmium and mercury films can be explained by supposing that it is impossible to form truly thin films of these two metals under ordinary conditions of deposition.

To test this supposition, we have attempted to gain some information concerning the structure of cadmium films by investigating the relation between their electrical resistivity and thickness. In the initial experiments the cadmium was condensed in vacuum on a glass plate at room temperature, and resistance measurements were made while the film was being driven off by warming the plate with a heating coil. The resistivity-thickness curve was found to be of the same general type as those that have been reported for many other metals; that is, as the average thickness of the film decreases, the resistivity increases from the value characteristic of the metal in bulk, at first slowly and then more rapidly, and finally, just beyond a so-called "critical thickness," rapidly approaches an infinite value.

Our initial experiments showed the critical thickness for cadmium to be not less than $200\text{–}300\times10^{-7}$ cm. In making this calculation, we estimated the value of the resistivity at the critical thickness to be twice that of the bulk metal. Experiences of various workers with other metals indicate that this assumed value is probably too small, and hence that the foregoing values for the critical thickness are smaller than the actual one.

To determine the critical thickness by a method not involving any assumption about the resistivity, the remaining experiments were made with a molecular beam apparatus, in which cadmium vapor effused through a pinhole from a vessel containing the vapor at a known pressure and deposited on a plate cooled by liquid air. The thickness of the deposit could be calculated from the vapor pressure and the geometry of the apparatus. The apparatus did not differ essentially from that used by Brady in photoelectric experiments[3] except for the use of a glass depositing surface equipped with a pair of tungsten electrodes and the addition of a magnetically-operated glass shutter placed in front of this surface; the purpose of the shutter was to shield the central portion of the surface from the cadmium beam during the time that thick cadmium terminals were being deposited over the tungsten wires and also while temperature equilibrium was being established in the apparatus.

Although measurements with this apparatus were disturbed because the electric current passing through the film tended to destroy the conductivity, enough data were obtained to place the value of the critical thickness of cadmium at 1800 molecular layers or about 400×10^{-7} cm. The total error in this determination may be as much as 25 percent. Now mercury, which also fails to exhibit photoelectric properties that are peculiar to the thin-film stage, has a critical thickness[4] of $200\text{–}300\times10^{-7}$ cm. On the

---

[1] J. Schmidt, R. F. Hughes, Helen Webb, Alice Hartley and D. Roller, unpublished.

[2] D. Roller, W. H. Jordan and C. S. Woodward, Phys. Rev. **38**, 396 (1931).

[3] J. J. Brady, Phys. Rev. **41**, 613 (1932).

[4] W. Braunbek, Zeits. f. Physik **59**, 191 (1930).

other hand, the published data on rubidium[5] indicate that its critical thickness is only about 8 or 10 times greater than the thickness for which the photoelectric threshold wave-length is a maximum; that is the critical thickness is less than 10×10^{-7} cm. Furthermore, the literature shows that the critical thicknesses of platinum, silver and gold are less than $5\times$, $20\times$, and 8×10^{-7} cm, respectively. Of the metals studied, then, the only ones which do not exhibit thin-film photoelectric anomalies are also the only ones which have a large critical thickness.

Such a correlation is to be expected. Most of the theories which have been advanced to account for changes in resistivity of metallic films with thickness involve the idea that the molecules, either before or after striking the depositing surface, group together into clusters, so that a comparatively large amount of material must be deposited to fill the gaps between clusters and thus render the film conducting. The larger the number of molecules in the clusters, the larger is the amount of material which must be deposited to establish conductivity; that is, the larger is the critical thickness. It seems reasonable to suppose that if a thin-film photoelectric effect is observed for one metal and not for another, it is because the first metal deposits more uniformly than does the second metal. When the surface area of metal exposed to the radiation has become large enough to give a measurable photoelectric current, or possibly when the particles of metal have finally established good electrical contact with the underlying iron surface, the actual thickness of the first metal film is still of molecular dimensions whereas that of the second metal film, due to the larger constituent particles, is of macroscopic dimensions. On this view, a dependence of photoelectric properties on film thickness will be observed only for metal films whose constituent particles, as indicated by the critical thickness, are small.

We wish to thank Miss Mary Louise Kropp and Mrs. Edith Townes for their invaluable assistance in the experimental work, and Mr. F. W. Crawford for his help in constructing parts of the apparatus. The spectroscopically pure cadmium used in this work was obtained through the generosity of the New Jersey Zinc Company.

DUANE ROLLER
DEAN WOOLDRIDGE

Department of Physics,
University of Oklahoma,
December 18, 1933.

[5] H. E. Ives and A. L. Johnsrud, Astrophys. J. **62**, 309 (1925).

Polarization of Fluorescence Radiation

The following problem has been investigated with the aid of the Dirac theory of light quanta. Light from a radiator falls upon a scattering atom in the ground state α_0 and raises the atom to the state γ from which it may fall to another, say a metastable level through an intermediate state β, emitting successively the light quanta ρ and δ. The intensity of the fluorescence radiation ρ polarized in a given direction was examined, taking into account the possibility of hyperfine structure and the effect of applying a magnetic field to the scatterer.

The result is found to be independent of the damping constant of the lower level β, only the damping constant Γ of the upper level γ entering into the final result. The formulae for the degree of polarization and the intensity of the scattered fluorescence radiation are therefore the same as those given by Breit for the case of resonance radiation.[1]

One may understand this result by observing that if the intermediate level β were metastable, then the polarization of the radiation emitted in the transition γ to β would depend on the interference of coherent transitions due to the atom coming back to the same sublevel of β. The effect of radiation is to broaden each sublevel of β into a band. Transitions to the same energy value in a given band may be regarded as giving rise to coherent radiations. The width of the band is however immaterial for the polarization of the fluorescence radiation.

This result is to be contrasted with that for the breadth of the line emitted in the transition γ to β, which as is known,[2] is equal to the sum of the breadths of the two levels.

IRVING S. LOWEN
G. BREIT

New York University,
December 22, 1933.

[1] G. Breit, Rev. Mod. Phys. **5**, 91 (1932). Eqs. (159), (164).

[2] Weisskopf and Wigner, Zeits. f. Physik **63**, 54 (1930)

Proceedings of the American Physical Society

MINUTES OF THE CINCINNATI MEETING, DECEMBER 1–2, 1933

THE 187th regular meeting of the American Physical Society was held at the University of Cincinnati, Cincinnati, Ohio, on Friday and Saturday, December 1 and 2, 1933. The presiding officers were Paul D. Foote, President of the Society, and J. H. Van Vleck.

The Netherland-Plaza Hotel was the headquarters and the Society's dinner was held there on Friday evening with seventy-six guests in attendance. President Foote presided and the after-dinner speakers were S. J. M. Allen, Arthur H. Compton, K. K. Darrow, L. T. More and Raymond Walters, President of the University of Cincinnati. The meeting was in celebration of the opening of the new Physics Laboratory. The Basic Science Laboratory was also open for inspection.

On Saturday afternoon a joint meeting was held with the American Mathematical Society in a symposium on *Spinor Analysis*. The speakers were Otto Laporte and Oswald Veblen. At one of the regular sessions L. T. More read a very interesting character sketch of Isaac Newton based on his recent research in England on this subject.

Meeting of the Council. At its meeting on Friday, December 1st, the Council approved the transfer of one member to the grade of fellow. Twenty-five candidates were elected to membership. *Transferred from membership to fellowship:* Harold M. Mott-Smith. *Elected to membership:* Clete Adams, Richard Bär, Robert B. Barnes, Willard F. Bartoe, Catharine M. Bergen, B. Edwin Blaisdell, John Paul Blewett, Walter L. Bond, George H. Burnham, W. F. Busse, Richard E. Carlson, Carl N. Challacombe, Sydney Chapman, Forrest F. Cleveland, Franklin S. Cooper, Clyde B. Crawley, Eugene Feenberg, C. E. Hablutzel, Jr., T. M. Hahn, Hirosi Hukusima, Theron W. Kilmer, Jr., Motoharu Kimura, Robert B. King, Andrew McKeller, A. O. C. Nier, Dwight O. North, Harold T. Olson, W. G. Penney, R. G. Piety, J. H. Plummer, Emil G. Purdom, Raymond Ricard, Severn Rinkob, Preston Robinson, Milward T. Rodine, William G. Shepherd, Brian O. Sparks, Ray L. Sweeny, Theodore A. Te Grotenhuis, Hiroshi Tsubota, Eugene E. Warner and Martin C. Watson.

The regular scientific session consisted of thirty-four papers, four of which, numbers 1, 14, 18, and 30, were read by title. A complete list of authors and abstracts will be found in the following pages.

W. L. SEVERINGHAUS, *Secretary*

ABSTRACTS

1. On a Formula to Determine the Direction of the Extraordinary Ray in a Uniaxial Crystal, Derived by a Method of Analytical Geometry. ROBERT V. BAUD, *Beaver Falls, Pa.*—The design of certain optical instruments necessitates the determination of the optical path of light rays through various substances which quite often offers difficulties, one of which may be the requirement of extreme accuracy. The graphical solution is not satisfactory when such a requirement exists due to the fact that the point of tangency of the wavefronts cannot be located accurately, even though the drawing be made to as large a scale as ordinary drafting accommodations permit. An analytical solution becomes therefore desirable in this case. As none of the standard texts contain such a solution, not even for the comparatively simple case of plane of incidence and principal plane coinciding, the author has endeavored to find one for this case that is not so complicated as the one given by Johannson in his book on *Petrographic Methods*. In deriving the formula the steps made in solving the problem graphically by means of Huyghen's construction were analytically formulated. Let β be the angle of incidence, θ the angle between the direction of the

extraordinary ray and a line perpendicular to the optical axis, α the angle between the crystal face and the optical axis, n_1 the index of refraction for rays perpendicular to the optical axis, n_2 the index for parallel rays, the derived formula reads as follows:

$$\theta = \arctan \frac{\cos\alpha - k(n_1/n_2)\sin\alpha}{\sin\alpha + k(n_2/n_1)\cos\alpha},$$

in which k is the value as determined by

$$k = (1/\sin\beta)(n_1^2\sin^2\alpha + n_2^2\cos^2\alpha - \sin^2\beta)^{\frac{1}{2}}.$$

2. A Photoelastic Method of Stress Evaluation in Structures Involving Two Parallel Systems of Plane Stresses. WALTER H. HAUPT, *University of Cincinnati.* (*Introduced by S. J. M. Allen.*)—To find stresses in each of two parallel plates in a model, polarized light is caused to vibrate in a plane corresponding to stress direction in the first plate, whereupon it reaches the second plate as plane polarized light. The image can then be analyzed directly for stresses in the second plate. To obtain stress directions for any given point of the two plates, white polarized light is transmitted through both, and the nicols are rotated until there is achromatic transmission. The nicol setting will then give the stress directions. When the stresses are parallel in the two plates the insertion of a half-wave plate between them with axis at forty-five degrees to stress direction will reverse the effect of the first plate from plus to minus. The images with and without the half-wave plate will give the value of the sum and difference of the two stress effects.

3. On the Comparison of Theoretical and Measured Hall Coefficients. K. K. SMITH AND N. A. HEDENBERG, *Northwestern University.*—From Kapitza's data, N. H. Frank calculated (Zeits. f. Physik **64**, 652, 1930) the coefficient C in his formula $\Delta\rho/\rho = BH^2/(1+CH^2)$, where ρ is the resistivity in the *presence* of the field. He found that $\rho(C)^{\frac{1}{2}}$ is *less* than the Hall coefficient, R (from tables), for bismuth and antimony. But Bellia's measurements (Zeits. f. Physik **74**, 655, 1932) on bismuth, and Barlow's on antimony show the reverse. We have made measurements of resistivity and Hall coefficient for each of two bismuth plates at room temperature in fields varying from 1000 to 13,000 gauss. When $H=0$, the resistivities are $\rho_0 = 14.2\times10^4$ e.m.u. and 12.8×10^4. For each plate C (found graphically) is 1.3×10^{-8} gauss^{-2}. Since the largest values of R are -7.4 and -2.6 e.m.u., $\rho(C)^{\frac{1}{2}}$ is greater than R. It appears that so far as this comparison is concerned, bismuth and antimony are like all the other metals for which Frank published calculations. We have recalculated C from Kapitza's data for the eight metals Cu, Ag, Au, Zn, Al, Cd, Sb, Bi. The result is an upward revision of Frank's values of $\rho(C)^{\frac{1}{2}}$. The discrepancy between the two sets of values is accounted for by noting that Kapitza plotted $\Delta\rho/\rho_0$, not $\Delta\rho/\rho$.

4. Nonmetallic Conducting Films. S. BLOOMENTHAL, *R. C. A.-Victor Co., Camden, N. J.*—Immutable conducting films, which adhere to any clean solid, have been formed from synthetic resin solutions holding finely ground carbon in suspension. Values of surface resistivity (Maxwell Treatise on E. & M., II, p. 287) for uniformly thin films were secured in the range 10 to 5×10^5 ohms referred to unit area of surface. When the thickness is held constant, the resistivity depends mainly upon the proportion of binder present and the kind of carbon used. The experimental error in repeating values of resistance is about ±20 percent when the same suspension is used, and somewhat higher when a second suspension, prepared identically, is used. The dependence of resistance upon resin content of the film appears to be in accord with the views of Frenkel (Phys. Rev. **35**, 1604, 1930) concerning gap contacts, and in definite disagreement with the classical Maxwell-Rayleigh theory for composite conductors. The behavior of various types of carbon, when used in the films, can be predicted qualitatively from electrical measurements made upon powdered samples subjected to high pressure.

5. The Scattering Coefficients of X-Rays at Short Wave-Lengths. S. J. M. ALLEN, *University of Cincinnati.*—The mass absorption coefficients μ/ρ of homogeneous x-rays have been measured for elements from hydrogen to uranium and down to $\lambda=0.05$A. Very especial care was taken to ascertain the impurities in each sample, so proper corrections could be made. This is very important for the light elements. An empirical law was used to calculate τ/ρ, the photoelectric coefficient. $\sigma/\rho = \mu/\rho - \tau/\rho$ was then calculated and reduced to electronic absorption. The values σ_e so obtained are shown in the following table for different elements at certain wave-lengths from $\lambda=0.005$A to 0.417A. Below $\lambda=0.05$A the data are from γ-ray absorption, and some few x-ray results of other experimenters. The results seem to me to be very interesting and important. For all elements at any λ, σ_e is constant and agrees very closely with that calculated from the Klein Nishina formula up to $Z=10$–15, when there is a rapid increase (excess scattering) for the heavier elements. This phenomenon for x-rays is identical with that noticed for γ-rays of radioactive bodies. Excess scattering in the case of γ-rays has been ascribed by many experimenters to

Electronic Scattering Coefficient $\times 10^{25}$.

	γ-rays and x-rays				*x-rays*				
Element	0.005A	0.010A	0.025A	0.050A	0.064A	0.098A	0.130A	0.200A	0.417A
H	128	195	270	380	410	460	530	620	640
Li					410	460		570	620
Be								580	600
B					440	480		570	590
C	128	197	270	390	420	460	500	550	570
N								540	
O		195			420	460		520	540
Ne								530	
Na					430	490		540	550
Mg					410	470		540	540
Al	129	197	270	380	420	490	510	530	550
S	128	198	270		420	460		600	600
Cl					430	500		660	680
A								700	
Ca					430	510		720	820
Fe	133	203	280	430	450	575	670	900	1000
Cu	134	206	290	450	470	709		1400	1500
M								1600	
Mo					1000	1600			
Sn	145	213	400	900	1300	2400	3200	5000	5500
Pb	172	300	950	2700	3500	4500	4100		

nuclear absorption. Is the similar phenomenon here shown for x-rays at much greater values of λ to be explained in the same manner? I do not attempt to answer that, but simply present the facts.

6. Electron Diffraction from Vacuum-Sublimated Layers. K. LARK-HOROVITZ, E. M. PURCELL AND H. J. YEARIAN, *Purdue University.*—The material for investigation is condensed in a high vacuum onto a volatile substance (camphor, naphthalene, etc.) held at liquid air temperature. By letting the volatile support evaporate after the desired thickness is reached it is possible to obtain thin, free films of the condensed material of varying thickness without using any dissolving agent as it is necessary in other methods. In this way films of zinc and zinc sulfide have been obtained. The electron diffraction pattern of zinc agrees with the x-ray diffraction pattern and shows no irregularity in the intensity distribution as compared with the corresponding x-ray pattern except for the first two lines. Zinc sulfide in thin layers forms colloidal particles; in thicker layers it is crystalline and the position of the lines agrees with the x-ray pattern. The intensities however are different in a similar way as reported previously in the case of ZnO. Copper, when deposited in this way, forms films of either pure cuprous oxide (Cu_2O) or a mixture of copper and cuprous oxide. The intensity distribution of the Cu_2O pattern agrees with the intensity distribution of the corresponding x-ray pattern.

7. Electron Scattering in Methane, Ethylene and Acetylene. A. L. HUGHES AND J. H. MCMILLEN, *Washington University, St. Louis, Missouri.*—Scattering coefficients for elastic collisions between electrons and molecules of these gases have been measured. Electron energies employed were from 10 to 800 volts for methane, to 100 volts for acetylene and to 225 volts for ethylene. Evidence for interference effects between the electron waves scattered by individual atoms within a molecule was indicated by the presence of maxima in the curves for the ratios of the scattering coefficients for C_2H_4 and CH_4 (also for the pair C_2H_2 and CH_4) expressed as functions of scattering angles. The ratios were also computed by the well-known formula for the intensity of the resultant waves emitted by a molecule, *viz.*,

$$\Psi^2 = \sum_1^n i \sum_1^n j \, \psi_i \psi_j (\sin x_{ij}/x_{ij}),$$

where ψ_i and ψ_j are the electron wave amplitudes due to the atoms i and j, and x_{ij} is a parameter involving the distance apart of the atoms. Fairly satisfactory agreement between experiment and calculations was obtained for the ratios for C_2H_4 and CH_4, provided that we assume that the scattering is done by the H atoms alone. But to get fairly satisfactory agreement in the case of C_2H_2 it was necessary to assume that the C atoms contribute their full share to the scattering.

8. Refocussing of Electron Paths by Means of a Magnetic Field. W. E. STEPHENS AND A. L. HUGHES, *Washington University, St. Louis.*—It is well known that, when electron paths diverge from a point in a magnetic field, they are refocussed when they have turned through 180°. This is a particular case of a more general relation. Consider a uniform magnetic field bounded by two planes, meeting at any angle, the magnetic field being parallel to the line of intersection of the two planes. Consider a third plane passing through the line of intersection and symmetrically orientated with respect to the other two planes. If a beam of electrons diverges from any point on this plane so that the central ray falls perpendicularly on the nearer face of the magnetic field and is then deviated by the magnetic field so that it emerges perpendicularly from the second face of the magnetic field, then all electron paths in a plane perpendicular to the three planes and diverging from the starting point, refocus at a point whose position in the third plane is the image of the starting point. The formula for the departure from perfect refocussing has been derived. The refocussing property has been verified experimentally. Refocussing of this type should be useful experimentally when the original 180° type of refocussing is inconvenient.

9. Some Aspects of Electromagnetic Forces and Waves. F. W. WARBURTON, *University of Kentucky.*—The force on a beam of cathode rays in a magnetic field due to conduction currents, developed from Weber's energy equation of moving charges, is equal to that obtained classically, provided the velocity of the conduction electrons is small compared with the velocity of the cathode particles. On the other hand, the contribution of neighboring electron orbital currents to the magnetic force on an electron in an orbit is half the classical value. An equal force acts on the nucleus. The relation of this to the gyromagnetic anomaly is considered. An error in the derivation of electric waves from Weber's energy equation (Phys. Rev. **44**, 319, 1933) is eliminated, making the wave equation read

$$\frac{\partial^2 A}{\partial r^2} = \frac{\mu\epsilon}{c^2}\frac{\partial^2 A}{\partial t^2} - \frac{\mu\epsilon v \sin^2\theta}{c^2 r \cos\theta}\frac{\partial A}{\partial t} - \frac{9\mu e' v' \sin\theta \sin\theta' \cos\gamma}{c r^3 \cos\theta},$$

where A is the magnitude of the vector potential; v', v the velocities of electrons in source and absorber; θ', θ the angles between v' and r, v and r; and γ the angle between the planes v, r and v', r. This equation is invariant under a Galileian transformation.

10. Spectral Distribution of the Photoflash Lamp. W. E. FORSYTHE AND M. A. EASLEY, *Lamp Development Laboratory, General Electric Company, Cleveland, Ohio.*—The distribution in the spectrum of the total quantity of radiation from the photoflash lamp has been measured by using a glass spectrometer with two 60° prisms and also the large crystalline quartz double monochromator[1] as the dispersing instrument and the measurements at the receiving slit made by means of a photoelectric tube connected to a very high sensitivity galvanometer. The values for the different wave-length intervals with the glass spectrometer were reduced to relative energy values by comparison with measurements made with the same instrument on the spectral energy distribution of a high intensity

tungsten lamp of known color temperature. The transmission of the quartz instrument and the spectral sensitivity of the photoelectric cell used with it were known so that the galvanometer deflections could be expressed in relative energy values directly. The distribution for the range measured agrees very well with data published by Ives[2] and his co-workers on the spectral distribution of energy in the spectrum of aluminum oxide when heated by means of a gas flame. The shape of the curve in the visible spectrum was found to be about the same as that of a black body at 3500°K.

[1] R. S. I. **4**, 289 (1933).
[2] J. Frank. Inst. **186**, 585 (1918).

11. Double-Coated Schumann Films. H. P. KNAUSS AND R. V. ZUMSTEIN, *Ohio State University.*—Hopfield's method (J. Opt. Soc. Am. **22**, 488, 1932) of preparing Schumann plates employs commercial photographic plates which are fixed and washed, to serve as a base for the Schumann emulsion. We have found that it is possible to precipitate a thin Schumann emulsion directly on the sensitive emulsion of Eastman 33 plates, thereby obtaining plates which are fast not only in the Schumann region, but also up to the long wave-length limit of the plates used. Plates so made have been compared with others prepared according to Hopfield's directions, as well as with Eastman ultraviolet sensitive plates, and plates sensitized with Eastman's ultraviolet sensitizing solution. A condensed copper spark in air was used as a source, with a small quartz spectrograph as a dispersing instrument. Plates of all four types were found to be practically alike in sensitivity for the extreme ultraviolet. Sensitivity for longer wave-lengths is an advantage only in using overlapping orders for comparison of wave-lengths.

12. The Spectrum of Rubidium in Mercury Arc. I. A. BALINKIN AND D. A. WELLS, *University of Cincinnati.* (*Introduced by S. J. M. Allen.*)—This is a continuation of the previously published work on the spectra of potassium and sodium in a specially designed mercury-arc lamp. Various low percentages of rubidium, $\frac{1}{4}$ to 2 percent, were introduced into the same type of mercury lamp and the spectra photographed in the visible and ultraviolet regions. Under proper conditions, 1.45 amp. and 40.0 volts, the lamp operates with full Rb glow, mercury lines being almost completely suppressed. The reduction in intensity of Hg lines is far greater in the visible than in the ultraviolet. The luminous efficiency of the Rb-Hg amalgam lamp has also been determined and compared with that of a similar lamp containing only mercury. The blackening of the glass so noticeable in lamps containing K and Na was absent in Rb mercury amalgam lamps.

13. Emission and Absorption from the $2\,^3P_0$ Metastable Level in Mercury. M. L. POOL AND O. W. PRASHUN, *Ohio State University.*—Mercury vapor at room temperature in the presence of nitrogen was optically excited by the total radiation from two mercury arcs. For nitrogen pressures from 1 to 200 mm the emission of the "forbidden line" 2656.6 ($1\,^1S_0-2\,^3P_0$) gradually increased in intensity. From 200 to 760 mm the intensity remained constant. When the intensity of the exciting radiation was reduced to one-half, the emission also decreased about one-half. The intensity of the 2537 line behaved similarly. The lines 5461, 4077, 3340, 2893, and 2752 showed a decrease in emission of only a little more than one-half when the excitation was decreased one-half. A decrease to one-fourth might be expected. The absorption of 2967 ($2\,^3P_0-^3D$) was found to be very strong up to 100 mm and then to decrease with further increase of nitrogen. The ratio of the emission from the $2\,^3P_0$ level to the absorption from that level indicated that the transition probability between the $2\,^3P_0$ and $1\,^1S_0$ levels increases rapidly with nitrogen pressure. The 4800 band due to $Hg_2(2\,^3P_0)$ increases in intensity with increase in nitrogen pressure from 200 to 760 mm and also increases in intensity with decrease of exciting energy.

14. Hydrogen-Isotope Effect in the OH Bands, λ3064 and λ3121. R. W. SHAW AND R. C. GIBBS, *Cornell University.*—Bands arising from the isotope of hydrogen of approximate mass 2 in the OH molecule have been photographed under high dispersion for the cases of the (0, 0) and (1, 1) vibrational changes. The spectrum was obtained by exciting in a Wood type discharge tube the vapor from a sample of "heavy" water which was made available to us through the courtesy of Professor G. N. Lewis. A concave grating of twenty-one feet radius of curvature and 30,000 rulings per inch was used in a stigmatic mounting. A high dispersion instrument is advantageous since, for the vibrational transitions under consideration, the main branches of these bands of the heavy isotope are completely overlapped by those of the lighter isotope. Precise wave-lengths of the band lines have been obtained and a rotational analysis has been made. It is of interest to note that the width of the spin doubling for the heavy isotope is greater than for the ordinary OH molecule. Moreover the separations in the former case do not contract as rapidly for large values of K as they do in the latter case.

15. Search for TiO Isotope Bands. H. P. KNAUSS, H. M. STRONG AND H. L. JOHNSTON, *Ohio State University.*—A carbon arc in air, fed with powdered TiO_2, was used as a source of TiO bands, and a search was made for bands of a molecule containing a predicted isotope, Ti^{46}. (J. Am. Chem. Soc. **53**, 2866, 1931.) The (1−0) band at 4955A gave promise of showing an isotopic shift, but the expected isotopic band was not observed. The spectrograms were taken in both first and second orders of a 21-foot grating. This does not exclude the possibility of the existence of Ti^{46}, since it is known (King and Birge, Astrophys. J. **72**, 251, 1930; Jenkins, Proc. Amsterdam Akad. **35**, 1212, 1932) that an arc is not a favorable source for observing isotopic bands.

16. Infrared Spectra of Acetylene Containing H^2. H. M. RANDALL AND E. F. BARKER, *University of Michigan.*—About 5 cc of acetylene gas was generated from a sample of "heavy" water generously supplied by Professor

G. N. Lewis. The infrared spectra show relatively few molecules of $C_2H_2^1$, and nearly equal concentrations of $C_2H^1H^2$ and $C_2H_2^2$. The molecules with equal H atoms have only two active fundamental vibrations, designated ν_3 and ν_4 (Cf. Sutherland, Phys. Rev. **43**, 883, 1933). The spectrum of the unsymmetrical molecule is much richer, all of the five fundamental vibrations and their combinations being active. A sufficient number of bands may be observed to provide a complete description of the potential function, assuming it to be independent of nuclear influences, and the moments of inertia may be obtained from the rotational structure. Thus the interatomic distances and forces are uniquely determined. The alternation of line intensities in the bands of $C_2H_2^2$ provides a measure of the nuclear spin of H^2. The long wave (perpendicular) bands have been observed with a prism spectrometer of very good resolving power, the prism being of KBr. The positions of the zero branches are as follows:

ν_4 ($C_2H_2^1$) 729 (13.7μ). ν_4 ($C_2H^1H^2$) 679 (14.7μ).

ν_4 ($C_2H_2^2$) 520 (19.2μ). ν_5 ($C_2H^1H^2$) 541 (18.5μ).

The bands of higher frequency are being measured with the grating spectrometer.

17. Isotope Shift in Magnesium. R. F. BACHER AND R. A. SAWYER, *University of Michigan.*—The spectrum of Mg I was excited in a hollow cathode tube at low current density. The lines in the region 4500A to 9000A were studied with a Fabry-Perot type interferometer used in conjunction with a Hilger E1 spectrograph. λ4571 ($3s^2\ {}^1S_0 - 3s3p\ {}^3P_1$) was found to have a strong central component and a much fainter component at about $+0.083$ cm^{-1}. The diffuse series lines ($3s3p\ {}^1P_1 - 3s\ n\mathrm{d}\ {}^1D_2$) were observed to show structure. The first two members λ8807 and λ5528 show two components which according to preliminary measurements have separations 0.085 cm^{-1} and 0.065 cm^{-1}, respectively. Since for the singlet diffuse series lines it may be shown that any structure due to the presence of a nuclear moment is negligible, the structure is attributed to isotope shift. Magnesium has three isotopes 24, 25 and 26 present in the ratio 7 to 1 to 1. If the displacement is due only to a mass effect it may be shown from the work of Bartlett and Gibbons (Phys. Rev. **44**, 538, 1933) that the three isotopes are expected to give rise to three lines almost equally spaced. It is believed that if the isotopes are present in the amounts given above, the presence of the third isotopic component would have been clearly apparent in the first two members of the diffuse series.

18. The Effect of Heat on the Intensity of Mercury Lines and Bands. J. G. WINANS, *University of Wisconsin.*—A reduced achromatic image of a quartz tube containing mercury was projected on the slit of a quartz spectrograph by a concave aluminum mirror. A discharge was produced in the tube through external electrodes by a low voltage Tesla coil. The mercury vapor pressure was controlled by a Bunsen burner. The center of the tube was heated by a blow torch. Comparison of center and edge of the spectrum obtained showed the effect of heat. The changes in intensity of Hg_2 bands were the same as the well-known effects in fluorescence. In addition the continuous spectrum from 2650–2536 was shown to follow the 3300 band in intensity changes. The reversals of the 2540 band and 2536 line were diminished by heat, the intensity correspondingly increased. Several unidentified bands were completely destroyed by heat. Others appeared only at the electrodes. The weakening by heat for the mercury arc lines was a maximum at about 340°C. Measurements of the relative intensities from heated and unheated regions were made by the photographic method. With one or two exceptions all lines originating from a given excited state showed the same weakening. From a sample plate $I_{\text{hot}}/I_{\text{cold}}$ equals 4% for $2\ {}^3S$, 24% for $3\ {}^3S$, 15% for $4\ {}^3S$, 16% for $5\ {}^3D$, 7% for $6\ {}^3D$, 9% for $7\ {}^3D$, and 12% for $8\ {}^3D$. One set of lines appeared only in the heated portion. These were tin lines. The experimental part of this work was done at Massachusetts Institute of Technology.

19. A Physico-Chemical Theory of Excitation and Inhibition. N. RASHEVSKY, *Westinghouse Elec. & Mfg. Co., East Pittsburgh, Pa.*—In various physical theories of nerve excitation it is usually assumed that the concentration of an exciting substance at the cathode must reach a certain threshold value for the excitation to occur. The substance is naturally identified with some cation. It is, however, known that only monovalent cations excite; the bivalent inhibit, and it is their ratio which determines the excitation. Hence a more general theory must consider the variations of concentration of two substances under the action of the current—one exciting, the other inhibiting. This is done in the present paper. A good agreement with a number of experimental data is found. In particular, the excitation at the anode by closing a current becomes intelligible in a very simple manner. The theory of two substances can be extended to the central excitation and inhibition, and gives a simple explanation of the "rebound phenomenon."

20. A Physico-Mathematical Theory of Organic Form. N. RASHEVSKY, *Westinghouse Elec. & Mfg. Co., East Pittsburgh, Pa.*—In a series of previous papers, the author has studied the thermodynamical properties of cells and cellular aggregates. From these investigations it follows that various forces, both attractive and repulsive, must exist between cells. An attempt is made in this paper to determine the general arrangement which the cells will assume under the influence of those forces in the early embryonic stages, when cells can move comparatively freely one with respect to another, and when the general shape of the future organism becomes determined. Depending on the values of various cell constants, forms are in this way obtained, which correspond in general with various forms of the animal kingdom.

21. The Effect of Soft X-Rays on the Germination of Wheat Seeds. HARRIS M. BENEDICT AND H. KERSTEN, *University of Cincinnati.* (*Introduced by Dr. Allen.*)—Wheat seeds were irradiated with the characteristic K lines of copper for various lengths of time, sprouted between

blotters and the diastase activity, the reducing sugar content, the respiratory rate, and the percentage of water in the seedlings determined. Those irradiated for five seconds showed an increase in both diastase activity and sugar content. Those irradiated for a longer time showed a decided and progressive decrease in these two substances as well as a decrease in the other quantities determined.

22. The Lethal Action of Radiant Energy on Living Cells. FRANCIS F. HEYROTH AND JOHN R. LOOFBOURROW, *Basic Science Research Laboratory, University of Cincinnati.*—The existence of a frequency threshold for the lethal action of radiant energy on living cells is discussed. Four changes which may be induced in the cell by radiant energy are pointed out as possible mechanisms of the lethal action: (a) the destruction of cell enzymes, (b) the precipitation of colloidal materials, including proteins, (c) changes in the permeability of cell membranes, and (d) the destruction of compounds of the cell nucleus. The first possibility seems to be ruled out by evidence which shows the threshold frequencies for the destruction of enzymes to be different from that for lethal action on cells. The second and third possibilities require future investigation. The fourth is shown to be of great importance, particularly in the action of radiant energy on certain types of cells, by comparison of the ultraviolet absorption spectra of nuclear materials with curves of bactericidal power against wave-length, and by comparison of the frequency thresholds for destruction of nuclear materials with those for the bactericidal action of light.

23. The Ultraviolet Absorption Spectra of Certain Compounds Derived from Living Cells. FRANCIS F. HEYROTH AND JOHN R. LOOFBOURROW, *University of Cincinnati.*—The ultraviolet absorption spectra of aqueous solutions of the pyrimidines derived from cell nuclei are characterized by a band extending from 2300 to 3100A, with the maximum at approximately 2600A, and apparently the result of the fusion of three or more finer bands. By comparing the absorption of 15 related compounds, various features of the effect of molecular constitution upon absorption are made evident. Saturation of the ethylene linkages of these ring compounds results in a loss of selective absorption. In those unsaturated compounds which, as e.g., barbituric acid, exist in solution in tautomeric equilibrium, the magnitude of the 2600A absorption is greater than in those compounds of fixed structure. The introduction of a second or third double linkage into the ring lessens the magnitude of the selective absorption. The effects of substitution upon these unsaturated 6-membered heterocycles depend both upon the position and nature of the substituents. The replacement of a hydrogen atom of position 5 of uracil by the hydroxyl group produces isobarbituric acid in which the absorption is shifted 200A toward the longer wave regions. Weighting the ring shifts the absorption toward longer wave regions. When this is done in position 5, it also decreases the molecular extinction values, but if the weighting group is attached at a position other than 5, it usually increases the absorption. Highly purified vitamin-B_1 preparations have absorption spectra apparently identical with those here discussed.

24. The Near Infrared Absorption Spectrum of Crystalline "Calciferol" (Vitamin D). ELIZABETH SHELOW, *Basic Science Research Laboratory, University of Cincinnati. (Introduced by J. R. Loofbourow.)*—Crystalline "calciferol," regarded by the English workers as being pure vitamin D, was prepared by the method of Askew, *et al.* It was dissolved in purified carbon tetrachloride and its infrared absorption spectrum determined. The persistence of bands at 1.55μ and 2.05μ, which are identified with the alcohol group, and the similarity of the general form of the absorption spectra curves of "calciferol" and ergosterol (its photochemical precursor), indicated the isomeric relationship of the two substances.

25. The Detection of Vitamin A by Means of the Magneto-Optic Apparatus. G. M. WISSINK AND JAY W. WOODROW, *Iowa State College, Ames, Iowa.*—The magneto-optic apparatus of Allison was modified somewhat so as to determine the positions of the minima. A large number of samples of materials were tested and a characteristic minimum was found for all substances investigated which contained vitamin A. This minimum was at 392. on a scale equivalent to that used by Allison. Materials which gave this minimum included cod-liver oil and Haliver oil, the juices from spinach, orange and tomato, egg yolk solution, and irradiated carotene, all of which contain vitamin A. This minimum was not obtained with strongly irradiated cod-liver oil, pure carotene, peanut oil and Wesson oil. The minimum for cod-liver oil became much less prominent after bubbling air through it.

26. The Magneto-Optic Method of Chemical Analysis. FRANCIS G. SLACK AND JAMES A. PEOPLES, JR., *Vanderbilt University, Nashville, Tenn.*—Attempts to reproduce the time-lag measurements and chemical analyses of Allison (Phys. Rev. **29**, 161, 1927; J.A.C.S. **52**, 3796, 1930), on an apparatus constructed and adjusted by a former staff member of Alabama Polytechnic Institute, have failed. The attempts followed a practise period in the laboratory of Dr. Allison where it is believed the observers learned to recognize "minima." Minima of light which appeared the same as those seen at Auburn were observed in our own laboratory but all objective attempts to correlate their occurrence with the position of the trolleys failed. Similar minima were observed with the coils and cells completely removed when the light was readjusted to its usual intensity. Experiments were tried in which a second spot of light was produced beside the normal spot. This light from a steady source and not affected by the magnetic fields was adjusted to the same color and intensity as the normal spot. No type of change in intensity was observed for one spot which did not appear similarly for the second spot. The intensity changes observed in our laboratory are ascribed to physiological and psychological effects.

27. On Spinors and Their Significance in Modern Physics. OTTO LAPORTE,* *University of Michigan.*—The significance of vector and tensor analysis in physics lies in the isotropy of space. The meaning of tensors as quantities generating representations of the 3 or 4-dimensional

rotation group is emphasized. Symmetry conditions among tensor components have as consequence the decomposition of the representation into its irreducible parts. From examples taken from various domains of physics one gains the impression that only those quantities which generate irreducible representations have physical significance. The best way to obtain irreducible representations of the rotation group is to transform spherical harmonics. An entirely new class of quantities was introduced into physics through the study of the spin of the electron. In order to prove the invariance in form of the Pauli or Dirac wave equations with spin, a new transformation law had to be assumed for the wave functions. It was found that these spin wave functions transform, not according to ordinary representations of the 3 or 4-dimensional rotation groups, but according to representations of the unitary group which was shown by Weyl to be isomorphic to the rotation group. The unitary group furnishes just twice as many representations as the ordinary rotation group; they may be regarded as two-valued representations of the rotation group. Upon a suggestion of Ehrenfest, van der Waerden developed a formalism, spinor analysis, which possesses all the advantages of tensor analysis but comprises both one- and two-valued representations. Covariance under Lorentz transformations is thus automatically restored for equations regardless of whether they contain wave functions or tensor quantities. A few applications of the spinor calculus to the Maxwell and Dirac equations are discussed.

Invited paper.

28. Spinor Analysis. OSWALD VEBLEN, *The Institute for Advanced Study, Princeton, New Jersey.*—A spinor is a physical object which has components which transform linearly, not only in response to changes of coordinates, but also in response to changes of gauge and of spin frame. The spin transformations are determined by arbitrary four-rowed matrices with complex elements. The spinors therefore have an interpretation in complex three-dimensional projective geometry. This interpretation points the way to a formal theory which can be developed without reference to the geometry which suggests it. In addition to these ideas drawn from projective geometry, the general theory of spinors contains a theory of covariant differentiation modeled on that of tensor analysis. For the application to relativity the general theory of spinors has to be specialized by introducing certain invariant spinors. These fundamental spinors extend the formal theory by providing a scheme of raising and lowering spin indices and shifting to "conjugate" indices and back again. They also provide for translating any tensor expression into spinor form. Thus introduced, the spinors are merely a new mathematical tool for the relativity theory involving no new physical assumption. The equations of Dirac appear as differential equations of a particularly simple type, and new physical considerations enter the discussion for the first time when we try to interpret these equations.

Invited paper.

29. A Rotating Flashometer. W. E. FORSYTHE AND M. A. EASLEY, *Lamp Development Laboratory, General Electric Company, Cleveland, Ohio.*—To study the time constants of the photoflash lamp a rotating photographic flashometer was designed. The cylinder carrying the photographic film was of such a diameter and as used for the most part, rotated at such a speed that 1/20 of an inch represented very accurately 1/1000 of a second. The shutter is opened and the current turned on through the lamp by using the contact mechanism of an oscillograph. A hard rubber cylinder with 6 v threads having the center v thread made of metal is used and two insulated contact brushes are dropped onto the thread of the insulated part and thus contact made when the threads on this rotating commutator move these contact brushes to the metal part and then after one rotation the two brushes pass beyond the metal portion and break the contact. The first contact brush opens the shutter in front of the particular part of the camera being used and then a short time after the second brush closes the lamp circuit. By means of cams and sliding contacts the contact brushes are returned to their neutral positions ready to be dropped on to the commutator for the next lamp.

30. Rotation in Polyatomic Crystals. HARALD H. NIELSEN, *Ohio State University.*—A generalization of the work of Pauling (Phys. Rev. **31**, 430, 1930) and Stern (Proc. Roy. Soc. **A130**, 551, 1931) on rotation in diatomic crystals to embrace rotation also in polyatomic crystals has been considered. The rotating configurations are treated as symmetric tops under the influence of the crystal fields. The potential energy is assumed expandable in spherical harmonics of the required symmetries. This discussion treats only cases where terms of higher order than the first in the potential energy are small and may be thought of as perturbations on the original system. The first term may be seen always to be a function only of θ in the usual Euler notation, multiplied by a parameter of magnitude μ. The problem has been solved where μ is small and where μ is large, in the first case by the method of perturbations on the symmetric rotator and in the second case by the method of perturbations on the isotropic oscillator in two dimensions. For μ small the solutions are expandable in hypergeometric functions, while for μ large, they are expansions of associated Laguerre polynomials. While solutions definitely valid for intermediate values of μ have not yet been obtained, it is possible to predict how energy levels where $\mu=0$ go over to energy levels where $\mu=\infty$.

31. The Absorption of Monochromatic X-Rays of Short Wave-Length. T. M. HAHN, *University of Chicago. (Introduced by A. H. Compton.)*—With a Société Genevoise double crystal spectrometer and calcite crystals reflecting the Kα' line of tungsten in the (1, 1) position, the mass absorption coefficients of paraffin, carbon, aluminum, copper, silver, tantalum, tungsten and lead were determined with a probable error of less than one percent in each case. By using the instrument with the first crystal removed as a single crystal spectrometer, the measurements were extended down to a wave-length of 0.139A. The values of the atomic absorption per electron calculated

from the above coefficients give values of the scattering coefficient σ/σ_0 as determined from the equation

$$\mu_a/Z = kZ^p\lambda^q + (\sigma/\sigma_0)\sigma_0$$

in good agreement with the theoretical value $1/(1+2\alpha)$.

32. An Improved Technique for the Determination of Transmittancy by Means of the Hilger Rotating Sector-Photometer. ANDREW DINGWALL, R. G. CROSEN AND H. T. BEANS, *Columbia University.* (*Introduced by W. L. Severinghaus.*)—The preliminary adjustment of the photometer and source with respect to the spectrograph is facilitated by using graduated scales with pointers, on the feet of the photometer, and on the spark stand. A series of spectrograms ranging from a sector setting of 0.00 to 0.4 is taken using distilled water in the cells. The cells are then filled with solution and solvent and the same series repeated, the variable sector settings being made on the solution. Microphotometer records are made at the desired wavelength on both halves of each spectrogram. From the results thus obtained a standard curve is constructed showing the relationship between sector setting and blackening of the plate. From this standard the transmittancy of the unknown solution may be obtained. A filter calibrated by the Bureau of Standards was used to check the method. Where sufficient observations are made agreement was found to within $\pm 0.5\%$. The measurements are at definite wave-lengths and it is not essential to have the two halves of the spectrograms in perfect adjustment. By constructing standard curves for chromium, using diphenyl carbazide to give colored solutions, the chromium content of human tumors was found to vary from less than 0.001% chromium to 0.25% of the tumor ash.

33. On the Distribution of Ferromagnetism Among the Metals. DAVID R. INGLIS, *Ohio State University.*—The essential condition for ferromagnetism, in Heisenberg's model, is that the wave functions of electrons in neighboring atoms overlap comparatively little near the nuclei, so as to make the negative term in the electrostatic exchange integral, the term involving attraction between nuclei and electrons, comparatively small and the exchange integral positive. Due to the angular distribution of electrons in an atom in a crystal, there is a tendency to limit ferromagnetism to crystals made of elements in the latter part of a period in the periodic table. To show this, we consider the $3d$-electrons that form an incomplete shell in the iron period. Further, we consider the case of a strong crystal field, expecting this to have some similarity to the actual intermediate case. In a field of cubic symmetry the five orientation states of a d-electron split into two sets of two and three (Bethe). The states of one set have the higher energy because their wave functions are small in the direction of the next nuclei. When an atom has more than enough d-electrons to fill the lower set of states (doubly, because of spin), only the spins of the electrons in the upper set are free. The wave functions of just these electrons are small near the next nuclei, so their exchange integrals tend to be positive, giving rise to ferromagnetism. The contrary tendency is found in the first part of a period. Slater has suggested that the right elements are apt to be theoretically ferromagnetic because the radial wave functions of their $3d$-electrons are comparatively small near the nuclei, but this tendency alone seems to be insufficient to explain ferromagnetism in iron. Numerical integration, with Slater's analytic interpolation of Hartree's radial functions, and the Fermi-Thomas atomic potential, evaluates the exchange integral as $5.1-8.1+1.8=-1.2\times10^{-12}$ erg. (1.8 is a second-order correction term). This gives paramagnetism, but, with the positive and negative terms so nearly balanced when reckoned with spherically symmetric wave functions, inclusion of the angular parts of the wave functions should easily suffice to bring about a ferromagnetic result.

34. Possible Modifications of the Lorentz-Maxwell Field Equations. (A preliminary report.) VIVIAN JOHNSON AND E. S. AKELEY, *Purdue University.* Instead of $f_i = F_{ij}J_j$, the classical equation for the force acting upon a charged particle in an electromagnetic field, we have assumed the equation $f_i = F_{ijk}J_jV_k$ from analogy to the gravitational equation. F_{ijk} is a third order tensor whose components depend only upon the electromagnetic field. We have considered two possibilities, that the charge is invariant and that the charge transforms as the mass. We have just started to work on the first case. For a longitudinal electric field we obtained an equation $f_1 = e(F_{111}V_1^2 + 2iecF_{114}V_1 + E)$, which must approximately check $f_1 = eE$. It is possible to choose values so that the integrated curves for velocity fit within the limits of experimental error for the work we have checked, that of Perry (Phys. Rev. **36**, 904, 1930). We intend to continue our work on this case and obtain more definite results. For the second case, that in which the charge transforms, the problem is simpler and more closely analogous to the gravitational case. Our equation becomes:

$$f_i = (e/c)(c\overline{E} + \overline{V}\times\overline{H})_i + \sum_1^3 F'_{ijk}J_jV_k \quad (i, j \neq k).$$

Integrating this equation to find the path of a charged particle, we obtained results consistent with the available experiments. Experiments may be devised to give a closer check to our equation. We hope to find a set of equations corresponding to the Maxwell equations by using our results for F_{ijk}.

AUTHOR INDEX TO ABSTRACTS OF THE CINCINNATI MEETING

Akeley, E. S.—see Johnson
Allen, S. J. M.—No. 5

Bacher, R. F. and R. A. Sawyer—No. 17
Balinkin, I. A. and D. A. Wells—No. 12
Barker, E. F.—see Randall
Baud, Robert V.—No. 1
Beans, H. T.—see Dingwall
Benedict, Harris M. and H. Kersten—No. 21
Bloomenthal, S.—No. 4

Crosen, R. G.—See Dingwall

Dingwall, Andrew, R. G. Crosen and H. T. Beans—No. 32

Easley, M. A.—see Forsythe

Forsythe, W. E. and M. A. Easley—Nos. 10, 29

Gibbs, R. C.—see Shaw

Hahn, T. M.—No. 31
Haupt, Walter H.—No. 2
Hedenberg, N. A.—see Smith
Heyroth, Francis F. and John R. Loofbourow—Nos. 22, 23
Hughes, A. L.—see Stephens
—— **and J. H. McMillen**—No. 7

Inglis, David R.—No. 33

Johnson, Vivian and E. S. Akeley—No. 34
Johnston, H. L.—see Knauss

Kersten, H.—see Benedict
Knauss, H. P., H. M. Strong and H. L. Johnston—No. 15
—— **and R. V. Zumstein**—No. 11

Laporte, Otto—No. 27
Lark-Horovitz, K., E. M. Purcell and H. J. Yearian—No. 6
Loofbourow, John R.—see Heyroth

McMillen, J. H.—see Hughes

Nielsen, Harald H.—No. 30

Peoples, James A., Jr.—see Slack
Pool, M. L. and O. W. Prashun—No. 13
Prashun, O. W.—see Pool
Purcell, E. M.—see Lark-Horovitz

Randall, H. M. and E. F. Barker—No. 16
Rashevsky, N.—Nos. 19, 20

Sawyer, R. A.—see Bacher
Shaw, R. W. and R. C. Gibbs—No. 14
Shelow, Elizabeth—No. 24
Slack, Francis G. and James A. Peoples, Jr.—No. 26
Smith, K. K. and N. A. Hedenberg—No. 3
Stephens, W. E. and A. L. Hughes—No. 8
Strong, H. M.—see Knauss

Veblen, Oswald—No. 28

Warburton, F. W.—No. 9
Wells, D. A.—see Balinkin
Winans, J. G.—No. 18
Wissink, G. M. and Jay W. Woodrow—No. 25
Woodrow, Jay W.—see Wissink

Yearian, H. J.—see Lark-Horovitz

Zumstein, R. V.—see Knauss

Proceedings of the American Physical Society

MINUTES OF THE STANFORD MEETING, DECEMBER 15–16, 1933

THE 188th regular meeting of the American Physical Society was held at Stanford University, Stanford, California, in the main lecture room of the Physics Department on Friday, December 15th, and Saturday, December 16th, 1933. Professor David L. Webster, Chairman of the Physics Department, Stanford University, presided.

The sessions lasted on Friday from 9:00 until 12:30 and from 1:30 until 5:00. The session on Saturday morning began at 9:15 and terminated at 12:00 noon. There was a luncheon for members of the society at the Stanford Union on Friday noon.

The sessions were attended by some sixty members of the society covering the territory ranging from Los Angeles to San Francisco. At 10:00 on Friday, December 15th, there was a short business session at which the following matters were brought up.

It was voted, in conformity with previous announcement, to hold the 192nd regular meeting of the American Physical Society on the Pacific Coast at Berkeley, California, during the week, June 18–23, 1934, in affiliation with the Pacific Coast meeting of Section B of the A.A.A.S. The decision as to details of the arrangements of the meetings at this time was left in the hands of the secretary who will early in 1934 request a committee to act in formulating plans for the meeting.

It was further voted to empower the representative of the Pacific Coast group of physicists delegated to the affiliations committee of the Pacific Division of the American Association for the Advancement of Science to be free to vote a change in the date of the 1935 meeting of the Pacific Division of the A.A.A.S. which had originally been set tentatively as September, 1935, if in the eyes of the Pacific Division a June meeting in 1935 at Southern California would be preferable to the September meeting. This vote was necessary in view of the fact that the Physical Society had unofficially committed itself to the September date at the Pullman meeting of the Society in consultation with the executive committee of the Pacific Division. Circumstances connected with the convention of the American Chemical Society in San Francisco in September, 1935, and the commitment of the Pacific Division to hold the 1935 meeting in the Los Angeles area have necessitated a change in plans as regards the 1935 Pacific Division meeting to prevent a serious conflict with the Chemical Society meetings. The vote taken thus enabled the representatives of the Physical Society on the affiliations committee of the Pacific Division to use their judgment in assisting the Pacific Division to arrive at a proper solution of the present complications concerning the time of the 1935 meeting.

There were forty papers on the regular scientific program of the Society. The abstracts of these papers are given in the following pages.

LEONARD B. LOEB,
Local Secretary for the Pacific Coast

ABSTRACTS

1. The Ratio of Fluorescence Yields of the L_{11} and L_{22} Sub-Series of Lead. B. E. FOSTER, *Stanford University.*—The intensity of an x-ray line depends upon the probability of excitation and the fluorescence yield of the series to which the line belongs. The ratio of total intensities, then, of the L_{11} and L_{22} groups equals the ratio of the products of their probabilities of excitation by their respective fluorescence yields. If one can obtain a comparison between the total fluorescence intensities of the L_{11} and L_{22} groups, the ratio of fluorescence yields of the two sub-series can be ob-

tained, since the comparative excitation probabilities can be gotten from the heights of the absorption discontinuities of the fluorescence material, provided the primary wavelength is near that of the L_{11} limit. This condition was satisfied here with Pb irradiated with Mo $K\alpha$-rays filtered through ZrO_2. The determination of the intensity of the L_{11} and L_{22} groups may be made by measuring a representative line or two in each sub-series and computing the total intensity from known relations existing between the lines in each sub-series. In this experiment $L\beta_6$ and $L\beta_5$ of the L_{22} group have been compared photographically with $L\beta_4$ of the L_{11} group. Rough preliminary measurements give the ratio of the total number of quanta coming from these two series as: $L_{11} : L_{22} = 6 : 70$. Data taken from unpublished work of C. G. Patten indicate that the ratio of the absorption discontinuities is: $L_{11} : L_{22} = 0.185 : 0.490$. This gives for the fluorescence yields: $L_{11} : L_{22} = 2 : 9$.

2. Relative Probabilities of the Ionization of K and L Electrons of Equal Ionization Energy. B. G. EATON, *Stanford University.*—The L_{22} excitation potential of thallium being 12.6 kv and the K of bromine being 13.4 kv, the compound TlBr has in it a K level and an L level which have approximately the same ionization voltage. Likewise in $Th(MoO_4)_2$ the L_{21} voltage of Th is 19.7 kv and the K of Mo is 20.0 kv. The relative probabilities of the ionization, by impact, of K and L electrons of equal ionization energy can be determined by measuring the relative numbers of quanta emitted from these levels when such a compound is bombarded by cathode rays. The x-ray spectra of these compounds were photographically recorded, and the ratio of the intensity of the $K\alpha_1$ of Mo to that of the $L\beta_1$ of Th was found to be about 1 : 1. This means that there are about 4/3 as many quanta in the K series altogether as in the L_{21}. The $K\alpha_1$ of Br was about 3/10 the intensity of the Tl $L\alpha_1$. Here the K level gives off 1/3 as many quanta as does the L_{22}. Since Allison's relative intensities in the Th L series give 100 to 40 as the ratio of the numbers of quanta emitted in L_{22} and L_{21} respectively, the ratio for equal numbers of electrons would then be about 1 : 0.8 for L_{22} and L_{21}. The relative intensities of TlBr and $Th(MoO_4)_2$ reported here therefore give 2/3 as many quanta emitted per K electron as per L_{21}. The number of quanta emitted divided by the fluorescence yield ϕ gives the number of ionizations taking place. ϕ for Mo K is given by Compton as 0.68, and for U L_{22} by Stephenson as 0.67; and the yield for Th L_{22} is probably about the same as for U L_{22}. As the K and L value are the same the relative numbers of quanta coming off are the same as the relative numbers of ionizations. Thus under cathode-ray bombardment any K electron is $\frac{1}{2}$ as likely to get ionized as any L_{22}.

3. Polarization of General X-Rays from Thick Targets. YEE FUNG CHENG, *Stanford University.*—The method applied in this experiment is that of 90° scattering combined with the balanced filter method. Bands of the x-ray spectrum between K-absorption limits of columbium and molybdenum, of palladium and rhodium, and of tungsten and tantalum from different targets of tungsten, copper and aluminum have been tested for polarization, using voltage from about 20 kv to 100 kv. From results so far obtained the following conclusions have been drawn. First, the polarization increases as the voltage decreases and increases very rapidly as the quantum voltage of each band is approached. Second, while the maximum experimental value of polarization obtained was not over 60 percent, the polarization at the quantum voltage of the band, obtained by extrapolation, is nearly complete. Third, the polarization of x-rays from the targets of lower atomic number is higher than from the targets of higher atomic number, except near the quantum voltage where they approach 100 percent.

4. X-Ray Line Intensities in Thick Targets of Nickel. L. T. POCKMAN, PAUL KIRKPATRICK AND D. L. WEBSTER, *Stanford University.*—$K\alpha$ line intensities of thick nickel have been measured as functions of voltage up to 180 kv for rays emerging from the target at various angles, by methods previously used for silver. (Phys. Rev. **44**, 258 (1933).) When the intensities are expressed as functions of U, the ratio of tube voltage to excitation voltage, the results are very much like those for silver up to its limit, $U=7$, but the limit for nickel is $U=21.6$. The effect of target absorption (estimated by Kulenkampff's method) is less for nickel than for silver at any given value of U, but greater at any given voltage. Intensities and emission efficiencies for nickel reach maxima as follows: for rays emerging at 1° from the target face, at 40 kv and 20 kv, respectively; 2°, 53 kv, 25 kv; 6°, 75 kv, 40 kv; 11°, 100 kv, 50 kv; 16°, 140 kv, 55 kv; 21°, 160 kv, 60 kv; 26°, 180 kv, 65 kv, with target absorption eliminated, over 180 kv, 110 kv. Beyond the maxima the intensities at all angles decline very slowly.

5. The True Absorption Coefficients for the Elements from Gold to Bismuth in the Neighborhood of the L-Absorption Edges. C. G. PATTEN, *University of California.* (*Introduced by R. B. Brode.*)—Thin films of thallium, lead and bismuth were made by evaporation of the metals onto very thin sheets of mica. Oxidation of the films was prevented by coating with a thin layer of aluminum. Effects due to possible irregularities in the films were averaged out by keeping the film in constant motion before the slits. The ionization currents were measured with a F.P. 54 Pliotron vacuum tube amplifier and the readings were constant within one percent. The true absorption coefficients τ_1, τ_2, and τ_3 corresponding to the photoelectric absorption by the three types of L electrons were found to vary approximately as $\lambda^{2.6}$ for each of the five elements gold to bismuth. The data for gold were obtained by Uber and Patten (Phys. Rev. **42**, 229 (1932)) and for mercury by Uber (Phys. Rev. **38**, 217 (1931)). With this relation the τ's were computed for a given wave-length. Their ratio $\tau_1 : \tau_2 : \tau_3$ (which is therefore independent of the wavelength) was found to be constant over the range 0.5 to 1.5A and to have approximately the same value for each of the five elements. The value of the ratio $\tau_1 : \tau_2 : \tau_3$ was found to be 19 : 32 : 49. This ratio also gives the relative numbers of photoelectrons ejected from the three L shells by radiation of a given frequency. Ratios of τ_1, τ_2, and τ_3 which are evaluated at their respective absorption edges L_{I}, L_{II}, and

L_{III} were also determined. This ratio of τ_2/τ_3 was found to be approximately 0.45 for each element and is in very good agreement with the value predicted by relativistic theory. (See abstract No. 6.) The ratio $\tau_1/(\tau_2+\tau_3)$ has been found theoretically only by means of a non-relativistic treatment of absorption. The experimental value, 0.163, is not in good agreement with the predicted value.

6. Theoretical Ratio of L_{II} and L_{III} X-Ray Absorption Coefficients. MELBA PHILLIPS, *University of California.*—On the assumption of a Coulomb field for the narrow range of the $2p$ electrons the relativistic radial wave functions may be used to calculate the ratio of the absorption coefficients for the L_{II} and L_{III} x-ray edges. Thus a correction for the coupling of spin and orbit is introduced. $\tau_{L_{II}}/\tau_{L_{III}}$ was found to have the value $1-0.35(\alpha Z_{eff})^2$ per electron, giving a correction to the "sum rule" ratio, 1 : 2, which holds for light elements. A reasonable choice of the effective nuclear charge for the elements Au to Bi makes $\tau_{L_{II}}/\tau_{L_{III}}=0.45$, in agreement with the observations of C. G. Patten.

7. A New Method of Measuring Doublet Separations with a Fabry-Perot Interferometer. WILLIAM V. HOUSTON, *California Institute of Technology.*—When the orders of interference of the two lines differ by Δp, the wave-number difference is $\Delta p/2d$, where d is the distance between the plates. The principal uncertainty in the ordinary method is due to the uncertainty in the location of the point on the fringe which should be measured. If one tries to find the plate separation, d_0, for which $\Delta p=1/2$, the accuracy can be much increased. The separation d_0 is characterized by the fact that all the minima of intensity are the same. This point can be located by means of interpolation by the following equation. If M_1 is the intensity of the minima between the members of the doublet, and M_2 is the intensity of the minima between the adjacent orders, $(1/\alpha)$ log (M_1/M_2) is a function of d which is zero for $d=d_0$, and is a linear function of d in the neighborhood of this point. The quantity α is given by

$$(L_1+L_2)/(M_1+M_2)=(1+2e^{-\alpha/4})/2e^{-\alpha/16},$$

where L_1 and L_2 are the intensities of the two maxima.

8. The Doublet Separations of the Balmer Lines. W. V. HOUSTON AND Y. M. HSIEH, *California Institute of Technology.*—An analysis of the theoretical shapes of the components of the Balmer doublets shows that, with the exception of $H\alpha$, they should be essentially symmetrical about the centers of gravity. Hence if the separation is measured by the method described in the previous abstract, the result will give the separation of the centers of gravity of the components. For $H\alpha$ a correction of about 1 percent must be applied. These measurements have been made on the first five members of the series. The source was a discharge-tube cooled in liquid air and operated under such conditions that the intensity ratios of the components were those expected theoretically. The results indicate that all of the doublets are about 3 percent narrower than is to be expected theoretically. This large discrepancy cannot be attributed to an uncertainty in the fine structure constant, and so must be attributed to a deficiency in the theory when this degree of precision is required.

9. The Spectrum of Fluorine, F II, F III, F IV. I. S. BOWEN, *California Institute of Technology.*—The spectrum of fluorine extending from 125A to 620A has been obtained with a two-meter grazing-incidence spectrograph. By using these new determinations and the previous measurements in the longer wave-length region made by Dingle and by the author, it has been possible to classify 37 additional lines in F II. The newly classified lines are largely due to transitions to the singlet and triplet terms of the s^2p^4 and sp^5 configurations. In F III, 96 new identifications have been made including 14 intercombination lines. These consist largely of transitions to terms of the s^2p^3 configuration, and of transitions between terms based on the ^1D state of the core. 21 new lines have been classified in F IV. These new identifications include most of the strong lines that had not already been accounted for. These analyses yield the following ionization potentials: F II 34.81 volts, F III 62.35 volts, F IV 87.34 volts.

10. Hyperfine Structure in the Arc Spectrum of Lanthanum. O. E. ANDERSON, *University of California.*—The hyperfine structure analysis previously reported for the arc spectrum of lanthanum has been extended to include a number of new lines and energy levels. These measurements afford a convenient experimental check on the formulas of Goudsmit and Bacher as applied to electron configurations involving three electrons. The spectrum was excited in a liquid-air-cooled Schüler tube and photographed with a three-meter flint prism spectrograph crossed with Fabry-Perot etalons. By setting the prisms off from minimum deviation a relatively high dispersion, sufficient to eliminate the troublesome overlapping of many of the lines, was obtained. Of particular interest in the measurements are the overall separations of the hyperfine structure terms arising from $5d^2\,6s$, $^4F_{3/2,\ 5/2,\ 7/2,\ 9/2}$. Both the hyperfine structure and the fine structure follow the Landé interval rule, and the overall separations are in good agreement with Goudsmit's and Bacher's equations.

11. Isotope Displacement in the Arc Spectrum of Tungsten. KENNETH R. MORE, *University of California.*—W I lines were excited in a liquid-air-cooled Schüler tube operated at 2000 volts with currents from 0.07 to 0.4 amp. The spectrum was photographed with a three-prism glass spectrograph crossed with silvered Fabry-Perot etalons. Invar etalon separators up to 30 mm were used. Several of the stronger W I lines in the region 4000 to 5600A show three components which are roughly equally spaced and are of the same order of intensity. The greatest overall splitting observed is 0.17 cm^{-1}. Aston (Nature **126**, 913 (1930)) reports four isotopes of tungsten of mass and abundance 182, 22.6%; 183, 17.2%; 184, 30.1%; 186, 30.0%. Since the components observed are roughly equally spaced they are attributed to the three even isotopes. The intensity ratios of the three components vary somewhat from line to line. This latter suggests that the odd isotope is present and is

showing a narrow hyperfine structure which is masked by the components due to the even isotopes. The electron configurations are known only for the ground states of W I. They are $5d^4\ 6s^2$, ^5D and $5d^5\ 6s$, ^7S. Most of the lines that show isotope displacement arise from transitions to the levels $5d^4\ 6s^2$, ^5D.

12. The Spectrum of Magnesium Fluoride. F. A. JENKINS AND RAFAEL GRINFELD (*Fellow of the Rockefeller Foundation*), *University of California.*—Measurements of the rotational structure and of the band heads of the three band systems observed in the absorption spectrum of MgF have been made on plates taken with a 21-foot grating. In the $^2\Sigma$, $^2\Sigma$ system at λ2689, wave numbers of 29 resolved lines of the R branch of the 0,0 band, combined with those of the band head and of the band origin (which appears as a sharp minimum at $\nu_{00}=37{,}187.4$), are used to determine the constants $B_0'=0.537$ cm^{-1}, $B_0''=0.518\pm0.010$ and $r_0''=1.75\ 10^{-8}$ cm. In the $^2\Pi$, $^2\Sigma$ system at λ3594, starting with the value of B_0'' found above, measurements of the P_1, P_2 and Q_2 heads, of a minimum at 27,829.4 cm^{-1}, and of some outer lines of the Q branch, the following constants are derived: $B_0'=0.529$, $\nu_{00}=27{,}846.5$, $A=-34.3$ cm^{-1}. The $^2\Pi$ state is assumed to be inverted, as in BeF. If it is normal, $A=+38.3$. By using these constants in the Hill and Van Vleck formula for $^2\Pi$ terms, good agreement is obtained with the measured wave numbers of the heads. In the newly-discovered system at λ2275, the data are insufficient for the determination of constants. The isotope effect of Mg is observed with definiteness for the first time in this spectrum.

13. Electronic and Vibrational Absorption in O_4 and O_2 Molecules. JOSEPH W. ELLIS AND HANS O. KNESER (*Fellow of the Rockefeller Foundation*), *University of California at Los Angeles.*—We have studied the infrared, visible and near ultraviolet absorption spectrum of liquid oxygen. At wave numbers 793, 943 and 1088 mm^{-1} a progression of bands occurs which we identify with the $^1\Delta+v\omega$ ($v=0, 1, 2$) system predicted by Mulliken for O_2 in the infrared. The wave numbers of the three well-known visible and ultraviolet progressions (1587, 1730, 1874, 2020, 2164), (2094, 2235, 2387, 2548) and (2621, 2765, 2896, 3040) we find to be expressible by $\nu=m\,^1\Delta+n\,^1\Sigma+v\omega$, in which $(m, n)=(2, 0)$, $(1, 1)$ and $(0, 2)$ respectively, $^1\Sigma$ represents the wave number of the electronic term of the red "atmospheric" system for O_2 at 1307 mm^{-1}, and ω is the average of the nearly equal vibration terms of the $^1\Delta$ and $^1\Sigma$ systems. These progressions we believe arise from simultaneous excitations of the two loosely coupled O_2 systems which constitute the O_4 molecule. The slight degradation toward the violet of the individual bands is probably caused by the unresolved vibrational terms of the O_2-O_2 molecule. The assumption that the infrared $^1\Delta$ system is primarily a characteristic of the O_2 molecule rests upon its appearance in the solar spectrum of Abbott and Freeman, although we could not detect it with a 64-meter atmospheric path.

14. Dissociation, Excitation and Emission in Condensed Sparks at High Pressure. WOLFGANG FINKELNBURG (*Fellow of the Rockefeller Foundation*), *California Institute of Technology.*—In the spectrum of condensed sparks at high pressure one gets broadened lines of normal and ionized atoms, especially of highly excited levels. The probability of such excitations, especially of dissociation and ionization by single electron collisions, is extremely small, because the potential difference per mean free path of an electron is only a few volts. In hydrogen, where all excitation conditions are known very well, one is able to prove that the emitting H-atoms (molecular spectra do not appear) cannot be formed in one collision, but by a series of two or more successive excitations. Generally in condensed sparks the probability of re-excitations during the lifetime of an excited atom is high because of the high current density. In the hydrogen spark studied one atom suffered 10^3 electron-collisions during the mean lifetime of 10^{-8} sec. Consequently excitation, dissociation and ionization will be a result of re-excitations, and the normal excitation rules do not apply. The enormous broadening of lines usually described as the result of a Stark effect produced by the inhomogenous field of the ions is explained more accurately by interactions of the single particles.

15. Band Spectrum of Nitrogen. JOSEPH KAPLAN, *University of California at Los Angeles.*—Further study of the unusual discharge tube described last December has led to several interesting nitrogen band spectra. In the present tube, the first negative bands are much more intense relative to the first positive bands than on the plates obtained last year. One of the most remarkable properties of the tube is the enhancement of bands which originate on high vibrational states of the molecule. This is shown by the discovery of at least a dozen new members of the Lyman bands of nitrogen. These bands arise in the $a\,^1\Pi-X\,^1\Sigma$ transition. In the first positive group, bands which arise on very high vibrational levels are also remarkably enhanced. The second positive group is nearly completely absent and the fourth positive group is present. The presence of the fourth positive group in an uncondensed discharge, as is the case in these experiments, is a rather unusual phenomenon. Two types of intensity distribution in the first negative bands are shown and their relationship to the spectrum of the aurora borealis is pointed out.

16. Analysis of the Infrared Bands of Formaldehyde. ARNOLD NORDSIECK, *University of California.*—The theoretically expected structure of the infrared bands of H_2CO, a slightly asymmetric coplanar molecule, has been worked out on the basis of Wang's theory of the asymmetric rotator (S. C. Wang, Phys. Rev. **58**, 730 (1929)), the calculations being modelled after those of D. M. Dennison (Rev. Mod. Phys. **3**, 289 (1931)) and H. H. Nielsen (Phys. Rev. **38**, 1432 (1931)). Four of these bands were resolved by J. R. Patty and H. H. Nielsen (Phys. Rev. **39**, 957 (1932)) and a larger number has recently been investigated under improved experimental conditions by Nielsen at Ann Arbor. Account being taken of the alternating intensities due to the presence of two H atoms, the structure seems to be explained satisfactorily. The moments of inertia found agree well with those deduced from the ultra-

violet spectrum by Dieke and Kistiakowsky (Proc. Nat. Acad. Sci. **18**, 367 (1932)).

17. The Value of e/m from the Zeeman Effect. L. E. KINSLER AND W. V. HOUSTON, *California Institute of Technology.*—The measurements of e/m by means of the Zeeman effect of the red singlet lines of Cd and Zn have been repeated with careful attention to all of the sources of experimental uncertainty. All apparatus has been duplicated and interchanged in such a way as to very much reduce the probability of instrumental errors. The magnetic field used in the solenoid was measured under the actual conditions of operation in order to determine the effects of the temperature rise and the mechanical stresses. The solenoid constant was found to decrease by about 1/1500 when the current was increased from 1 amp. to 190 amp. The field determination is believed to be correct to one part in three thousand. The results of the spectroscopic measurements, which were made with a Fabry-Perot interferometer, give $e/m=1.7570\pm0.0010$ e.m.u. The interpretation of these results in terms of e/m depends, of course, upon the theory of the Zeeman effect. If this theory should be incorrect these measurements would give the splitting of these two lines, but would not necessarily give this value of e/m.

18. Anomalies in the Zeeman Effect of Helium. L. E. KINSLER AND W. V. HOUSTON, *California Institute of Technology.*—Measurements of the Zeeman splitting of three singlet lines of helium have shown that they differ among themselves by much more than the experimental error. If e/m is taken as 1.7570 e.m.u., the splitting of λ4921 is 1.0016 times the expected value. This is just at the limit of the experimental uncertainty, and its difference from 1.0000 may not be real. However, on the same plates, λ5015 shows 1.0055 and λ6678 shows 1.0106 times the normal splitting. These differences are much larger than can be accounted for by the ordinary theory of perturbation by the triplet levels, and they point to an inadequacy of the theory of the Zeeman effect when results of this precision are desired.

19. Hyperfine Structure in the Solar Spectrum. EDWIN MCMILLAN (*National Research Fellow*), *University of California.*—The possibility of observing hyperfine structure (including isotope shifts) in the solar spectrum has been investigated. This is of interest since it may give some evidence concerning the isotopic constitution of elements in the sun. Because of the large intrinsic breadths of solar lines, it is impossible to resolve any hyperfine structures; only a broadening of the lines can be observed. This has been studied on a number of plates taken in the third order of the grating belonging to the Astronomy Department of the University. Information has also been obtained from Rowland's Table of Solar Spectrum Wave-Lengths, where many broad lines are listed as double. Studies of the isotope shift in the solar lines of H and Ti have been published by Menzel (J. Astron. Soc. of the Pacific **44**, 33 (1932)) and McMillan (Phys. Rev. **44**, 240 (1933)) respectively. In the present work the following additional lines have been found to show observable evidence of hyperfine structure in the sun:

Element	Listed as double by Rowland	Photographed by author	Correlation with known hyperfine structures
Mn I	11 lines	9 lines	Complete
Cu I	3 lines	3 lines	
Ba II	1 line	2 lines	
La II	2 lines		
Co I	12 lines		Probably complete
Sc II	8 lines		No laboratory data on hyperfine structure
Ti II	9 lines		
Ce II	1 line		

The laboratory data on cobalt, obtained by N. S. Grace in this laboratory, are not complete. Seven of the above lines are found to have large structures, and the others will undoubtedly be found to have also when the work is completed. The case of titanium is interesting, as it would not be expected to have large structure, but nothing further can be said until this is examined in the laboratory. The question of correlation with terrestrial data was also approached from the other side; all lines known to have large structure were examined in regard to their occurrence in the sun. None were found with sufficient intensity or freedom from overlapping for observation of structure, except those listed above. Thus, as far as the observations go at present, there are no differences between the solar and terrestrial hyperfine structures.

20. An Absolute Determination of the Efficiency of Production of Silver $K\alpha$ X-Rays as a Function of Voltage. J. C. CLARK, *Stanford University.*—Ross' method of balanced foils was used with foils of Rh and Mo to isolate a small region of the x-ray spectrum from thin silver targets (about 1400A), the Ag $K\alpha$ lines being included. The ratio of line energy to the continuous for this region was calculated from data taken by Webster, Hansen and Duveneck (Phys. Rev. **43**, 839 (1933), and **44**, 258 (1933)). Preliminary measurements give the ionization cross section per atom as about 5.6×10^{-23} cm^2 at 70 kv. Rosseland's theory would predict 4.6×10^{-23} cm^2 and a more complete classical theory 7.1×10^{-23} cm^2. The departure of these measurements from the theories is of the same order as that of Smith's measurements (Phys. Rev. **36**, 1923 (1930)) on helium. The ionization cross section per atom can be determined as a function of voltage by using the value here obtained in the work of the above reference (Phys. Rev. **44**, 258 (1933)).

21. Compton Effect. P. A. ROSS AND PAUL KIRKPATRICK, *Stanford University.*—The Compton effect has been studied with a double-crystal spectrometer and a special x-ray tube. An annular target and cathode distributed the focal energy over a ring 3 inches in diameter. A small scattering block was placed so that a cone of x-rays from the ring focus converged upon it. Scattering to the spectrometer took place along the axis of the cone. By

turning the tube through 180° supplementary angles were used with each position of the scattering block. This eliminated a large part of the error due to uncertainty in scattering angle, since for supplementary angles $\theta+\theta'=\pi$, $\Delta\lambda=(h/mc)(1-\cos\theta)$, $\Delta\lambda'=(h/mc)(1-\cos\theta')$ and by addition $\Delta\lambda+\Delta\lambda'=2h/mc$. We believe that we have obtained a more accurate value of the "Compton constant" than has hitherto been experimentally obtained and that this accuracy is sufficient to give a value of m (in terms of e, h and c) comparable in accuracy with that obtained by spectroscopic and deflection methods. Curves showing the modified and unmodified components from beryllium, carbon, aluminum and sulphur have been taken at scattering angles between 30° and 150°. Modified widths from carbon and beryllium agree well with DuMond's theory (Rev. Mod. Phys. **5**, 1 (1933)). Radiation scattered by aluminum and sulphur shows a narrow modified line and evidence of some complex structure. The study of the variation of the modified line shape and width is being continued.

22. Determination of h by X-Rays. PAUL KIRKPATRICK AND P. A. ROSS, *Stanford University.*—A determination of the Planck constant has been performed by the method of measuring the minimum potential required to produce continuous spectrum x-rays of specified wave-length. The wave-length employed was that of the $K\alpha_1$ line of silver, a radiation which has been measured with precision by many investigators. No wave-lengths were measured in this research. A double spectrometer was adjusted to receive the $K\alpha_1$ line from a silver target after which isochromats from a tungsten target were observed without disturbing the spectrometer adjustment. X-ray tube potentials were measured by a potential divider and potentiometer system, and the potential during a single observation could be held effectively constant to about 0.01 percent. Though experimental work is complete, the final numerical result must unfortunately be withheld pending action by the Bureau of Standards upon our standard cells and resistances. It is certain at this time that the probable error to be assigned to our final value of $h/e^{4/3}$ will be much smaller than that associated with the presently accepted value. Methods for the attainment of further precision are indicated.

23. A 400 Kilovolt X-Ray Tube for Therapy. R. R. NEWELL, F. B. DUVENECK AND A. W. HACKNEY, *Stanford University.*—The anode end of the tube is a large, grounded, water-jacketed brass cylinder, 80 cm of which is designed to project horizontally into the treatment room. The x-rays come through a belt thinned to three millimeters near the free end. A roof-shaped target with two 45° gold surfaces, water-cooled, and two cathode filaments permits the use of the rays downward, upward, horizontally or at any intermediate inclination. The cathode is a long steel pipe extending axially through a large thick porcelain tube into the brass cylinder to within about 15 cm of the target. In order to make use of a Villard potential-doubling arrangement a valve is built into the tube itself by setting a kenotron filament, at ground potential, into that part of the brass cylinder which will be behind the wall. The plate for this valve is the cathode pipe. The tube is assembled with lead gaskets and is run on the pump.

24. The Crystal Structure of Cadmium Hydroxychloride, CdOHCl. J. L. HOARD AND J. D. GRENKO, *Stanford University.*—The closely related structures of cadmium chloride and cadmium hydroxide, each representative of a large class of halides or hydroxides of bivalent elements, are built up by the superposition of neutral layers of composition MX_2. The crystal structure of a compound of intermediate composition, cadmium hydroxychloride, was determined in order to investigate further the factors determining the order of succession of these layers. Laue and oscillation photographs fix the symmetry as hexagonal with $a_0=3.66$A, $c_0=10.27$A, and the space-group as $C_{6v}{}^4-C\,6mc$. The structure, uniquely determined by semiquantitative but rigorous arguments, places the two molecules of CdOHCl as follows: Cd at $\frac{1}{3}$, $\frac{2}{3}$, 0; $\frac{2}{3}$, $\frac{1}{3}$, $\frac{1}{2}$, Cl at $\frac{1}{3}$, $\frac{2}{3}$, u; $\frac{2}{3}$, $\frac{1}{3}$, $u+\frac{1}{2}$ with $u=0.337\pm0.010$, OH at 0, 0, v; 0, 0, $v+\frac{1}{2}$ with $v=0.100\pm0.010$. The structure is seen to be built up from neutral layers of composition CdOHCl. The order of succession of atomic layers is accounted for by considering the degree of polarization of each type of anion, and these criteria suffice to determine whether the $CdCl_2$ or the $Cd(OH)_2$ type of structure will be assumed by a compound MX_2. Certain slight peculiarities of interatomic distances and the absence of a pronounced basal cleavage in CdOHCl are correlated with the presence of the proton in each hydroxyl group.

25. Spray Electrification of Liquids. SEVILLE CHAPMAN, *University of California.* (*Introduced by Leonard B. Loeb.*)—The problem of spray electrification of aqueous solutions and pure water has been extensively investigated by Lenard and his school. While the phenomenon is known to be applicable to other liquids, little is known of the nature of the phenomenon in these cases. This work represents an attempt to make a more quantitative study of the phenomena by using the Millikan oil drop method, with a view to correlating if possible drop size, sign of charge, magnitude of charge, surface tension, and dielectric constant. A brass-nozzled atomizer operated by clean compressed air was used. Difficulties were encountered due to evaporation and the measurements covered only drop sizes from 3×10^{-5} cm to 7×10^{-4} cm. The results on specially purified liquids are best represented in the table. The data on water are in order of magnitude only, owing to the evaporation of the droplets. It is seen that the larger drops in general have the larger charges, that no

Substance	Dielectric constant	Surface tension in dynes/cm	Smallest Drops: Average charge in electrons	Smallest Drops: Radius in cm	Smallest Drops: Predominating sign of charge	Largest Drops: Average charge in electrons	Largest Drops: Radius in cm	Largest Drops: Predominating sign of charge
Ameroil	1.9	27	2	4×10^{-5}	neither	2	1×10^{-4}	neither
Nitrobenzene	35.7	46	150	1×10^{-4}	neither	800	4×10^{-4}	neither
Aniline	7.3	44	100	1.5×10^{-4}	neither	450	5×10^{-4}	neither
Glycerine	56.2	65.2	40	5×10^{-5}	neither	500	2.5×10^{-4}	neither
Water	80	72.8	125	1.5×10^{-4}	neither	600	5×10^{-4}	neither

preference in sign attaches to drop size in this range, and that higher dielectric constants in general give higher charge values.

26. The Elastic Scattering of High Velocity Electrons by Mercury Atoms and the Agreement with Mott's Theory. EDWARD B. JORDAN, *University of California.*—The angular distribution of electrons scattered elastically by single mercury atoms has been studied for electrons of 900, 1160, 1600 and 2000 volts energy. The angle range was 8° to 48°. The values of the scattered intensities have been plotted and compared with the corresponding theoretical curves computed in accordance with Mott's theory. The theoretical and experimental curves for 900 volt-electrons differ markedly in shape. The slope of the experimental curve is much greater for small angles than that of the theoretical curve. The departure from Mott's curve decreases progressively for electron velocities corresponding to 1160, 1600 and 2000 volts energy. The 2000 volt curve shows good agreement with the corresponding theoretical curve.

27. The Measurement of Natural Alpha-Particles Ejected from Solids. ROBLEY D. EVANS (*National Research Fellow*), *University of California.*—Exact expressions for the ionization due to the emission of alpha-particles from radioactive solids are set up and the results of their graphical integration are given. The total ionization per cm^2 of surface, both with and without absorbers; the variation of ionization with height above the radioactive surface; the ionization from thin films; the ionization from substances containing all members of the U, Th and Ac series, both with and without absorbers; and the counting rate for alpha-particle counting chambers, are given in equations accompanied by appropriate graphs and tables. The older approximate theories break down for actual alpha-particles, particularly those of short range. If q is the number of ion pairs per cm^2 per sec. formed above the surface of a radioactive solid; N, the number of alpha-particles per sec. per cm^3 emitted in the solid; k, the number of ion pairs per alpha-particle of range R in air; and R', the alpha-particle range in the solid: then $q=\epsilon NkR'$, and the numerical coefficient ϵ has values between 0.114 and 0.150 for the alpha-particles from all known radioactive substances.

28. The Crystaldiamagnetism of Single-Crystalline Solid Solutions of Bi. A. GOETZ AND A. B. FOCKE, *California Institute of Technology.*—Previous work on polycrystalline material has shown large influences by metallic admixtures when within the solubility limits. The effect of the type of insertion is found to be non-existing in case of complete insolubility (Bi–Cu), to be random for macroscopic solubility (eutectic) (Bi–Ag) and large and directional for atomic solubility, no matter whether the admixture enters the crystal as atom (Sn, Pb and probably Ge) or as intermetallic compound (BiSe, Bi_2Te_3). The effect is smallest for an isomorphous admixture (Sb) with complete atomic solubility. The dependence of the susceptibilities parallel and normal to [111] on the concentration and the type of the foreign atom shows a critical concentration N_e for low temperatures which exists only in one direction of the crystal: normal to [111] for an atom with an electropositive, parallel to [111] for an atom with an electronegative valency configuration. An isomorphous atom has an electropositive effect normal to [111] and an electronegative parallel to [111]. N_e has the following values for: Te = 0.01%; Sn = 0.03%; Pb = Se = 0.09%. These phenomena contradict any assumption based on a volume effect; however, by introducing a superstructure of planes according to previous suggestions of the authors with a parameter of 10^3–10^4A on which the admixture is adsorbed and accepting the Ehrenfest-Raman hypothesis of crystal-diamagnetism the entire phenomenology can be accounted for. The parameters obtained from N_e are in good agreement with the results of etch figures and the "critical" sizes of colloidal crystals.

29. The Maximum Range of Cosmic Rays. PAUL S. EPSTEIN, *California Institute of Technology.*—As was pointed out by Zwicky, the astronomical red shift seems to indicate that cosmic rays can travel only a finite distance before completely losing their energy. A closer investigation shows that the problem of their travel time is the same as that of the time scale of the universe. It can be generally shown that the types of expansion of the universe discussed by Friedmann and Lemaitre for a special model are the only possible ones under all circumstances. If the cosmological constant is zero or negative, the maximum range of light quanta and material particles is below $2\cdot10^9$ years; if the constant is positive, it can have any value, up to infinity. The difficulties pointed out by Zwicky form, therefore, an additional argument in favor of a finite, positive cosmological constant.

30. On the Production of Positives by Nuclear Gamma-Rays. L. NEDELSKY AND J. R. OPPENHEIMER, *University of California.*—A gamma-ray emitted by a nucleus may be absorbed by the creation of an electron and positive. The probability of this process does not depend essentially on the electrostatic field of the nucleus, and is, for light elements and high energies, very much greater than the probability of internal conversion by the ejection of an atomic electron. The probability that a dipole gamma-ray of energy γmc^2 should eject a positive of energy ϵmc^2 and an electron of energy $\epsilon' mc^2$ (with $\epsilon+\epsilon'=\gamma$) is then

$$d\epsilon\,\frac{2e^2}{hc\gamma^2}\left[2(\epsilon^2-1)^{\frac{1}{2}}(\epsilon'^2-1)^{\frac{1}{2}} + (\epsilon^2+\epsilon'^2)\ln\frac{\epsilon\epsilon'+1+(\epsilon^2-1)^{\frac{1}{2}}(\epsilon'^2-1)^{\frac{1}{2}}}{\gamma}\right]; \qquad (\epsilon,\ \epsilon'>1).$$

The total probability that a pair be created increases with $\ln\gamma$. For $\gamma=12$, which corresponds roughly to the radiation emitted by disintegrating Be, the probability is 0.003 Almost identical results are obtained for a quadripole gamma-ray. The positives observed by Curie and Joliot when Be was disintegrated by Po alpha-particles may be accounted for by this theory. The positives observed in disintegrating Al are far too numerous, and high energy electrons far too infrequent to admit this explanation.

31. Production of High Energy Electron Pairs. W. H. FURRY (*National Research Fellow*) and J. F. CARLSON, *University of California.*—The production of a high energy electron pair (electron and positive) by a γ-ray traversing the field of a nucleus was first discussed by Oppenheimer and Plesset (Phys. Rev. **44**, 53 (1933)). This problem has now been studied in considerable detail and by a more rigorous method. The production of pairs by five million volt γ-rays is reasonably consistent with the experimental results obtained with artificial γ-rays from beryllium. For energies above twenty million volts the predicted pair production is even greater than that computed by Oppenheimer and Plesset, and hence even more irreconcilable with experiment. It seems possible to connect this discrepancy with the fundamental inadequacies of quantum electrodynamics.

32. The Nature of Statistical Fluctuations. ROBLEY D. EVANS (*National Research Fellow*), *University of California.* —I. The square of the mean deviation, D, of the combined effect of several random processes releasing an average of $x, y, z \cdots$ particles per unit time, and producing $a, b, c \cdots$ ion pairs respectively per particle, is $D^2=a^2x+b^2y+c^2z+\cdots$, regardless of whether the separate effects are added or subtracted by the experimental arrangement. For tube-counters, point-counters, scintillation screens, and particle counting chambers, $a=b=c=1$; for ionization chamber $a, b, c \cdots$ are unequal. II. From the standpoint of statistical fluctuations, the use of two identical instruments in a differential circuit is inferior to the use of a single instrument. III. The natural observation limit for the measurement of x particles against a background of y particles is $x=0.67(y)^{\frac{1}{2}}$. IV. The statistical fluctuations in the ionization produced by cosmic rays in a spherical ionization chamber are treated rigorously, and the fluctuations due to heterogeneity of range and to showers are derived. V. Application to existing data shows that the showers observed in cloud-chamber photographs of the penetrating radiation are also present in the ionization chamber, in about the same frequency and multiplicity as indicated by the cloud-chamber results. The tube-counter investigations of the cosmic-ray flux are also in agreement with the deductions from the statistical fluctuations in the ionization chamber. An upper limit of 70 ± 10 ion pairs per cm in air at 1 atmosphere is set for the total ionization along the path of an individual cosmic-ray secondary. The size and the relative frequency of occurrence of showers is several times greater at 14,700 feet elevation than at sea level. These showers are quite distinct from the ionization bursts or "Stösse" observed by Hoffmann, Steinke and others.

33. Radium Content of the Lavas of the Lassen Volcanic National Park, California. ROBLEY D. EVANS (*National Research Fellow*) AND HOWEL WILLIAMS, *University of California.*—Joly and Piggot have determined the radium content of lavas from Vesuvius and Hawaii respectively. The present authors chose the lavas of the Lassen region for study because of their wider range of chemical and mineralogical composition. One of the authors (H. W.) has already described the petrographic characters of these rocks in detail (Univ. Calif. Publ. Bull. Dept. Geol. Sci. **21**, 195 (1932)). The direct-fusion method of radium analysis was employed (Evans, Rev. Sci. Inst. **4**, 223 (1933)). Within the silica range of 47.43 percent and 70.93 percent, the radium content varies from 0.30 to 1.14×10^{-12} g Ra per g rock. There is a strict correlation between these constituents, irrespective of the age or mode of occurrence of the rocks. Experiments are now being made to determine the extent to which the radium is concentrated in certain definite minerals.

34. The Mass of the Neutron. R. M. LANGER, *California Institute of Technology.*—The reaction $Li^7+H^2\rightarrow 2He^4+n$ has been studied by Oliphant, Kinsey and Rutherford (Proc. Roy. Soc. **141**, 722 (1933)) who find all energies up to 8.3×10^6 volts for the resulting alpha-particles. These data can be used to calculate the mass of the neutron with less error than is involved in any other case known. The result is 1.0062 with an error less than 0.001. This means that the binding in the case of H^2 is of the order of 5×10^5 volts and if the proton consists of a neutron and a positive electron (Science **76**, 294 (1932)) its ionization potential is very small. This value of the neutron's mass is apparently in disagreement with disintegration experiments of Kurie (Phys. Rev. **43**, 771 (1933)). However, if Kurie's data (which he has kindly furnished) are computed on the assumption that the neutron is not captured, it turns out that there is no difficulty with the conservation of energy with the mass 1.0062. Moreover, it can be shown that while the evidence for non-capture disintegrations with neutrons in nitrogen is good, that for capture disintegrations is very weak, because the usual criterion for capture applies in this case almost as well for non-capture. Further, only those exceptional neutrons are able to disintegrate nitrogen without capture which have almost their maximum energy. The more abundant kind below 8×10^6 volts play no part in such disintegrations.

35. The Interaction Between Neutrons and Protons. R. M. LANGER, *California Institute of Technology.*—The scalar product $(\mu\cdot\sigma)$ (where μ is the magnetic moment and σ the mechanical moment) seems, according to Bacher (Phys. Rev. **41**, 1001 (1932)) to have about the same numerical value for the neutron and the proton but the sign is opposite. This may be taken as an indication that the interaction between the neutron and the proton is mainly magnetic. In fact two bar magnets free to rotate would be in their lowest energy state when their moments were opposite in direction. In the case under discussion it would follow that the spins would add. The H^2 nucleus in its lowest state should then have a spin of one unit and a magnetic moment close to zero. If the He^4 nucleus is a closed shell the same should apply to Li^6. If O^{16} is a closed shell then N^{14} lacks one neutron and one proton and the same conclusion holds for it as well as for O^{18}. Other results can be obtained for certain more complex nuclei. The expectations are in agreement with all available

experiments. Without the hypothesis here proposed it is hard to see why N^{14} for example should have a spin of 1 instead of 0.

36. Theory of the Origin of Cosmic Radiation. R. M. LANGER, *California Institute of Technology.*—The radical assumption that nuclear charges can disappear slowly has no valid experimental or theoretical evidence against it. If this is a general property of matter it follows that in our portion of the universe there should be a negative space charge which would accelerate positive charges from the outside. Even for exceedingly low rates of annihilation, the total drop could be sufficient to account for cosmic-ray positive particle energies. At the same time the difficulties raised recently by Swann and Zwicky disappear. The primary charged particles shown by the latitude effect have higher energy than the average because they have fallen through the whole field. The more abundant secondaries of lower energy are either parts of showers involving many particles or result from photons formed part way in. The east-west differences seem to indicate that all of the primary charged particles are positive as would be required if the radiation is due to a cosmical field as here supposed. The lack of a dependence on sidereal time is however surprising. Of course the otherwise mysterious atmospheric electrical currents are immediately accounted for as already discussed by Swann (Phil. Mag. **3**, 1088 (1927)). Certain puzzling properties of the aurora also find explanation. In fact a whole series of cosmic and terrestrial phenomena can be interpreted with the help of this single harmless lapse from conservatism.

37. Active Nitrogen. JOSEPH KAPLAN, *University of California at Los Angeles.*—The afterglow in the nitrogen tube described in abstract No. 15 has been photographed in the visible on panchromatic and astronomical green plates and in the ultraviolet on Eastman 33's. In addition to a very unusual intensity distribution in the first-positive group, different from that in normal nitrogen afterglows, this afterglow contains the first-negative and second-positive bands. The two latter groups of bands have never before been reported in nitrogen afterglows. In the present afterglow the first-negative and the first-positive groups are more intense relative to the second-positive group than they are in the exciting discharge itself. It was for this reason that the second-positive bands were not observed on my first afterglow plates, since these were in the visible and there the second-positive bands are very weak. This intensity relationship between the three systems is very similar to that in the aurora spectrum. This fact, together with the experiment performed by me at Princeton, in which the green aurora line was produced in the nitrogen afterglow without the simultaneous excitation of any other oxygen lines, shows that it is possible to produce the entire aurora spectrum in an afterglow.

38. Supernovae and Cosmic Rays. W. BAADE, *Mt. Wilson Observatory*, AND F. ZWICKY, *California Institute of Technology.*—Supernovae flare up in every stellar system (nebula) once in several centuries. The lifetime of a supernova is about twenty days and its absolute brightness at maximum may be as high as $M_{\text{vis}}=-14^{M}$. The visible radiation L_{ν} of a supernova is about 10^8 times the radiation of our sun, that is, $L_{\nu}=3.78\times10^{41}$ ergs/sec. Calculations indicate that the total radiation, visible and invisible, is of the order $L_{\tau}=10^7L_{\nu}=3.78\times10^{48}$ ergs/sec. The supernova therefore emits during its life a total energy $E_{\tau}\geq10^5L_{\tau}=3.78\times10^{53}$ ergs. If supernovae initially are quite ordinary stars of mass $M<10^{34}$ g, E_{τ}/c^2 is of the same order as M itself. In the *supernova* process *mass in bulk is annihilated.* In addition the hypothesis suggests itself that *cosmic rays are produced by supernovae.* Assuming that in every nebula one supernova occurs every thousand years, the intensity of the cosmic rays to be observed on the earth should be of the order $\sigma=2\times10^{-3}$ erg/cm² sec. The observational values are about $\sigma=3\times10^{-3}$ erg/cm² sec. (Millikan, Regener). With all reserve we advance the view that supernovae represent the transitions from ordinary stars into *neutron stars*, which in their final stages consist of extremely closely packed neutrons.

39. The Motion of Electrons Near a Plane Photo-Electrode in the Presence of a Gas. AUSTIN M. CRAVATH, *University of California.*—When electrons leave a photoelectric cathode in the presence of a gas, some are reflected back to the cathode and only a fraction i/i_0 escapes to the anode. The mean energy and density of the electrons vary with distance from the cathode, approaching constancy at large distances if the field is uniform. Previous theoretical calculations of i/i_0 (Bradbury, Phys. Rev. **40**, 980, 1932; Young and Bradbury, Phys. Rev. **43**, 35, 1933) have been found to be not even approximately valid. The differential equation for the current involves diffusion and thermal effusion as well as mobility. The energy equation involves *flows* of energy due to thermal conductivity of the electron gas, diffusion, and electric field, as well as the energy gained from the field and that last in collision. These equations have been solved numerically. None of the above terms can be neglected under all conditions. $i_0/i=0.25(V_e/W_{\infty})(N_e/N_{\infty})+0.5$ where V_e is the average speed with which the electrons leave the cathode, W_{∞} the drift velocity in terminal state of motion, and N_e and N_{∞} the electron densities at and far from the cathode. For most of the range covered by Bradbury's experiments, N_e/N_{∞} is nearly unity, giving practically the equation which he found to fit his results.

40. About the Origin of the Mosaic Structure in Metal Crystals. A. GOETZ, *California Institute of Technology.*—In order to explain the appearance of periodicities of higher orders (secondary or mosaic structures) it is suggested that an aggregation of groups takes place during an interval of temperature of a few degrees *above* the melting point. These aggregates ("groups") are of approximately equal size and their existence is essential for the formation of a solid crystal. If their formation is prevented, undercooling results down to a temperature at which the group formation is more probable. The support of this hypothesis is partly found in experiments of the author concerning

the "survival" of crystalline qualities of single crystals beyond the melting point, partly in the experiments about the phenomena of undercooling as function of previous overheating by Webster, partly by the fact that the x-ray analysis of liquid metals whose structure in the solid state deviates much from close-packed arrangements does not give an indication of a statistical distribution of the molecules in the liquid. The mosaic structure in solids is suggested to be caused by the slight structural deformation which the molecules at the surface of the groups possess in the moment of the transition into the solid state. The variation in the size of these groups as well as slight inaccuracies of their packing may serve for explaining the failure to observe diffraction patterns of such structures and also the dependence of such structures on the methods of growth of the crystal.

AUTHOR INDEX TO ABSTRACTS OF THE STANFORD UNIVERSITY MEETING

Anderson, O. E.—No. 10

Baade, W. and F. Zwicky—No. 38
Bowen, I. S.—No. 9

Carlson, J. F.—see Furry
Chapman, Seville—No. 25
Cheng, Yee Fung—No. 3
Clark, J. C.—No. 20
Cravath, Austin M.—No. 39

Duveneck, F. B.—see Newell

Eaton, B. G.—No. 2
Ellis, Joseph W. and Hans O. Kneser—No. 13
Epstein, Paul S.—No. 29
Evans, Robley D.—Nos. 27, 32
—— **and Howel Williams**—No. 33

Finkelnburg, Wolfgang—No. 14
Focke, A. B.—see Goetz
Foster, B. E.—No. 1
Furry, W. H. and J. F. Carlson—No. 31

Goetz, A.—No. 40
—— **and A. B. Focke**—No. 28
Grenko, J. D.—see Hoard
Grinfeld, Rafael—see Jenkins
Hackney, A. W.—see Newell
Hoard, J. L. and J. D. Grenko—No. 24
Houston, William V.—No. 7
—— see Kinsler
—— **and Y. M. Hsieh**—No. 8
Hsieh, Y. M.—see Houston

Jenkins, F. A. and Rafael Grinfeld—No. 12
Jordan, Edward B.—No. 26

Kaplan, Joseph—Nos. 15, 37
Kinsler, L. E. and W. V. Houston—Nos. 17, 18
Kirkpatrick, Paul—see Pockman
—— see Ross
—— **and P. A. Ross**—No. 22
Kneser, Hans O.—see Ellis

Langer, R. M.—Nos. 34, 35, 36

McMillan, Edwin—No. 19
More, Kenneth R.—No. 11

Nedelsky, L. and J. R. Oppenheimer—No. 30
Newell, R. R., F. B. Duveneck and A. W. Hackney—No. 23
Nordsieck, Arnold—No. 16

Oppenheimer, J. R.—see Nedelsky

Patten, C. G.—No. 5
Phillips, Melba—No. 6
Pockman, L. T., Paul Kirkpatrick and D. L. Webster—No. 4

Ross, P. A.—see Kirkpatrick
—— **and Paul Kirkpatrick**—No. 21

Webster, D. L.—see Pockman
Williams, Howel—see Evans

Zwicky, F.—see Baade